Studies on red color-related pigment-binding protein derived from the shell of Pacific white shrimp Litopenaeus vannamei

Doctoral Dissertation

STUDIES ON RED COLOR–RELATED PIGMENT–BINDING PROTEIN DERIVED FROM THE SHELL OF PACIFIC WHITE SHRIMP *Litopenaeus vannamei*

September 2018

Graduate School of Marine Science and Technology

Tokyo University of Marine Science and Technology

Doctoral Course of Applied Marine Biosciences

Pan Chuang

Doctoral Dissertation

STUDIES ON RED COLOR–RELATED PIGMENT–BINDING PROTEIN DERIVED FROM THE SHELL OF PACIFIC WHITE SHRIMP *Litopenaeus vannamei*

September 2018

Graduate School of Marine Science and Technology

Tokyo University of Marine Science and Technology

Doctoral Course of Applied Marine Biosciences

Pan Chuang

[課程博士・論文博士共通]

博士学位論文内容要旨
Abstract

専　攻 Major	応用生命科学	氏　名 Name	Pan Chuang
論文題目 Title	Studies on red color–related pigment–binding protein derived from the shell of Pacific white shrimp *Litopenaeus vannamei* (バナメイエビ殻由来の色素結合タンパク質に関する研究)		

Crustaceans like shrimps and crabs have a remarkable red color change during cooking. In addition to reflecting the freshness of crustaceans, the red color change also plays a significant role in consumer acceptability of commercial crustacean species. Studies on crustacean shell color change were mainly focused on lobsters like American lobster (*Homarus americnaus*), European lobster (*H. gammarus*), and Western Australia lobster (*Panulirus cygnus*). It revealed that this well–know red color change is caused by the releasing of pigments from denatured pigment–binding proteins, which is consist of apoprotein and astaxanthin (ATX), named crustacyanin. However, information on the red color–related pigment–binding proteins derived from other crustacean species is insufficient. To our knowledge, there has been few report on the pigment–binding proteins involved in the red color change on the shell of Pacific white shrimp, *Litopenaeus vannamei*. Therefore, this study dealt with the purification, identification, and elucidation of the structural and thermal properties of the red color–related pigment–binding protein in the shell of *L. vannamei*. In addition, specificity of the red color–related protein derived from *L. vannamei* was investigated among *H. americanus*, *Marsupenaeus japonicus*, and *Panulirus japonicus*.

In order to clarify the red color change on *L. vannamei* shell surface, the red color–related protein was purified from shell by ammonium sulfate precipitation, gel filtration and anion exchange HPLC in Chapter 2. The purified red color–related protein afforded a major single peak as analyzed by gel filtration HPLC on a TSKgel G3000SW$_{XL}$ column and a single band in native– and SDS–PAGE, indicating that this protein was a hemogeneous monomer with molecular mass of ~75 kDa and was termed as LvPBP75 (*Litopenaeus vannamei* pigment–binding protein with molecular mass ~75 kDa). Peptide mass fingerprinting (PMF) analysis revealed a protein that named hemocyanin (GenBank accession number: CAA57880) matched LvPBP75 with a nominal mass of ~74,992 Da. Absorption spectrum of acetone extract from the precipitate of heated LvPBP75 was typical of ATX with absorption maxima at 481 nm. The results suggested that the red color change on *L. vannamei* shell surface is correlated with a novel red color–related pigment–binding protein, LvPBP75, which is consist of hemocyanin and astaxanthin, but not the previous described crustacyanin in lobster shell.

In chapter 3, in order to elucidate the structural properties of LvPBP75, cDNA cloning and circular dichroism spectroscopy analysis were carried out. On the basis of the partial amino acid sequences determined by PMF analysis, a full length cDNA of 2,183 bp including an ORF of 1,986 bp that encodes 662 amino acid residues (GenBank/EMBL/DDBJ accession number KY695246) was cloned. Multiple sequence alignment indicated that LvPBP75 shows a high similar identity (~80%) with the hemocyanin or

its subunits derived from the hepatopancreas of *L. vannamei*. α–Helix, β–sheet, β–turn, and random coil contents of unheated LvPBP75 were calculated to be 51.0 ± 0.216, 19.5 ± 0.262, 16.4 ± 0.216, and 13.6 ± 0.245%, respectively. Meanwhile, to investigate the thermal properties of LvPBP75, studies on the effects of temperature, ion strength, pH, and alcohol on the red color change of LvPBP75 were carried out. As results, initial color change of LvPBP75 occurred at 30 °C and no significant changes were observed before heated at 60 °C. Within the increasing of heating temperatures, the protein color increased significantly in both the redness and yellowness scales. Color change of LvPBP75 is reversible at 30 ºC with low NaCl concentrations (< 0.05 M), but irreversible when heated with high NaCl concentrations (> 0.1 M). No significant color change was detected under the pH of 6, 7, and 8. The red color values of acidic or alkali pH–treated LvPBP75 were significantly moved to red and yellow scales after heat treatments. Before heating, LvPBP75 changed to pink when 20% methanol and 30% ethanol was added. A yellow color was detected when 40% methanol and 60% ethanol was added. All samples turned to both redness and yellowness scales after heat treatments. The results suggested a novel function of hemocyanin as binding with pigment and its involvement in *L. vannamei* shell color change.

In chapter 4, in order to demonstrate the pigment–binding property of LvPBP75, tissue distribution of LvPBP75 and reconstruction of artificial LvPBP75 were carried out. It was found that LvPBP75 has the highest expression level in hepatopancreas, mediate level in heart, hemolymph, epithelium, and intestine, and the lowest in eyestalk, nerve, and muscle based on the analysis of tissue distribution. LvPBP75 was successfully expressed in *E. Coli* using the pET–44a vector system and a prominent 75 kDa protein band corresponding to His–tagged recombinant LvPBP75 (rLvPBP75) was observed in the precipitate fraction of IPTG–induced bacteria. After overnight incubation at 4 ºC, the rLvPBP75 was successfully combined with ATX. However, ATX peak (~ 480 nm in acetone) was not detected in the binding experiment when using the hemocyanins derived from the hemolymph of *Megathura crenulata* and *Limulus polyphemus*, indicating that hemocyanins with oxygen transportation function do not possess the pigment–binding functions. Three–dimensional structural analysis revealed that LvPBP75 monomer possesses four spatial structural differences compared with the hemocyanin monomer which was derived from *L. vannamei* hepatopancreas. The results suggested that the pigment–binding ability of hemocyanins has species– or tissue–specificity and their unique structural features play an important role in binding ability.

In chapter 5, in order to illuminate the relationship between small molecular weight proteins (< 40 kDa) and red color change in *L. vannamei*, the < 40 kDa proteins were separated and subjected to color change experiments. As results, no significant red color change could be detected after heat treatment, indicating that *L. vannamei* shell color change was not correlated with < 40 kDa proteins. Meantime, to investigate whether the LvPBP75 is specific in *L. vannamei* or not, red color–related proteins derived from the shell of *H. americanus*, *M. japonicus*, and *P. japonicus* were purified using gel filtration and ion exchange HPLC, respectively. As results, the 75 kDa protein was correlated with the red color change on the surface of *L. vannamei*, *M. japonicus*, and *P. japonicus*, while the 22 kDa protein was correlated with the red color change in *H. americanus*. The results suggested that the red color change on *L. vannamei* surface is mainly correlated with LvPBP75 and it is not specific in *L. vannamei*, further investigation is necessary to

understand the red color–related proteins among a variety of crustacean species.

This study identifies a novel red color–related hemocyanin–ATX binding protein, LvPBP75, from the shell of *L. vannamei* and strongly suggests a novel function of hemocyanin as binding with pigment and involved in *L. vannamei* shell red color change.

Content

List of Figures..... i

List of Tables..... vi

Abbreviation of Amino Acids..... vii

Chapter 1 General introduction and literature review..... 1

1.1 Pigment–binding protein (PBP) in animals..... 1

1.2 Relationship between PBP and red color change in crustaceans..... 3

1.3 Research objectives..... 5

1.4 Research summary..... 6

Figures and Tables..... 9

Chapter 2 Purification and identification of red color–related PBP derived from the shell of *L. vannamei* (LvPBP)..... 11

2.1 Introduction..... 11

2.2 Materials and Methods..... 12

2.2.1 Extraction of different soluble proteins..... 12

2.2.2 Purification of LvPBP..... 13

2.2.3 In–gel digestion and peptide mass fingerprinting (PMF) analysis of LvPBP..... 14

2.2.4 Pigment analysis of LvPBP..... 15

2.2.5 Analysis of protein color change..... 15

2.2.6 Statistical analysis..... 15

2.3 Results..... 16

2.3.1 Isolation and color change of different soluble proteins..... 16

2.3.2 Purification and identification of LvPBP..... 17

2.4 Discussion..... 18

Figures and Tables..... 22

Chapter 3 Structural and thermal properties of red color–related protein LvPBP..... 31
3.1 Introduction..... 31
3.2 Materials and Methods..... 32
3.2.1 Materials.....32
3.2.2 Primer design..... 32
3.2.3 RNA extraction and cDNA synthesis..... 32
3.2.4 Cloning of full–length cDNA encoding LvPBP.....33
3.2.5 Bioinformatic analysis..... 34
3.2.6 Circular dichroism (CD) spectroscopy analysis.....34
3.2.7 Thermal properties of LvPBP.....35
3.2.8 Statistical analysis.....35
3.3 Results.....36
3.3.1 cDNA cloning and sequence analysis of LvPBP..... 36
3.3.2 Secondary structure of LvPBP..... 37
3.3.3 Thermal properties of LvPBP.....38
3.4 Discussion.....39
Figures and Tables.....43

Chapter 4 Gene distribution and functional expression of red color–related protein LvPBP..... 60
4.1 Introduction..... 60
4.2 Materials and Methods..... 61
4.2.1 Shrimp and tissue collection.....61
4.2.2 RNA extraction and cDNA synthesis..... 61
4.2.3 Semi–quantitative and quantitative real time PCR..... 62
4.2.4 Expression and purification of recombinant LvPBP (rLvPBP).....62
4.2.5 Identical analysis between LvPBP and rLvPBP..... 64
4.2.6 Construction of artificial LvPBP.....64
4.2.7 Structural analysis of artificial LvPBP.....65

4.2.8 Statistical analysis.....65
4.3 Results.....65
4.3.1 Tissue distribution of LvPBP.....65
4.3.2 Expression and purification of rLvPBP.....66
4.3.3 Identical analysis between LvPBP and rLvPBP..... 67
4.3.4 Construction and structural analysis of artificial LvPBP.....67
4.4 Discussion.....69
Figures and Tables.....72

Chapter 5 Specificity analysis of red color–related protein LvPBP..... 81
5.1 Introduction..... 81
5.2 Materials and Methods..... 82
5.2.1 Materials.....82
5.2.2 Relationship between small molecular weight proteins and red color change in *L. vannamei* shrimp.....82
5.2.3 Purification of red color–related PBP from the shell of kuruma shrimp, American lobster, and Japanese spiny lobster..... 82
5.2.4 Electrophoretic analysis of shell derived PBPs.....83
5.2.5 Analysis of protein color change..... 84
5.2.6 Statistical analysis.....84
5.3 Results.....84
5.3.1 Relationship between small molecular weight proteins and red color change in *L. vannamei* srhimp..... 84
5.3.2 Purification of red color–related proteins derived from kuruma shrimp, American lobster, and Japanese spiny lobster.....85
5.4 Discussion.....86
Figures and Tables.....90

Chapter 6 Summary of main finding and discussion..... 98

6.1 Summary.....98
6.2 Discussion.....99
6.3 Prospect for future study..... 101

Acknowledgements..... 102

References..... 103

List of Figures

Fig. 1–1 The detailed layout of the astaxanthin–binding sites at the end–ring molecular environments in β–crustacyanin (C1–6 end ring of astaxanthin1 bound to crustacyanin A1 subunit).

Fig. 1–2 Photographs of the *Litopenaeus vannamei*: (a) frozen, (b) after cooking.

Fig. 2–1 (A) Protein files of different soluble proteins extracted from *L. vannamei* shell (Lane M: protein marker). (B) Color changes of different soluble proteins from *L. vannamei* shell after heat treatment at 100 ºC for 10 min.

Fig. 2–2 Calibration curve for the determination of protein concentration.

Fig. 2–3 Effect of heating temperature on crude water–soluble proteins derived from *L. vannamei* shell (Lane M: protein marker).

Fig. 2–4 Purification of red color–related protein by gel filtration HPLC (A) and anion–exchange HPLC (B). (A) Crude proteins obtained by 60% ammonium sulfate were applied to a Superdex 200 gel filtration column. (B) The red color–related fraction (Fr. 2) from the Superdex 200 column was applied to a Mono Q column. (C) SDS–PAGE on a 5–20% precast gel (Lane M: protein marker).

Fig. 2–5 (A) HPLC of LvPBP75 on a TSK gel G3000SW$_{XL}$ column. The following proteins were used as a reference: 1, β–amylase (200 kDa); 2, alcohol dehydrogenase (150 kDa); 3, albumin (66 kDa); 4, carbonic anhydrase (29 kDa); 5, cytochrome C (12.4 kDa). (B) Native–PAGE on a 12% hand–made gel.

Fig. 2–6 (A) Spectrum of peptide mass fingerprinting analysis of the 75–kDa band (m/z: mass numbers/charge numbers). (B) Absorption spectra of the unheated LvPBP75 and acetone extract from the precipitate of heated LvPBP75.

Fig. 3–1 Alignment of the amino acid sequences of hemocyanin from different shrimp species. The peptides of LvPBP75 obtained from MALDI–TOF–MS were highlighted with bold red. The primer regions were framed. Multiple

sequence alignments were performed using Clustal W. Accession numbers were (GenBank nucleotide sequence databases): *L. vannamei*, AHN85635; *P. monodon*, AEB77775; *F. chinensis*, ACM61982; *F. merguiensis*, AGT20779; *M. japonicus* subunit L, ABR14693; *M. japonicus* subunit Y, ABR14694.

Fig. 3–2 Multiple sequence alignment of nucleotide sequences of hemocyanin from different shrimp species. Multiple sequence alignments were performed using Clustal W. The positions of internal amplification primers were marked with red. Accession numbers were (GenBank nucleotide sequence databases): *L. vannamei* (X82502), *P. monodon* (JF357966), *F. chinensis* (FJ594414), *F. merguiensis* (KC920897), *M. japonicus* subunit L (EF375711) and subunit Y (EF375712).

Fig. 3–3 Strategy for the cDNA cloning of LvPBP75 derived *L. vannamei* shell (Meaning of letters: Inter, internal amplification primer; Gsp, gene–specific primer; F, forward primer; R, reverse primer).

Fig. 3–4 (A) 1.2% agarose gel electropherogram of amplified internal region (M: 100 bp DNA ladder). (B) Nucleotide sequence alignment of internal fragment and hepatopancreas derived hemocyanin (Accession No.: KJ151291). The identical residues are shown by dots.

Fig. 3–5 1.2% agarose gel electrophoregram of 3'–end/5'–end products (A) and end to end amplification products (B) (M: 100 bp DNA ladder).

Fig. 3–6 Nucleotide sequence and deduced amino acid sequence of LvPBP75. The initial methionine codon is at position 70 and indicated with bold, whereas the stop codon is at position 2,056 of the nucleotide sequence and indicated with an asterisk. The polyadenylation signal is in italics. The landmark peptides of arthropod hemocyanin are indicated with frame. Transmembrane domains are in bold and italics, tyrosinase copper binding domain is double underlined. N– and C–terminals are shadowed.

Fig. 3–7 Multiple sequence alignment of deduced amino acid sequence of LvPBP75 with other known hemocyanins and their subunits derived from the

hepatopancreas of *L. vannamei*. Sequence similarity is delineated as identical (asterisk), strongly similar (colon), and weakly similar (dot). The predicted secondary structure is indicated by α or β (α, α–helices; β, β–strands). Accession numbers (DDBJ/EMBL/GenBank amino acid sequence databases): hemocyanin, AIN41163; subunit L1, AHY86475; subunit L2, AHY86476; subunit L3, AHY86477; subunit V4, AKI81624.

Fig. 3–8 Circular dichroism spectra analysis. (A) Changes of CD spectra in LvPBP75 induced by different heating temperatures. Colored spectra refer to the native state (black), heated at 30 ºC (orange), 45 ºC (green), 60 ºC (blue), 80 ºC (pink) and 100 ºC (red). (B) Plots of the β–sheet (▲), turn (■) and random coil structure (●) contents against the α–helix content for heat–treated LvPBP75.

Fig. 3–9 Changes of CD spectra in LvPBP75 induced by different concentrations of NaCl at different heating temperatures. (A) room temperature, (B) 30 ^{o}C, (C) 60 ^{o}C and (D) 100 ^{o}C. Colored spectra refer to the unheated (blue), NaCl concentration at 0.01 M (yellow), 0.05 M (gray), 0.1 M (black), 0.5 M (purple) and 1.0 M (green).

Fig. 3–10 Changes of CD spectra in LvPBP75 induced by different pHs at different heating temperatures. (A) room temperature, (B) 30 ^{o}C, (C) 60 ^{o}C and (D) 100 ^{o}C. Colored spectra refer to pH 3–red, pH 4–black, pH 5–blue, pH 6–yellow, pH 7–brown, pH 8–green, pH 9–gray, pH 10–pink, pH 11–purple

Fig. 3–11 Changes of CD spectra in LvPBP75 induced by different alcohols at different heating temperatures. Colored spectra refer to the native state–black and alcohol concentration of 10%–blue, 20%–green, 30%–gray, 40%–brown, 50%–yellow, 60%–purple and 70%–pink.

Fig. 4–1 Procedure for expression of recombinant LvPBP75 (rLvPBP75).

Fig. 4–2 Tissue distribution of LvPBP75 mRNA in *L. vannamei*, as determined by semi–quantitative real–time PCR (A) and quantitative real–time PCR (B). LvPBP75 expression was normalized to β–actin expression. Bars represent

the mean of triplicate tissue samples ± SD.

Fig. 4–3 1.2% agarose gel electrophoresis of restriction enzymes digested pET–44a vector (A) and amplification of mature LvPBP75 with restriction enzyme sites (B).

Fig. 4–4 Insert check of recombinant expression vector LvPBP–pET44a. (A) LvPBP–pET44a digested by two restriction enzymes; (B) Colony PCR screening of LvPBP–pET44a using pET upstream and Colidown primers (Lane numbers mean different positive single colonies).

Fig.4–5 SDS–PAGE analysis of different incubation conditions: temperature (30 and 37 ^{o}C), induction time (1, 2, 4 and 6 h) and IPTG concentration (0.1, 0.5 and 1.0 mM).

Fig. 4–6 (A) Purification of rLvPBP75 on the affinity chromatography. (B) Analysis of expression and purification of rLvPBP75 by SDS–PAGE. Lanes: M, protein marker; 1, soluble fraction from non–induced *E. coli*; 2, unsoluble fraction from non–induced *E. coli*; 3, soluble fraction from IPTG–induced *E. coli*; 4, unsoluble fraction from IPTG–induced *E. coli*; 5, purified rLvPBP75.

Fig. 4–7 (A) The absorption spectra of hemocyanin astaxanthin binding complexes (▬▬▬ *Limulus polyphemus* derived hemocyanin, ····· *Megathura crenulata* derived hemcoyanin, ▬ · ▬ · recombinant LvPBP75). (B) CD spectra of LvPBP75 (·····) and rLvPBP75 (▬) in 20 mM phosphate buffer (pH 7.0) at room temperature.

Fig. 4–8 (A) 3D model of red color–related pigment–binding protein derived from the shell of *L. vannamei*, LvPBP75. (B) Ribbon diagram of LvPBP75 monomer (B–1) and *L. vannamei* hepatopancreas derived hemocyanin monomer (B–2).

Fig. 5–1 Purification (A) and protein pattern (B) of small molecule weight proteins derived from the shell of *L. vananmei* using ion exchange HPLC on IEC QA–825 column.

Fig. 5–2 Protein files of crude water–soluble proteins derived from kuruma shrimp (A),

American lobster (B) and Japanese spiny lobster (C) after heated at 100 ^{o}C, 10 min (Lane M: marker).

Fig. 5–3 Purification (A) and protein pattern (B) of red color–related protein derived from kuruma shrimp shell by using Superdex 75 gel filtration column.

Fig. 5–4 Purification of gel filtration derived fraction No.1 (A) and fraction No.2 (B) using ion–exchange HPLC on IEC QA–825 column. The inserts were protein patterns of purified fractions.

Fig. 5–5 Purification (A) and SDS–PAGE analysis (B) of red color–related proteins derived from American lobster shell using ion–exchange HPLC on an IEC QA–825 column. (C) Protein files of ultracentrifugation fractions of fraction No. 1 which was collected from ion exchange HPLC.

Fig. 5–6 Purification of the red color–related proteins derived from Japanese spiny lobster shell using gel filtration HPLC on a Superdex 200 column (A) and ion–exchange HPLC on an IEC QA–825 column (B). The inserts were protein patterns of purified fractions.

List of Tables

Table 2–1 Color change of different soluble proteins

Table 2–2 Color change of crude water–soluble proteins

Table 2–3 Color change of LvPBP75 under different heating temperatures

Table 2–4 Amino acid sequences of LvPBP75 peptide fragments identified by MALDI–TOF–MS

Table 3–1 List of primers for LvPBP75 cDNA amplification

Table 3–2 Secondary structure contents of LvPBP75 under different heat treatments

Table 3–3 Color measurement of LvPBP75 heated with different concentrations of NaCl at different heating temperatures

Table 3–4 Color measurement of LvPBP75 heated with different pHs at different heating temperatures (RT: room temperature; 30, 60, and 100 mean heated at 30, 60, and 100 ^{o}C, respectively)

Table 3–5 Color measurement of LvPBP75 heated with different alcohols at 100 ^{o}C, 15 min (Upper, EtOH; Lower, MeOH)

Table 4–1 Nucleotide sequences of primers used in this chapter

Table 4–2 Secondary structure contents of rLvPBP75–ATX under different heat treatments

Table 5–1 Color changes of different fractions (</> 50 kDa) derived from the crude water–soluble proteins of *L. vannamei*

Table 5–2 Color changes of fractions purified from American lobster by using IEC QA–825 column (Upper: before heat treatment, Lower: 100 ^{o}C, 10 min. 1–8: fraction numbers)

Abbreviation of Amino Acids

Table of amino acids and their abbreviations, one letter abbreviations were only used in the description of deduced amino acid sequence, three letter abbreviations were used in the remaining descriptions.

Amino Acid	Abbreviation (3 Letter)	Abbreviation (1 Letter)
Alanine	Ala	A
Cysteine	Cys	C
Aspartate	Asp	D
Glutamate	Glu	E
Phenylalanine	Phe	F
Glycine	Gly	G
Histidine	His	H
Isoleucine	Ile	I
Lysine	Lys	K
Leucine	Leu	L
Methionine	Met	M
Asparagine	Asn	N
Proline	Pro	P
Glutamine	Gln	Q
Arginine	Arg	R
Serine	Ser	S
Threonine	Thr	T
Valine	Val	V
Tryptophan	Trp	W
Tyrosine	Tyr	Y

Chapter 1 General introduction and literature review

Color plays a significant role in consumer acceptability of food product, especially in crustacean species (Erickson et al., 2007; Parisenti et al., 2011; Wade et al., 2012; Ertl et al., 2013). In nature status, all colored organic substances are considered as pigments, although sometimes they may be colorless, as are some pigment–binding complexes (Shahidi & Brown, 1998). Pigment–binding proteins (PBP), as the most common forms of pigments present in animals, has been widely studied in the past decades (Zagalsky, 1985; Shahidi & Brown, 1998; Matsuno, 2001; Senphan et al., 2014; Goncalves & Menezes de Oliveira, 2016).

1.1 Pigment–binding protein (PBP) in animals

Pigments are widely distributed in almost all living creatures, from the most primitive bacteria (Archebacteria) to the highly developed plants (Angiospermae), from the unicellular organisms (protozoa) to higher mammals, including human (Shahidi & Brown, 1998). After combined with the hydrophobic sites of proteins, the pigment–binding protein (PBP) was formed (Lee, 1966). Formation of PBP brings some changes to the pigments: 1) it makes the pigment to become water–soluble and easy to transport or penetrate through the membranes into other tissues (Zsila et al., 2002; Green et al., 2006), 2) PBP may possess different characterizations and color change mechanisms in different individuals (Cianci et al., 2002; Chayen et al., 2003; Elizabeth et al., 2009; Wade et al., 2008, 2009, 2012).

Among insects, the most extensively studied PBP is a carotenoid–binding protein which was purified from the silkworm, *Bombyx mori* (Tabunoki et al., 2004; Bhosale & Bernstein, 2007). The color of cocoons obtained from farmed silkworm showed various colors, while the wild–type silkworms only made yellow cocoons due to the presence of lutein. The pigments are transported from midgut to the lipophorin, and from lipophorin into the silk gland, where the cocoon is produced (Bhosale &

Bernstein, 2007). Jouni and Wells reported that a specific lutein–binding protein with a molecular mass around 35 kDa, has been purified from the midgut of silkworm. It possessed maximum absorbances at 432, 460, and 492 nm and showed a significant bathochromic shift at 22–38 nm compared with the spectrum of lutein in hexane or acetone (Jouni & Wells, 1996). Tabunoki et al. studied a series of mutant silkworms with colorless cocoons and found new lutein–specific carotenoid binding protein with a molecular mass around 33 kDa. The maximum absorbance of this protein was determined at 436, 461, and 493 nm (Tabunoki et al., 2002). The followed functional characterization studies revealed that the lutein–binding protein is ultimately responsible for the pigmentation of yellow cocoons (Tabunoki et al., 2004).

In marine animals, PBP is mainly responsible for the coloration and can be found from skin and muscle to eggs, gonads, and shells (Cheesman et al., 1967; Zagalsky, 1985; Lakshman & Okoh, 1993; Bhosale & Bernstein, 2007). Unlike plants, animals couldn't synthesize the pigment by themselves, the distribution and diversity of pigments and PBPs are mainly depend on 1) dietary habits, 2) metabolic transformations, 3) absorption and storage capacity, etc. (Herring, 1969; Gross, 1991). It was reported that the red coloration of salmonid fish muscle was mainly generated from astaxanthin (Shahidi et al., 1998; Matsuno, 2001). 88% of the pigments found in the muscle of chum salmon was astaxanthin, 99.8% in sockeye salmon, and 95.7% in coho salmon (Crozier, 1970; Saito & Regier, 1971; Kitahara, 1984). Schiedt et al. reported that the pigments in the skin and muscle of wild rainbow trout were almost similar to the farmed samples which were fed with astaxanthin (Schidet et al., 1985a, b). They also mentioned that astaxanthin was the predominant pigment in the skin and muscle of rainbow trout. However, Matsuno & Katsuyama found that rhodoxanthin, an in vivo oxidative metabolite of zeaxanthin, was the main pigment in the skin of *Tilapia nilotica*, *T. mossambica*, and red Tilapia (Matsuno & Katsuyama, 1982; Matsuno, 2001). In addition, more than 90% of the pigments in the skin of stripped jack *Caranx delicatissimus* were composed of tunaxanthin, lutein, and zeaxanthin (Shahidi & Brown, 1998).

In crustaceans, PBPs can be found in many tissues including shell, epithelium, eggs, and blood. They display various colors like green, brown, blue, and black (Shahidi & Brown, 1998; Wade et al., 2017). PBP in crustaceans can be divided into two types: 1) lipovitellins, composed of lipoproteins and pigments, are mainly found in the ovaries and eggs of crustaceans, they may also be present in blood and epithelium. They display a blue, green, or purple color (Zagalsky, 1985, Shahidi & Brown, 1998). 2) Carotenoproteins, such as crustacyanin, are mainly found in the exoskeleton of crustaceans. They are formed from apoproteins and pigments, almost always astaxanthin, by the Schiff base bonds or carbonylamino bonds (Ghidalia, 1985; Shahidi & Brown, 1998), and usually appear to be correlated with the crustacean surface color, such as the shore crab (*Carcinus maenas*) showed a green or orange–red color, while the English freshwater crawfish (*Astacus pallipes*) has a greenish brown shell. Different tissues may display different colors even though they were derived from one sample. In the lobster *Homarus vulgaris*, the shell is black, tentacle is red, and the eggs are dark green (Shahidi & Brown, 1998).

1.2 Relationship between PBP and red color change in crustaceans

The color of crustacean shells changes from dark blue to bright red–orange when cooked (Wade et al., 2012; Ertl et al., 2013). In addition to reflecting the freshness of crustaceans, the red color change also plays a significant role in consumer acceptability of commercial crustacean species (Erickson et al., 2007; Parisenti et al., 2011). A pioneering study on lobster shell revealed that this well–known red color change is due to the release of pigments from denatured PBPs, named crustacyanin (Wald & Nathanson, 1948; Zagalsky, 1985; Chayen et al., 2003; Durbeej & Eriksson, 2003; Elizabeth et al., 2009; Wade et al., 2009). Crustacyanin extracted from a lobster shell comprises apoproteins and astaxanthin (Wald & Nathanson, 1948). The predominant PBP in the lobster shell is α–crustacyanin (λmax: 632 nm, ~320 kDa), which contains 16 protein subunits and 16 astaxanthin molecules (Zagalsky, 1985;

Chayen et al., 2003). After irreversible dissociation, β–crustacyanin (λmax: 585 nm, ~40 kDa) appears; eight units of β–crustacyanin can form one unit of α–crustacyanin. Both α– and β–crustacyanin can easily dissociate into apoproteins (~20 kDa) under experimental conditions (Elizabeth et al., 2009).

Crustacean shell color change was recently shown to be determined by crustacyanin and the interaction between astaxanthin and apoproteins (Fig. 1–1) (Chayen et al., 2003; Wade et al., 2008; Michael et al., 2009; Parisenti et al., 2011; Reszczynskaab et al., 2015). In nature, PBP in crustaceans can be influenced by many factors, including amount of carotenoids in the daily diet, background substrate color, light intensity, water quality, and growth stage (Palma & Steneck, 2001; Chayen et al., 2003; Wade et al., 2008, 2009, 2012). It was reported that American lobster (*Homarus americanus*) shell color is mainly influenced by ultraviolet light; moreover, in the absence of ultraviolet light, lobster shell matches the background color after long–term exposure (> 60 days) (Michael et al., 2009). Meanwhile, the mechanism of shell color change in prawn (*Penaeus monodon*) has been reported to strongly correlated with the background substrate color (Wade et al., 2012). The prawns fed in black background showed a much more orange color compared with those grown in white background after cooking. This was due to the prawns are grown in different background color need to adjust the accumulation of pigment–binding protein in their shell to match the environment. In another word, the prawns in black tanks need much more pigment–binding protein to dark their shell color compared with the ones grown in white tanks. Background color not only affects the prawns but also determines the shell color change on crabs (Hemmi et al., 2006; Kronstadt et al., 2013). In addition, study on the different body color of burrowing crab (*Neohelice granulata*) revealed that the colors are determined by its habitat (Casariego et al., 2011). Study on the effects of background and temperature on body color of fiddler crab (*Uca panacea*) revealed that the shell color could be affected by habitat and sex (Kronstadt et al., 2013). Furthermore, other studies demonstrated that crustacean shell colors are also associated with body size, molting stage, migration, and even water quality (Palma &

Steneck, 2001; Melville–Smith et al., 2003; Yanar et al., 2004; Zadorozhny et al., 2008). When crustaceans are cooked, the shell colors are influenced by storage conditions, heating temperatures, processing methods, and food additives (Brookmire et al., 2013; Ando et al., 2014; Huang et al., 2016). These studies suggesting that even though crustacean shell color change is associated with the release of pigment, but 1) PBPs derived from different crustacean species may differ with each other, 2) distribution, accumulation, and protein–pigment interaction mechanism of PBPs is still not clear (Nur–E–Borhan et al., 1995; Velu et al., 2003; Porter et al., 2009; Begum et al., 2015).

1.3 Research objectives

Crustaceans are cultured widely throughout the world, with 90% of shrimp cultured in Asia. Pacific white shrimp (*Litopenaeus vannamei*) is one of the economically important species of shrimp culture (~70%). It is mainly cultured in Asian countries, both as a food item for domestic consumption and as a valuable export commodity (Nirmal & Benjakul, 2009). Although it is well known that *L. vannamei* shell color changes from pale gray to bright red–orange after cooking (Fig. 1–2), the underlying mechanism and red color–related pigment–binding proteins derived from *L. vannamei* shell are poorly understood.

The main objective of this research is to illuminate the red color change on the surface of *L. vannamei* by studying the red color–related protein derived from its shell, as well as to help to promote the usage of shrimp by–products.

The specific objectives of this research are:

1) To purify and identify the red color–related proteins derived from the shell of *L. vannamei*.

2) To illuminate the structural and thermal properties of the red color–related protein.

3) To illuminate the pigment–binding ability of the red color–related proteins.

4) To demonstrate the specificity of this red color–related protein among shrimp

species.

1.4 Research summary

In chapter 2, the red color–related protein was purified from the shell of *L. vannamei* using ammonium sulfate precipitation, gel filtration, and anion exchange HPLC. Gel filtration HPLC and SDS–PAGE analysis demonstrated that the pure protein has a molecular mass of ~75 kDa. It was a homogeneous monomer with a purity more than 90%. Peptide mass fingerprinting analysis revealed a protein named hemocyanin matched this 75 kDa protein. The pigment was confirmed as astaxanthin. Next, in chapter 3, the structural and thermal properties of this red color–related protein were studied. On the basis of the partial amino acid sequences determined by peptide mass fingerprinting, a full–length cDNA of 2,183 bp including an ORF of 1,986 by that encodes 662 amino acid residues was cloned. Blast analysis revealed that it belongs to the hemocyanin family. Circular dichroism analysis illuminated that it was a protein rich in α–helix conformation. This red color–related protein was determined as a thermal sensitive protein. Color changes of this protein can be promoted after being subjected to conditions of high concentrations of NaCl, acidic or alkaline pH, and high concentrations of alcohols. In chapter 4, pigment–binding ability of this protein was studied. Tissue distribution revealed that LvPBP75 has the highest expression level in hepatopancreas, mediate level in heart, hemolymph, epithelium, and intestine, and the lowest in eyestalk, nerve, and muscle. Recombinant and structural analysis revealed that astaxanthin could bound to the shell derived hemocyanin and this pigment–binding complex had closely corresponded to *Litopenaeus vannamei* shell color change. But unlike crustacyanin, astaxanthin does not bring any structural changes to the binding complex. Three–dimensional structural analysis revealed a unique spatial structure of this red color–related protein. In chapter 5, specificity of this red color–related protein among shrimp species were determined. The 75 kDa protein was correlated with the red color change on the surface of *L.*

vannamei, *Marsupenaeus japonicus*, and *Panulirus japonicus*. Meanwhile, 22 kDa protein was correlated with the red color change in *Homarus americanus*. Accordingly, the red color–related pigment–binding protein LvPBP75 is not species–specific among shrimps.

Published paper

Chuang Pan, Shoichiro Ishizaki, Yuji Nagashima, Jialong Gao, Shugo Watabe. 2018. Isolation and cDNA cloning of a novel red colour–related pigment–binding protein derived from the shell of the shrimp, *Litopenaeus vannamei*. **Food Chemistry**, 241, 104–112. (Represent: Chapter 2 and 3)

Submitting

Chuang Pan, Shoichiro Ishizaki, Yuji Nagashima, Shugo Watabe. Functional and structural properties of red color–related pigment–binding protein from the shell of *Litopenaeus vannamei*. Submitted to "**Journal of the Science of Food and Agriculture**". (Represent: Chapter 3 and 4)

Preparing

Chuang Pan, Shoichiro Ishizaki, Shugo Watabe. Study on specificity of red color–related protein derived from the shell of *L. vannamei* among decapoda crustaceans (*Marsupenaeus japonicus*, *Panulirus japonicus*, and *Homarus americanus*). (Represent: Chapter 2 and 5).

Oral Presentation

Isolation and characterization of a novel red color–related protein derived from shrimp *Litopenaeus vannamei* shell (バナメイエビ殻の赤色化関連タンパク質の精製および特性). Chuang Pan, Yuji Nagashima, Shoichiro Ishizaki. The 2016 Autumn Meeting of the Japanese Society of Fisheries Science. Sep. 7th~10th, 2016, Kindai

University, Nara, Japan.

Reconstruction and structural analysis of red color–related pigment–binding protein derived from *Litopenaeus vannamei* (バナメイエビ殻の赤色化関連タンパク質の組換え体構築および構造解析). Chuang Pan, Shoichiro Ishizaki, Yuji Nagashima. The 2018 Autumn Meeting of the Japanese Society of Fisheries Science, Sep. 15th~18th, 2018, Hiroshima University, Hiroshima, Japan.

Poster Presentation

Isolation and secondary structure analysis of a novel red color–related pigment–binding protein derived from shrimp *Litopenaeus vannamei* shell. (バナメイエビ殻の赤色化関連色素結合タンパク質の単離および二次構造解析). Chuang Pan, Shoichiro Ishizaki, Yuji Nagashima. International Symposium "Fisheries Science for the Future Generations" (2017). Conference abstract, Tokyo, Japan.

cDNA cloning and expression analysis of red color–related hemocyanin gene in shrimp *Litopenaeus vannamei*. Chuang Pan, Shoichiro Ishizaki, Yuji Nagashima. 19th International Conference on Food Processing & Technology (2017). Conference abstract, Paris, France.

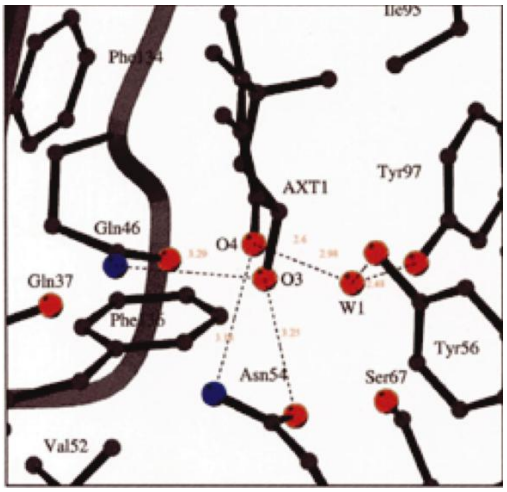

(Ref.: Chayen et al., 2003)

Figure 1–1 The detailed layout of the astaxanthin–binding sites at the end–ring molecular environments in β–crustacyanin (C1–6 end ring of astaxanthin1 bound to crustacyanin A1 subunit).

Figure 1–2 Photographs of the *Litopenaeus vannamei*: (a) frozen, (b) after cooking.

Chapter 2 Purification and identification of red color–related PBP derived from the shell of *L. vannamei* (LvPBP)

2.1 Introduction

Carapace coloration has been reported for a number of functions in crustaceans, like communication (Detto et al., 2006; Crothers et al., 2011), camouflage (Cuthill et al., 2005; Stevens & Merilaita, 2009), and thermo–regulation (Silbiger & Munguia, 2008). The various colors displayed on crustacean shell is correlated with a complex named carotenoprotein which is consist of pigment (almost astaxanthin) and protein (Wald & Nathanson, 1948; Zagalsky, 1985; Chayen et al., 2003; Castillo et al., 2013). The pigment–binding protein is also reported to be responsible for the red color change on crustacean shell when they are cooked (Wade et al., 2012; Ertl et al., 2013).

Isolation strategies of pigment–binding complex from crustacean shell or processing waste are various. Sila et al., (2012) reported the effect of barbel (*Barbus callensis*) trypsin on the recovery of carotenoprotein from pink shrimp (*Parapenaeus ongirostris*) waste, consisting of head, thorax, and appendix. The freeze–dried carotenoproteins recovered contained 71.09% protein, 16.47% lipid, 7.78% ash, and 87.42 μg total astaxanthin/g of sample. Senphan et al., (2014) extracted the carotenoprotein from shells of Pacific white shrimp (*Litopenaeus vannamei*) with the aid of proteases from hepatopancreas of the *L. vannamei* at various levels for different times. Carotenoprotein consisted of 73.58% protein, 21.87% lipids and 2.63% ash contents. Babu et al., (2008) compared the extractability of three different proteolytic enzymes (trypsin, pepsin, and papain) on the recovery of carotenoprotein from intact shrimp head waste. Trypsin showed the highest recovery ability, and the percent of recovery ratio was *Penaeus indicus* > *P. monodon* (farmed) > *Metapenaeus monocerous* > *P. monodon* (wild). In addition, another extraction method of carotenoprotein is a combination of ammonium sulfate precipitation and HPLC chromatography. This method is widely used for the isolation of crustacyanins from

lobsters, like *Homarus americanus*, *H. gammarus*, *Jasus lalandii*, and *Panulirus cygnus* (Zagalsky, 1985, Wade et al., 2008; Elizabeth et al., 2009; Michael et al., 2009).

In this chapter, a novel red color–related pigment–binding protein was isolated and purified from the shell of *Litopenaeus vannamei* by ammonium sulfate precipitation, gel filtration, and anion exchange HPLC. Then, the red color change ability of this pigment–binding protein was determined by subjecting it to different heat treatments. Furthermore, identification of the binding protein was illuminated by peptide mass fingerprinting analysis.

2.2 Materials and Methods

2.2.1 Extraction of different soluble proteins

Water–soluble proteins

Water–soluble proteins were prepared as described by Zagalsky (1985) and Elizabeth et al. (2009) with some modifications. Briefly, specimens of shrimp *L. vannamei* were purchased from the Tokyo Central Wholesale Fish Market (Tokyo, Japan). Shells were obtained, thoroughly freed from the underlying tissue by scrubbing with ice water, and dried overnight at 4 °C. The shells were minced with an electric food processor, and soaked for 16 h with agitation in 0.3 M boric acid adjusted to pH 6.8 with solid Tris and then transferred into pre–cooled (4 ^{o}C) 10% (w/v) EDTA solution (pH 7.0; 25 g shell with 1000 mL solution). The shells were removed by filtration after overnight stirring and the filtrate was brought to 60% saturation with ammonium sulfate. After stirred overnight at 4 °C, the precipitate was collected by centrifugation at 15,000 × *g* for 20 min at 4 °C, and then resuspended in 50 mM phosphate buffer (pH 7.0). The interfering proteins were removed by precipitation with ammonium sulfate to 30% saturation. The blue–colored filtrate, containing water–soluble proteins, was precipitated by increasing the saturation to 60%.

Non–water–soluble proteins

In addition to the traditional water–soluble protein, non–water–soluble proteins were also scanned for the existence of red color–related proteins. They were divided into salt–, acid–, and alkaline–soluble parts based on protein solubility and extracted according to Fernlund's method (Fernlund & Josefsson, 1968). 30% interfering precipitate was re–dissolved into 50 mM phosphate buffer containing 1 M NaCl and collected the salt–soluble extract by centrifugation at 15,000 × *g* for 20 min at 4 °C. The precipitate was soaked in 0.1 M HCl or NaOH to extract acidic– and alkaline–soluble proteins, respectively. All precipitate obtained from the previous step was washed with distilled water (pH 7.0) three times before subjecting to subsequent extraction experiments.

2.2.2 Purification of LvPBP

The crude water–soluble proteins were applied to gel filtration HPLC on a Superdex 200 10/300 GL column (1 × 30 cm, GE Healthcare Biosciences, Buckinghamshire, UK) that was equilibrated and washed with 0.15 M NaCl/50 mM phosphate buffer (pH 7.0) at a flow rate of 0.5 mL/min. Red color–related fractions were collected and subjected to HPLC on a Mono Q 5/50 GL column (5 × 50 mm, GE Healthcare Biosciences), the column was equilibrated with 50 mM phosphate buffer (pH 7.0) and developed by a linear gradient of NaCl (0–1 M over 50 min) in 50 mM phosphate buffer (pH 7.0) at a flow rate of 0.5 mL/min. At each chromatographic step, the proteins were monitored by recording A280 and the red color change was determined after heating in a 100 °C hot water bath by using a colorimeter (CLR–7100F, Shimadzu, Kyoto, Japan). The purified red color–related protein was termed as LvPBP75.

LvPBP75 was analyzed for its homogeneity by PAGE system. Native–PAGE was performed on a 12% handmade gel. SDS–PAGE was carried out on a 5–20% precast gel (Atto, Tokyo, Japan) with an AE–7300 (Atto, Japan) compact PAGE system.

Before SDS–PAGE, LvPBP75 was mixed with an equal volume of 0.125 M Tris–HCl buffer (pH 6.8) containing 4% SDS and 10% 2–mercaptoethanol and heated in a boiling water bath for 5 min. After being run, the gel was stained with a Rapid Coomassie Brilliant Blue (CBB) R–250 (Kanto Chemical Co., Inc. Tokyo, Japan), and Precision Plus Protein Standards (Bio–Rad Laboratories, Hercules, CA, USA) were used as a reference.

The molecular mass of non–denatured LvPBP75 was determined by gel filtration HPLC using a TSKgel G3000 SW_{XL} column (0.78 × 30 cm, Tosoh, Tokyo, Japan) with 0.15 M NaCl/50 mM phosphate buffer (pH 7.0) at a flow rate of 0.5 mL/min and monitored by recording A280. Five reference proteins were used to calibrate the column: β–amylase (200 kDa), alcohol dehydrogenase (150 kDa), albumin (66 kDa), carbonic anhydrase (29 kDa), and cytochrome C (12.4 kDa) (Sigma–Aldrich, St. Louis, MO, USA). The molecular mass of denatured LvPBP75 was determined by SDS–PAGE as described above.

2.2.3 In–gel digestion and peptide mass fingerprinting (PMF) analysis of LvPBP

Peptide mass fingerprinting (PMF) analysis of LvPBP75 was performed according to the method of Li et al. (2012) with slight modifications. The LvPBP75 spot was manually cut from the SDS–PAGE gel that was stained with CBB solution and incubated in 10 mM DTT (Dithiothreitol)and 55 mM IAA (Iodoacetamide) in the dark for 30 min. Next, the gel pieces were de–colorized in solution A (50 mM NH_4HCO_3: CH_3OH, 1:1) and followed by solution B (50 mM NH_4HCO_3: Acetonitrile, 1:1) for 15 min. The gel pieces were then dehydrated with 100% acetonitrile and subsequently rehydrated with 20 ng/μL trypsin for 30 min on ice. 50 mM NH_4HCO_3 was added after removing the supernatant. The digestion was performed at 37 °C for 16 h and subsequently stopped by adding 0.2% TFA. The digestion liquid was collected and then subjected to a 4800 Plus MALDI–TOF/TOF Analyzer (AB SCIEX, Redwood City, CA, USA). PMF data were collected using reflective and positive ion

modes, with a mass range of 800–4000 Da. The collected data were submitted to search for candidate proteins using MASCOT software (http://www.matrixscience.com). MS spectra were searched in the SwissProt/NCBInr database using the following search parameters: fixed modification, carbamidomethylation; variable modification, methionine oxidation; mass values, monoisotopic; peptide mass tolerance, ± 0.2 Da; max missed cleavages, 1. MASCOT research score of greater than 91 was considered statistically significant ($p < 0.05$).

2.2.4 Pigment analysis of LvPBP

The pigments released from cooked LvPBP75 were extracted based on the method of Yanar et al. (2004) with some modifications. After heating, the red colored precipitate was collected by centrifugation at 10,000 × *g* for 10 min at room temperature. Then it was mixed with equal amounts of anhydrous sodium sulfate and soaked into 5 mL acetone overnight. The mixture was homogenized and centrifuged at 10,000 × *g* for 10 min. The UV–visible absorption spectra of uncooked LvPBP75 and acetone extract were determined by a micro–volume spectrophotometer from 220 to 800 nm (BioSpec–nano, Shimadzu, Kyoto, Japan).

2.2.5 Analysis of protein color change

Investigation of the color change of the proteins derived from shrimp shell was performed by heating at temperatures of 30, 45, 60, 80, and 100 °C for 10 min. Unheated samples were set as controls. Temperatures and color changes were monitored and recorded. Color changes were investigated by using the colorimeter (CLR–7100F). The results are expressed as L* (brightness), a* (+a red, –a green), and b* (+b yellow, –b blue).

2.2.6 Statistical analysis

All measurements were conducted in triplicate and expressed the results as the

mean ± SD of three parallel measurements. Data were subjected to one–way ANOVA, followed by Student's t–test using JMP version 10.0 (SAS Institute Inc., Cary, NC, USA) and differences were considered statistically significant at $p < 0.05$.

2.3 Results

2.3.1 Isolation and color change of different soluble proteins

As shown in Fig. 2–1A, the molecular weight of water–soluble proteins were located in 3 parts, 55–100, 35–45 and lower than 30 kDa. Salt–soluble proteins showed almost the same bands with water soluble parts except 210 kDa band. Two obvious bands with the molecular weight around 35 and 27 kDa were found in acidic soluble parts. In alkaline soluble parts, 210, 75 and 45 kDa protein bands can be observed. After heat treatment at 100 °C, the L* values of the water– and salt–soluble extracts decreased significantly ($p < 0.05$). Both the a* and b* values in the water–soluble extract changed significantly to the redness and yellowness scales, respectively ($p < 0.05$) (Fig. 2–1B, Table 2–1). In the salt–soluble extract, the b* value changed significantly to the blueness scale after heat treatment ($p < 0.05$). No significant color change was observed ($p > 0.05$) in either acidic– or alkaline–soluble extracts (Table 2–1). The results suggested that non–water–soluble proteins have no effect on the red color change on shrimp surface. The possible explanation for the shell color change in salt, acidic, or alkaline solution is that the red color change was mainly produced by water–soluble proteins, and it was accelerated by the salt, acid, or alkaline in some way. Hence, the red color–related proteins were preliminarily located in the water–soluble fraction. Total 178.75 mg of water soluble protein was obtained from 25 g shell calculated by the calibration curve (Fig. 2–2). The salt–, acidic, and alkali–soluble proteins were calculated to be 26.14, 24.39 and 46.74 mg, respectively.

To confirm the red color change of the water–soluble extraction, the crude water–soluble extract was subjected to thermal treatment of 30, 45, 60, 80, and 100 °C for 10 min. Regarding the color change of the crude water–soluble extract, the L*

value decreased significantly with increasing temperature ($p < 0.05$). Meanwhile, the a* and b* values of unheated samples were initially low negative values or near one, respectively, and increased significantly in both the redness and yellowness scales ($p < 0.05$) with increasing temperature (Table 2–2).

2.3.2 Purification and identification of LvPBP

Proteins with molecular weights from 45–140 kDa disappeared with increasing temperature (Fig. 2–3). Meanwhile, slight changes were observed in the proteins located less than 45 kDa. Therefore, proteins ranged from 45–140 kDa were selected for further purification.

The red color–related protein was obtained by ammonium sulfate precipitation and subsequently purified by two–step column chromatography. Gel filtration HPLC yielded five different protein peaks, and the red color–related fraction was eluted at retention times between 20 and 25 min (Fig. 2–4A). Finally, the red color–related protein was purified by HPLC using a Mono Q 5/50 GL anion–exchange column, in which it appeared between retention time of 28 to 31 min with 0.39 M NaCl (Fig. 2–4B). SDS–PAGE analysis showed that the pure red color–related protein had a molecular mass of ~75 kDa (Fig. 2–4C). Therefore, it was termed as LvPBP75 (*L. vannamei* pigment–binding protein with molecular mass ~75 kDa). 2.44 mg of red color–related protein was purified from 178.75 mg crude water–soluble fraction.

LvPBP75 showed a major single peak at a retention time of 26 min as analyzed by gel filtration HPLC on a TSK gel G3000SW$_{XL}$ column, and its molecular mass was calculated to be ~72 kDa (Fig. 2–5A), which is concordant with the results of SDS–PAGE (Fig. 2–4C). In native–PAGE analysis, LvPBP75 afforded only one band (Fig. 2–5B). These results indicating that LvPBP75 was a homogeneous monomer.

The color change of LvPBP75 was determined by heating the solution at different temperatures. The results showed that the initial color change of the complex occurred at 30 °C. However, no significant changes were observed when heated at 60 °C.

Within the increasing of heating temperatures, the a* and b* values increased significantly in both the redness and yellowness scales when compared with the control and low–heat treatments (Table 2–3).

Analysis of LvPBP75 was performed by PMF analysis using MALDI–TOF–MS. The mass numbers of the peptides obtained from the digestion of LvPBP75 ranged from 842.49–3248.57 (Fig. 2–6A). Of these digested peptide fragments, 11 (fragments 1–11 in the order of corresponding position of LvPBP75) were sequenced (Table 2–4). A protein that named hemocyanin (GenBank accession number: CAA57880), which has a nominal mass of ~74,992 Da and a calculated pI of 5.27, matched LvPBP75 with a maximum score of 109.

In the experiment of pigment confirmation, the absorption spectrum of acetone extract from the precipitate of heated LvPBP75 is typical of astaxanthin with absorption maxima at 481 nm (Fig. 2–6B).

2.4 Discussion

Pigment–binding proteins derived from different crustacean species have different molecular masses. In the lobster shell, they range from 40–90 kDa (Buchwald & Jencks, 1968; Simpson et al., 1993). However, Wade et al., (2012) reported that the proteins found in black tiger shrimp (*Penaeus monodon*) ranged from 21–100 kDa. Cremades et al. (2003) separated two different types of pigment–binding proteins, carotenoprotein–1 and carotenoprotein–2, from crayfish (*Procambarus clarkii*) by–products by using a solid filtration method. Carotenoprotein–1 has molecular mass from less than 10 kDa to more than 400 kDa. Meanwhile, carotenoprotein–2 comprises two main proteins weighing 40 and 22 kDa, respectively, followed by a series of proteins with small molecular masses. Extraction methods can also affect the molecular masses of pigment–binding proteins. Klomklao et al. (2009) extracted carotenoprotein from *P. monodon* shells with the aid of bluefish trypsin. The

predominant 211 kDa protein band vanished entirely, but the 45 kDa band remained and appeared as the major protein. In contrast, Senphan et al. (2014) report that the 45 kDa protein derived from *L. vannamei* shell disappeared completely with the aid of proteases extracted from the hepatopancreas of the same species. In our study, the appearance of red color corresponded with the disappearance of proteins ranging from 40–140 kDa (Fig. 2–3 & Table 2–1). This may be due to the differences of proteins and pigments that make up the pigment–binding proteins. Besides, the complexes weighing more than 100 kDa may correspond to the aggregates of myofibrillar–like proteins, and the small compounds weighing less than 45 kDa may correspond to some free amino acids, oligopeptides or dissociations of large–sized proteins (Cremades et al., 2003; Elizabeth et al., 2009; Gamiz–Hernandez et al., 2015). Pure protein was finally eluted using anion exchange HPLC with 0.39 M NaCl between retention times of 28 and 31 min (Fig. 2–4B), which is concordant with the separation results of β–crustacyanin from South African lobster, *Jasus lalandii* (Elizabeth et al., 2009).

Pigment–binding proteins derived from different crustacean species show different relationships with the red color change. Elizabeth et al. (2009) found two main pigment–binding proteins with molecular masses around 40 and 300 kDa from *J. lalandii* shell, respectively. They exhibited a reversible color change after removing their pigment group. The color change of both proteins started at 45 °C, and complete denaturation occurred at 70 °C. Moreover, a noticeable bathochromic shift was observed at 85 °C. Ando et al. (2014) determined the improvement of red color development on the surface of kuruma prawn (*Marsupenaeus japonicus*). Significant red color change required a minimum heating temperature of 60 °C. In our study, the initial red color change of LvPBP75 occurred at about 30 °C, and the red color change increased significantly with increasing temperature. Significant red color change was detected around 80 °C (Table 2–3). In the pigment–binding protein, covalent bonds between protein and pigment are some of the most important chemical bonds that maintain its conformational stability (Buchwald & Jencks, 1968; Cianci et al., 2002; Chayen et al., 2003). Once the covalent bonds have been destroyed, which releases

pigments from the denatured proteins, a red color change can be detected. Furthermore, the denatured proteins can protect the un–denatured part from heating before the temperature reaches a critical point. Significant color changes of the red color–related proteins derived from different crustacean species are detected at various heating temperatures, suggesting that these proteins may possess different structural characteristics.

The majority of crustaceans and crustacean tissues attribute their coloration to the presence of carotenoprotein, which is consisted of proteins and carotenoids (Castillo et al., 2013; Matsuno, 2001; Maoka, 2011). It was reported that the predominant carotenoid in crustacean species was free and esterified forms of astaxanthin (ATX). As the major carotenoid in crustacean tissues, ATX performs various functions that include pigmentation, photoprotection, antioxidant and a source of vitamin A. Among these functions, the best–established function was reported to be pigmentation (Liñán–Cabello et al., 2002; Niu et al., 2014), the coloration of crustacean was correlated with the distribution and amount of ATX and carotenoproteins in crustacean tissues (Ribeiro et al., 2001; Sachindra et al., 2005). Crustacyanin, a pigment–binding protein consists of apoprotein and ATX, is linked to the production and modification of lobster colors (Wald & Nathanson, 1948; Zagalsky, 1985; Elizabeth et al., 2009; Wade et al., 2009). Interestingly, our results show that the red color change of *L. vannamei* shell corresponds with a novel pigment–binding protein that consists of hemocyanin (Fig. 2–6). However, hemocyanin is considered a respiratory protein and is well known for its oxygen transportation and inner defense functions (Paul & Pirow, 1997). The possible explanation is that there's a novel function of the hemocyanin as binding with pigment, and involved in *L. vannamei* shell color change. PMF analysis provided a limited match of peptide fragments between LvPBP75 and hemocyanin (Fig. 2–6). Further studies are needed to demonstrate the relationship between *L. vananmei* shell color change and LvPBP75.

In conclusion, a novel red color–related protein (LvPBP75) was purified from the shell of *L. vannamei* using ammonium sulfate precipitation, gel filtration, and anion

exchange HPLC. It had closely corresponded with *L. vannamei* shell color change under heat treatment. The temperature–sensitive and color change properties of this binding protein show potential use as an edible temperature indicator in food processing area. However, the information on its structural and red color change properties is very limited. In next chapter, 1) to confirm the result of PMF analysis, the primary structure of LvPBP75 was studied, 2) to illuminate the relationship between LvPBP75 and red color change, the secondary structure and thermal properties of LvPBP75 were studied.

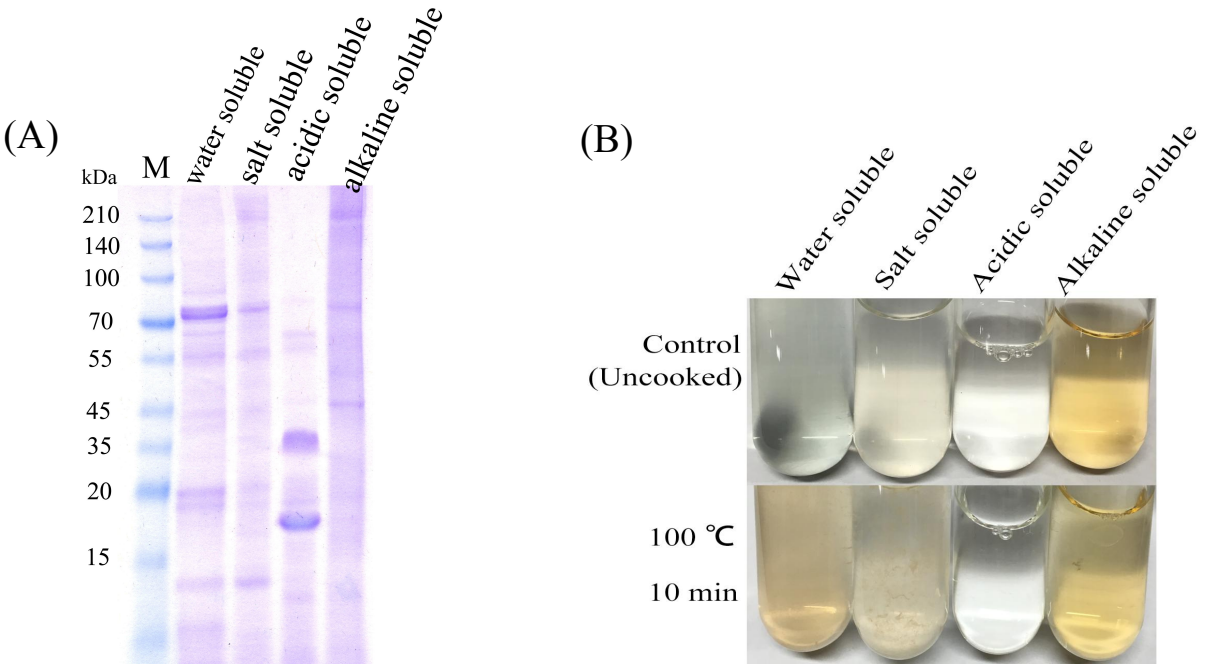

Figure 2–1 (A) Protein files of different soluble proteins extracted from *L. vannamei* shell (Lane M: protein marker). (B) Color changes of different soluble proteins from *L. vannamei* shell after heat treatment at 100 ºC for 10 min.

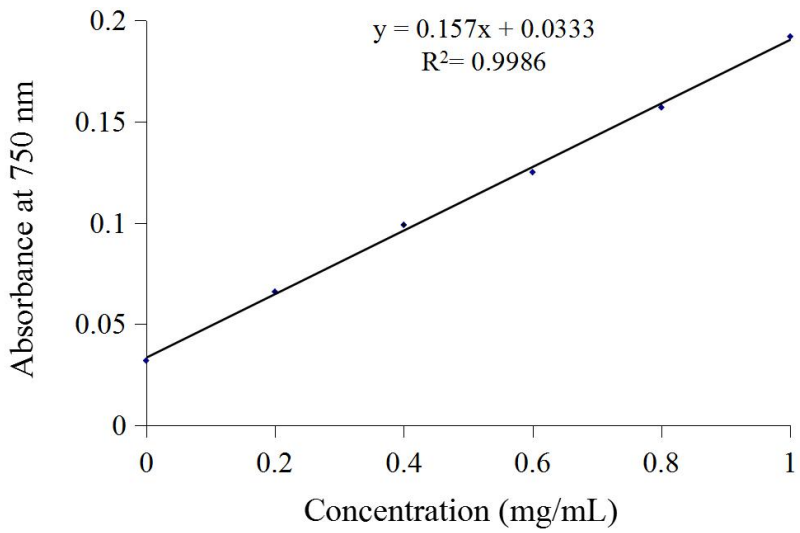

Figure 2–2 Calibration curve for the determination of protein concentration.

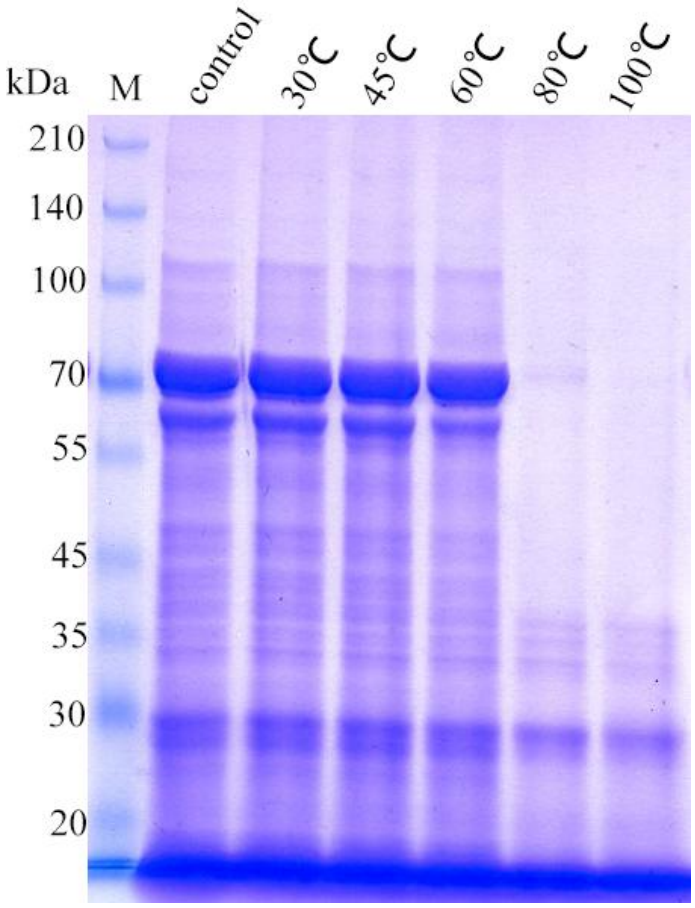

Figure 2–3 Effect of heating temperature on crude water–soluble proteins derived from *L. vannamei* shell (Lane M: protein marker).

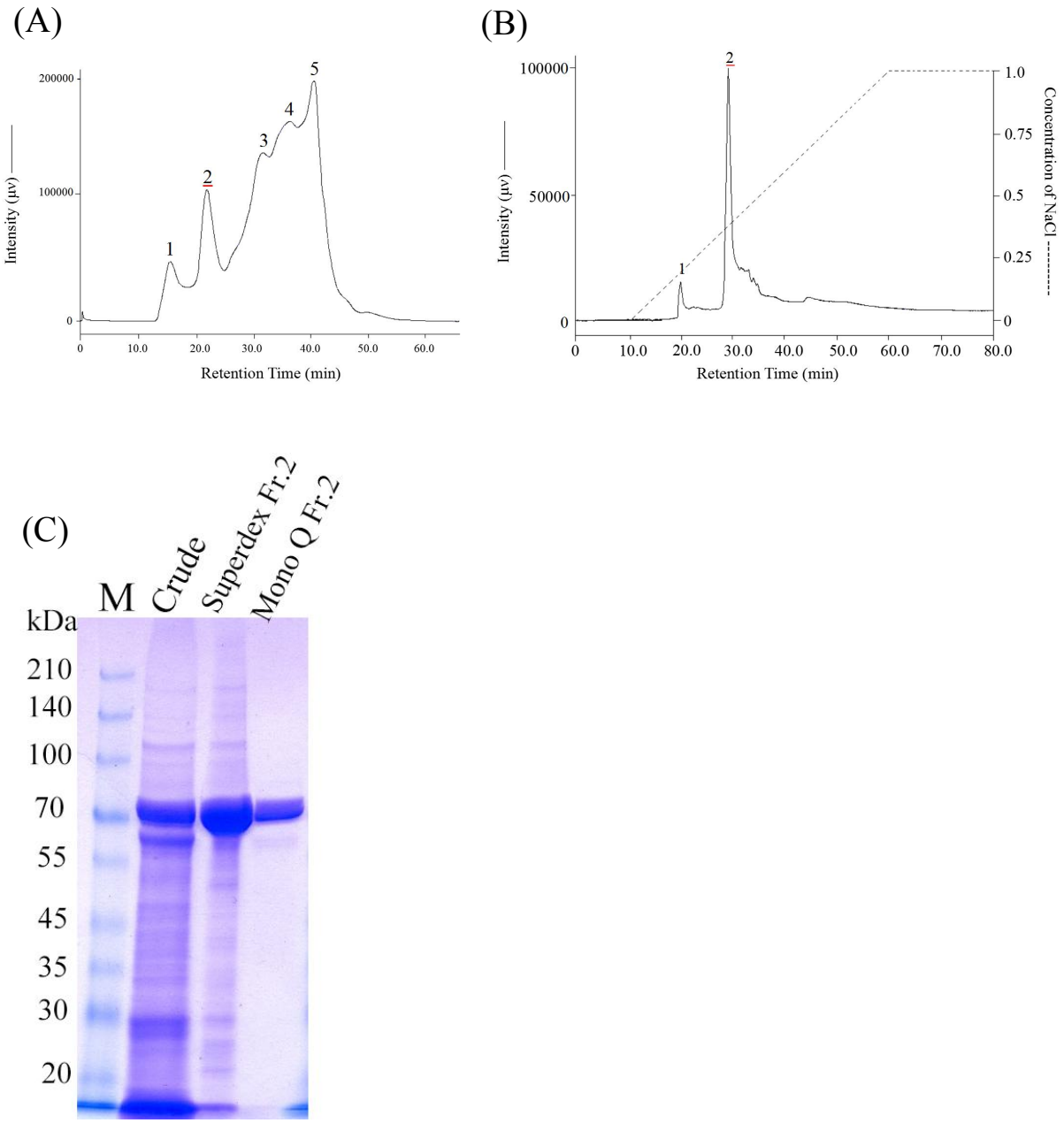

Figure 2–4 Purification of red color–related protein by gel filtration HPLC (A) and anion–exchange HPLC (B). (A) Crude proteins obtained by 60% ammonium sulfate were applied to a Superdex 200 gel filtration column. (B) The red color–related fraction (Fr. 2) from the Superdex 200 column was applied to a Mono Q column. (C) SDS–PAGE on a 5–20% precast gel (Lane M: protein marker).

(A) (B)

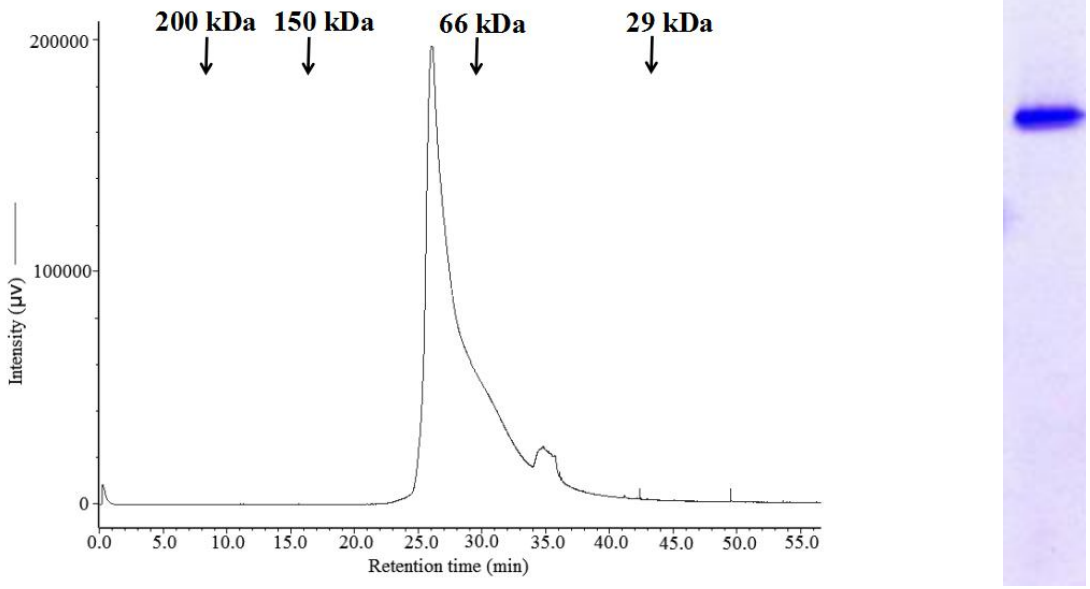

Figure 2–5 (A) HPLC of LvPBP75 on a TSK gel G3000SW$_{XL}$ column. The following proteins were used as a reference: 1, β–amylase (200 kDa); 2, alcohol dehydrogenase (150 kDa); 3, albumin (66 kDa); 4, carbonic anhydrase (29 kDa); 5, cytochrome C (12.4 kDa). (B) Native–PAGE on a 12% hand–made gel.

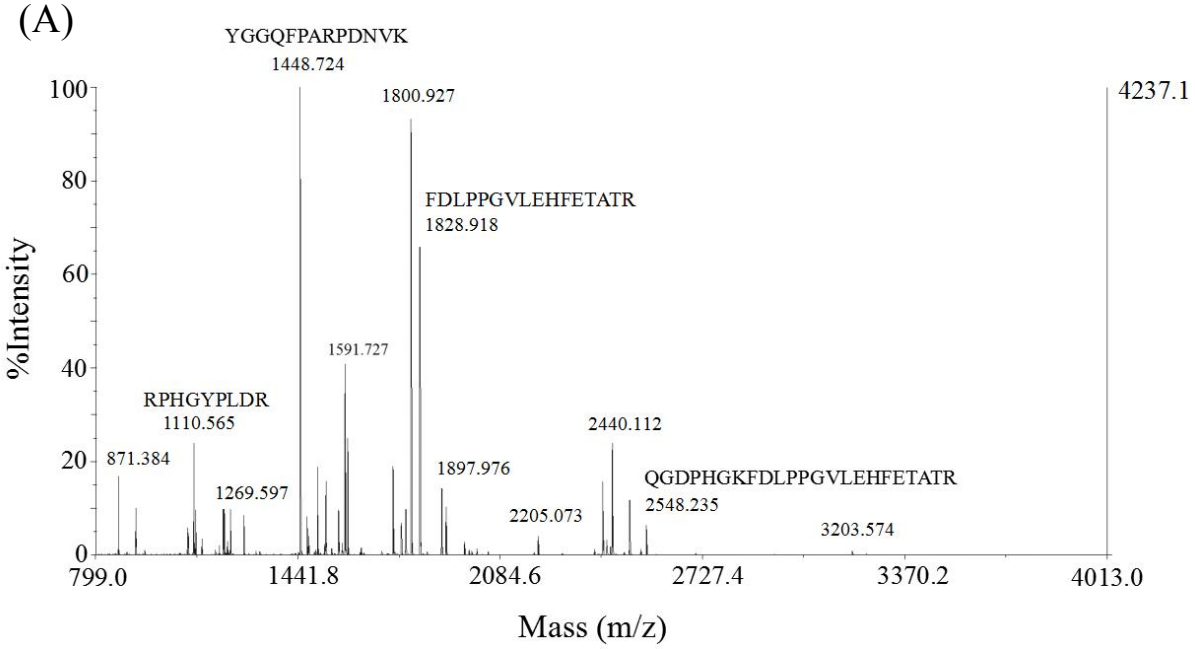

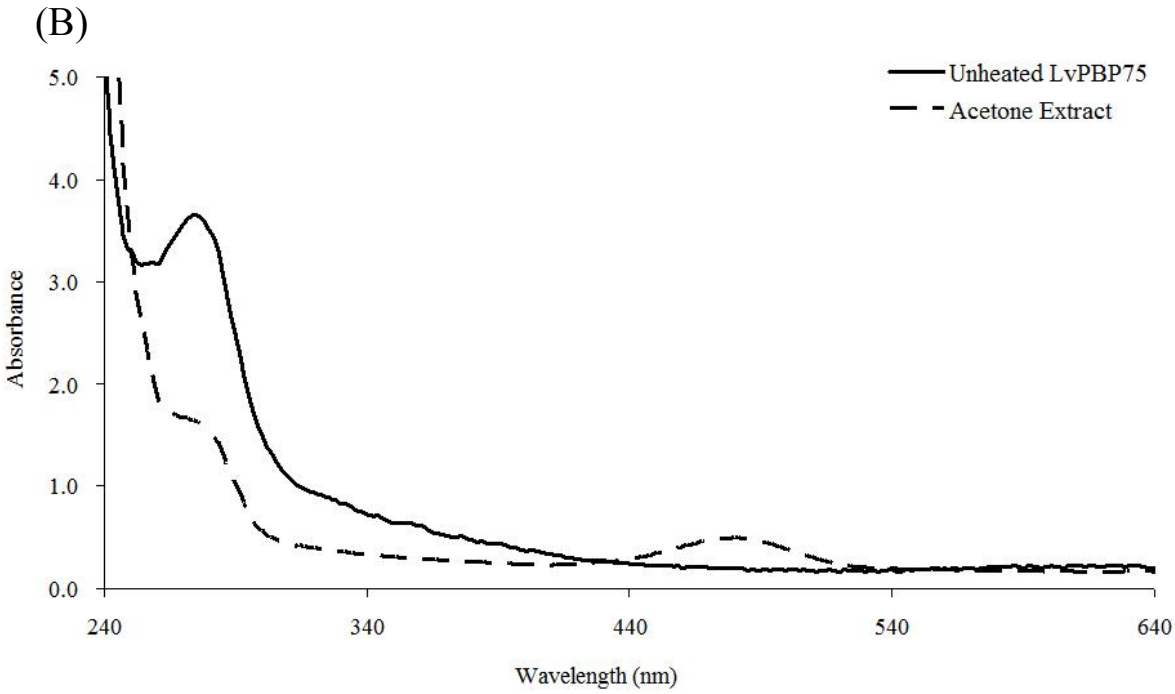

Figure 2–6 (A) Spectrum of peptide mass fingerprinting analysis of the 75–kDa band (m/z: mass numbers/charge numbers). (B) Absorption spectra of the unheated LvPBP75 and acetone extract from the precipitate of heated LvPBP75.

Table 2–1 Color change of different soluble proteins

	Water–soluble		Salt–soluble		Acidic–soluble		Alkaline–soluble	
	Unheated	Heated	Unheated	Heated	Unheated	Heated	Unheated	Heated
L*	5.84 ± 0.014[a]	5.17 ± 0.014[b]	2.83 ± 0.017[a]	1.82 ± 0.024[b]	4.95 ± 0.005[a]	5.03 ± 0.045[a]	5.40 ± 0.022[a]	5.59 ± 0.033[b]
a*	–0.56 ± 0.005[a]	0.01 ± 0.005[b]	0.16 ± 0.012[a]	0.14 ± 0.029[a]	–0.29 ± 0.012[a]	–0.30 ± 0.019[a]	–0.19 ± 0.012[a]	–0.21 ± 0.012[a]
b*	0.76 ± 0.016[a]	2.27 ± 0.014[b]	1.74 ± 0.021[a]	1.26 ± 0.045[b]	0.92 ± 0.025[a]	0.93 ± 0.029[a]	2.82 ± 0.029[a]	2.87 ± 0.017[a]

(Means followed by different lower–case letters within the same protein solutions differ significantly at $p < 0.05$ versus unheated samples. Data are expressed as mean ± standard deviation, n = 3)

Table 2–2 Color change of crude water–soluble proteins

Temperature (°C)	L*	a*	b*
25 (control)	6.84 ± 0.000[a]	–0.38 ± 0.005[a]	1.15 ± 0.005[a]
30	6.75 ± 0.005[b]	–0.34 ± 0.005[b]	1.11 ± 0.005[b]
45	6.04 ± 0.005[c]	–0.22 ± 0.005[c]	1.47 ± 0.009[c]
60	5.20 ± 0.005[d]	0.05 ± 0.005[d]	1.83 ± 0.004[d]
80	3.79 ± 0.005[e]	0.03 ± 0.000[e]	2.09 ± 0.005[e]
100	2.84 ± 0.005[f]	0.33 ± 0.000[f]	3.52 ± 0.000[f]

(Means followed by different lower–case letters within the same column differ significantly at $p < 0.05$ versus the control. Data are expressed as mean ± standard deviation, n = 3)

Table 2–3 Color change of LvPBP75 under different heating temperatures

Temperature (°C)	L*	a*	b*
25 (control)	6.76 ± 0.014[a]	–0.35 ± 0.009[a]	1.16 ± 0.009[a]
30	6.70 ± 0.009[b]	–0.31 ± 0.012[b]	1.20 ± 0.009[ab]
60	6.67 ± 0.012[b]	–0.28 ± 0.008[b]	1.22 ± 0.022[b]
80	3.76 ± 0.009[c]	0.16 ± 0.012[c]	1.53 ± 0.017[c]
100	3.38 ± 0.021[d]	0.21 ± 0.012[d]	1.75 ± 0.012[d]

(Means followed by different lower–case letters within the same column differ significantly at $p < 0.05$ versus the control. Data are expressed as mean ± standard deviation, n = 3)

Table 2–4 Amino acid sequences of LvPBP75 peptide fragments identified by MALDI–TOF–MS

Peptide	Sequence	Corresponding position of LvPBP75*
1	HWFSLFNTR	84–92
2	NEALMLFDVLIHCKDWASFVGNAAYFR	95–121
3	KGENFFWIHHQLAVR	230–244
4	LSNYLDPVGELQWNKPIVDGFAPHTTYKYGGQF PARPDNVKFEDVDDVAR	250–299
5	DMVIVESRIRDAIAHGYIVDSEGK	302–325
6	QGDPHGKFDLPPGVLEHFETATR	368–390
7	LNHKEFTFRIDVENGGAERLATVRIFAWPHKDNN GIEYTFDEGR	469–512
8	FESATGLPNR	566–575
9	RPHGYPLDR	625–633
10	VFEDLPNFK	640–648
11	VFNHGEHIH	654–662

(*: the number of amino acid residue of LvPBP75 refers to Chapter 3 Fig. 3–6)

Chapter 3 Structural and thermal properties of red color–related protein LvPBP

3.1 Introduction

Crustacean shell color change was shown to be determined by crustacyanin (a pigment–binding protein formed by apoprotein and astaxanthin) and the interaction between pigments and proteins (Wade et al., 2008; Michael et al., 2009; Parisenti et al., 2011; Reszczynskaab et al., 2015). In nature, pigment–binding proteins can be influenced by many factors, like amount of carotenoids in the daily diet, background substrate color, light intensity, water quality, and growth stage (Palma & Steneck, 2001; Chayen et al., 2003; Wade et al., 2008, 2009, 2012). It was reported that American lobster (*Homarus americanus*) shell color is mainly influenced by ultraviolet light; moreover, in the absence of ultraviolet light, lobster shell matches the background color after long–term exposure (Michael et al., 2009). Meanwhile, the mechanism of shell color change in prawn (*Penaeus monodon*) has been reported to strongly correlated with the background substrate color (Wade et al., 2012, 2017). In addition, study on the different body color of burrowing crab (*Neohelice granulata*) revealed that the colors are determined by its habitat (Casariego et al., 2011). Furthermore, crustacean shell colors are associated with body size, molting stage, and migration (Yanar et al., 2004; Zadorozhny et al., 2008). When crustaceans are cooked, their shell colors are influenced by storage conditions, heating temperatures, processing methods, and food additives (Brookmire et al., 2013; Ando et al., 2014; Huang et al., 2016). Even though crustacean shell color change is associated with the release of pigment from denatured pigment–binding proteins, but their structural and thermal properties were reported to be differ among crustacean species (Nur–E–Borhan et al., 1995; Velu et al., 2003; Porter et al., 2009; Begum et al., 2015).

In this chapter, the study was aimed to elucidate: 1) primary structure of the pigment–binding protein in LvPBP75 by using cDNA cloning, 2) secondary structure

of LvPBP75 by using circular dichroism (CD) spectroscopy, 3) thermal characterization of LvPBP75.

3.2 Materials and Methods

3.2.1 Materials

Eighty Pacific white shrimp (*Litopenaeus vannamei*) with 2.0 g in body weight, and 6 cm in body length were collected in living status from a farm in Myoko City, Niigata prefecture, Japan. They were transported to the lab and acclimated in tanks containing aerated artificial seawater (2.5%) for 24 h before use.

3.2.2 Primer design

Nucleotide sequences of the degenerate and gene–specific primers designed in this study are summarized in Table 3–1. First, hemocyanin amino acid sequences from *L. vannamei* (AHN85635), *P. monodon* (AEB77775), *Fenneropenaeus chinensis* (ACM61982), *F. merguiensis* (AGT20779), *Marsupenaeus japonicus* subunit L (ABR14693), *M. japonicus* subunit Y (ABR14694) were aligned to search the conservative peptide sequences. The peptide fragments obtained from MALDI–TOF–MS were highlighted with bold red (Fig. 3–1). Then, hemocyanin nucleotide sequences from *L. vannamei* (X82502), *P. monodon* (JF357966), *F. chinensis* (FJ594414), *F. merguiensis* (KC920897), *M. japonicus* subunit L (EF375711) and subunit Y (EF375712) were aligned. Finally, two internal primers (Inter–F and Inter–R) were designed based on the highly conserved zone of nucleotide sequence (Fig. 3–2), which is corresponded to the amino acid regions of $^{Phe}270$–$^{Tyr}278$ and $^{Val}381$–$^{Thr}389$ (numbering in this chapter is on the basis of the amino acid sequence of LvPBP75 shown in Fig. 3–6). The other gene–specific primers were all designed based on the determined nucleotide sequences.

3.2.3 RNA extraction and cDNA synthesis

Total RNA was isolated from the epithelium (about 500 mg) with 5 mL TRIzol reagent (Invitrogen, Carlsbad, CA, USA) and digested with recombinant DNase I (RNase–free, Takara, Otsu, Japan) to remove the possible genomic DNA contamination. Poly A^+ RNA was isolated from total RNA using Oligotex–dT 30 (super) mRNA purification kit (Takara, Otsu, Japan) according to the manufacturer's instructions and then concentrated by using NucleoTrap mRNA Mini Kit and NucleoSpin RNA Clean–up XS Kit (Macherey–Nagel, Duren, Germany), respectively.

Synthesis of double–strand and adaptor–ligated cDNA was performed by 1 μg of poly A^+ RNA with a Marathon cDNA Amplification Kit (Clontech, Mountain View, CA, USA) according to the manufacturer's introductions and applied to full–length cloning as a template.

3.2.4 Cloning of full–length cDNA encoding LvPBP

The cDNA amplification strategy of LvPBP75 was showed in Fig. 3–3. The encoding cDNA of LvPBP75 was obtained by two steps of PCR amplification. Firstly, a pair of primers Inter–F and Inter–R were used to amplify the internal cDNA sequence. Amplification conditions were: pre–incubation at 94 °C for 5 min, followed by 35 cycles of: 30 s at 94 °C, 30 s at 63 °C and 1 min at 72 °C, with the final extension step at 72 °C for 7 min. Secondly, the full–length cDNA of LvPBP75 was obtained according to the procedures of rapid amplification of cDNA ends method. Briefly, the 5'–and 3'–end amplifications were performed using the set of adaptor primers (AP1: CCATCCTAATACGACTCACTATAGGGC) with Gsp–F (3'–end) and Gsp–R (5'–end), respectively. PCR thermal cycling conditions were 94 °C for 30 s, 30 cycles of 94 °C for 5 s, 72 °C for 3 min. All amplifications were carried out using Ex Taq polymerase (Takara, Otsu, Japan).

Amplified products were subcloned into the pGEM–T easy vector (Promega, Masison, WI, USA) and sequenced using a BigDye Terminator v3.1 Cycle Sequencing Kit and an ABI 3130 Genetic Analyzer (Applied Biosystems, Foster City, CA, USA).

Sequence data were analyzed by Seq Ed Version 1.0.3 software (Perkin Elmer, Foster City, CA, USA). The LvPBP75 cDNA sequence was generated by overlapping the three fragments. A pair of primers 5'–Gsp and 3'–Gsp were used to confirm that the assembled sequence was corresponded to a single transcript.

3.2.5 Bioinformatic analysis

The cDNA sequence and deduced amino acid sequence were analyzed using DNAMAN 8 (Lynnon Biosoft, CA, USA). The open reading frame (ORF) was identified using ORF Finder at NCBI (http://www.ncbi.nlm.nih.gov/projects/gorf/), and sequence similarity was searched using BLAST program (http://blast.ncbi.nlm.nih.gov/). Sequence alignment among *L. vannamei* hemocyanin subunits was performed using ClustalW program (http://clustalw.ddbj.nig.ac.jp). Secondary structure prediction was obtained using the Secondary Structure Consensus webware tool combined three different prediction methods (MLRC, DSC, and PHD) (https://npsa–prabi.ibcp.fr/). The prediction of functional sites or domains of the deduced amino acid sequence was performed using the PROSITE program (http://www.expasy.org/prosite) and InterPro program (http://www.ebi.ac.uk/interpro/). Transmembrane segments were analyzed using TMPred program (http://http://embnet.vital–it.ch/software/TMPRED). The signal peptide of LvPBP75 was determined using the software SignalP 4.0 (http://www.cbs.dtu.dk/servies/SignalP).

3.2.6 Circular dichroism (CD) spectroscopy analysis

Investigation of the changes of secondary structure of LvPBP75 was performed by using a circular dichroism (CD) spectropolarimeter (J–725, JASCO, Tokyo, Japan) based on the description of Sreerama & Woody (2004) and Greenfield (1996) with some modifications.

Spectra in the far UV region (200–260 nm) was recorded using a suprasil quartz

cell with a path length of 2 mm (T–11–UV–2) at room temperature. The resolution ratio was set at 0.1 nm, while the scanning speed was 50 nm/min, and the band width and response were 1.0 nm and 1.0 s, respectively. All of the spectra were measured against the baseline corrected using the phosphate buffer, and presented as an average of three independent scans and expressed in moore ellipticity. The changes of secondary structure contents of LvPBP75 under different heating treatments were determined using the CDSSTR program of the CDPro package (http://sites.bmb.colostate.edu/sreeram/CDPro/).

3.2.7 Thermal properties of LvPBP

The effects of ion strength, pH, and alcohol on the thermal properties of LvPBP75 were studied in this part. The concentration of LvPBP75 was first adjusted to 0.5 mg/mL using 20 mM phosphate buffer (pH 7.0) and then separated into three groups. In the first group, different concentrations of NaCl (0.01, 0.05, 0.1, 0.5, and 1.0 M) were added for the study on effect of ion strength. In the second group, protein solution was adjusted to different pHs (3, 4, 5, 6, 8, 9, 10, and 11) using 0.5 M CH_3COOH and 1.0 M Na_2CO_3, respectively. In the third group, samples were mixed with ethanol (EtOH) and methanol (MeOH) with different concentrations (10, 20, 30, 40, 50, 60, and 70%), respectively. All protein samples were heated at 30, 60, and 100 ºC for 15 min. The supernatants were collected using ultra–centrifugation at 10,000 × *g*, 20 ºC, 10 min and then subjected to a circular dichroism (CD) spectropolarimeter (J–725, Jasco) using a 2 mm quartz cell.

Color changes of heat treated samples were investigated by using the colorimeter (CLR–7100F, Shimadzu). Unheated samples were set as controls. Temperatures and color changes were monitored and recorded. The results are expressed as L* (brightness), a* (+a red, –a green), and b* (+b yellow, –b blue).

3.2.8 Statistical analysis

Statistical analysis of all data was followed with the description in 2.2.6.

3.3 Results

3.3.1 cDNA cloning and sequence analysis of LvPBP

As shown in Fig. 3–4A, a cDNA sequence of 295 bp was amplified using β–actin primers (Table 3–1) and sequence analysis revealed that it has a 100% similarity with *L. vanamei* beta actin nucleotide sequence (Data not shown), suggesting the cDNA template obtained from marathon kit is acceptable for further amplification. A partial cDNA sequence of 357 bp was amplified using primers (Inter–F & Inter–R) derived from conserved regions in the hemocyanin sequences of penaeidaes (Fig. 3–4A). Blast analysis revealed that this 357 bp region had a 99% similarity with hemocyanin family from other organisms (Fig. 3–4B). The ^{25}C was mutated from ^{1130}T of the hemocyanin that derived from hepatopancreas (KJ151291). However, these two different combinations encoded the same amino acid residue, Y (Tyrosine). In order to obtain the complete cDNA sequence and confirm the mutated nucleotide base, 5'– and 3'–end amplification were performed using primers (Gsp–R and Gsp–F) designed from the obtained partial sequence. The product lengths were 1,200 bp (3'–end amplification) and 1,100 bp (5'–end amplification), respectively (Fig. 3–5A). After overlapping the three fragments, a complete cDNA sequence (2,183 bp) of *L. vannamei* epithelium encoding hemocyanin gene was obtained, which was confirmed by 5'–Gsp and 3'–Gsp primers (Fig. 3–5B). The determined nucleotide sequence was then deposited in the GenBank/EMBL/DDBJ databases under the accession number of KY695246.

The complete cDNA sequence of LvPBP75 induced an open reading frame (ORF) of 1,986 bp by surrounded on both sides by 5' and 3' un–translated region (UTR) of 69 and 128 bp, respectively (Fig. 3–6). A putative polyadenylation signal AATAAA and poly (A) tail were found in 3'–UTR. The ORF coded for a 662 amino acid protein with a theoretical isoelectric point of 5.44 and predicted molecular weight of 74,878 Da.

Predicted signal peptide was found between segment of $^{Met}1$ and $^{Ala}20$. Arthropod hemocyanin landmark peptides corresponded to segments of $^{Tyr}197$–$^{Thr}216$ and $^{Thr}387$–$^{Phe}395$. A putative tyrosinase cooper–binding domain was displayed between segments of $^{Asp}391$–$^{Asp}402$. Predicted transmembrane domains were located between segments of $^{Leu}4$–$^{Ala}20$ and $^{Gly}127$–$^{Val}146$. The amino acid fragments 1–11 determined by MALDI–TOF–MS were all recognized (Table 2–4).

Multiple sequence alignment indicated that LvPBP75 shows a high similar identity with the hemocyanin or its subunits derived from the hepatopancreas of *L. vannamei* (Fig. 3–7). LvPBP75 shares 79.55% identity with hemocyanin derived from the hepatopancreas (AIN41163), 79.31% with subunit L1 (AHY86475), 79.64% with subunit L2 (AHY86476), 79.43% with subunit L3 (AHY86477) and 79.46% with subunit V4 (AKI81624). Based on the result of identity, the potential secondary structure was established using mLRC algorithm. The secondary structure elements were 22.36% for α–helices and 21.45% for β–strands, which was indicated by the letter "α" for α–helices and "β" for β–strands (Fig. 3–7).

3.3.2 Secondary structure of LvPBP

The α–helix, β–sheet, β–turn and random coil are the four main types of secondary structures of protein (Sreerama & Woody, 2004). Each structure has its distinctive CD spectra, α–helical proteins have two negative peaks at 222 and 208 nm and one positive peak at 193 nm, β–sheet ones possess one negative peak and one positive peak at 218 and 195 nm, respectively. β–turn shows one positive peak at 206 nm while one negative peak ranges at 180–190 nm (Clarke 2012). The changes in the CD spectra of heat–treated LvPBP75 are presented in Fig. 3–8A. The results showed that unheated LvPBP75 had two negative bands at 223 and 208 nm, indicating that it was a protein rich in α–helix conformation.

Secondary structural changes are presented in Table 3–2. It shows that the α–helix,

β–sheet, β–turn and random coil contents of unheated LvPBP75 were 51.0 ± 0.216%, 19.5 ± 0.262%, 16.4 ± 0.216%, and 13.6 ± 0.245%, respectively. Compared with unheated sample, the α–helix content of LvPBP75 decreased significantly when heated at 30 ºC ($p < 0.05$). However, the secondary structure content of LvPBP75 treated with the temperature at 30–45 ºC had minor changes, but these changes were not significant ($p > 0.05$). Once the temperature was heated over 60 ºC, the α–helix content was significantly decreased to 15.7 ± 0.262% (100 ºC), and the contents of β–sheet, β–turn and random coil were increased to 31.6 ± 0.249%, 29.6 ± 0.249%, and 22.9 ± 0.236%, respectively ($p < 0.05$). Fig. 3–8B plots the contents β–sheet, turn and random coil against the α–helix contents for the LvPBP75 complex denatured by heat treatment. It shows that the newly decreased α–helix are transformed dominantly to β–sheet and turn ($r^2 = 0.9764$, $r^2 = 0.9025$, respectively) and weaker correlation to random coil ($r^2 = 0.74$).

3.3.3 Thermal properties of LvPBP

As shown in Fig. 3–9, the α–helix content showed minor changes when only added with NaCl (Fig. 3–9A). At low heating temperatures (30 and 60 ºC), α–helix contents showed no significant change with low NaCl concentrations (0.01 and 0.05 M) when compared with high NaCl concentrations (> 0.1 M) (Fig. 3–9B and C). While heating at 100 ºC, the α–helix content decreased gradually within the increasing of NaCl (Fig. 3–9D). Color measurements revealed that a* and b* values of LvPBP75 were significantly moved to red and yellow scales ($p < 0.05$) when heated with high NaCl concentrations at the same temperatures (Table 3–3).

Slight changes of CD spectra were detected under the pHs of 6, 7 and 8 without heating (Fig. 3–10A). However, the α–helix contents decreased significantly under the pHs of 3, 4 and 5 compared with 10 and 11 (Fig. 3–10A). Elizabeth et al. (2009) reported the pigment–binding proteins derived from the shell of *Jasus lalandii* showed an immediate color change in pH below 5 or above 9 before any heat treatments. In

addition, the CD spectra of heat treated LvPBP75 decreased significantly and the decreasing ratio of acidic treated samples was sharper than alkali treated ones (Fig. 3–10B, C and D). Color measurements revealed that a* and b* values of LvPBP75 treated with acidic or alkali pHs were both significantly moved to red and yellow scales ($p < 0.05$) after heat treatments. Furthermore, these values changed significantly in acidic pH treated samples when compared with alkali pH treated ones (Table 3–4). It might be due to the ionic bond inside LvPBP75 is sensitive to any combination of the various acidic or alkaline pHs (Wang, 2007). Further studies on the identification of affected amino acids may help with illuminating the relationship between pH and color change. Further studies on the identification of affected amino acids may help with illuminating the relationship between pH and color change.

α–Helix contents of LvPBP75 changed significantly within the increasing of alcohol concentrations before heating and these changes were much more significant in MeOH group compared with EtOH group (Fig. 3–11). When heated at 100 ^{o}C, the α–helix content decreased within the increasing of alcohol concentration. Color measurements revealed that color changes could be detected in both alcohol groups before heat treatment (Table 3–5). LvPBP75 changed to pink when 20 and 30% MeOH were added, while this pink color only occurred when the EtOH concentration was reached at 30%. Furthermore, protein color changed to yellow once the MeOH concentration was over than 40%. This phenomenon can be observed in EtOH only when the EtOH concentration was higher than 60%. The possible explanation is protein denaturation could be occurred due to the formation of new hydrogen bonds between alcohol molecules and protein side chains (Matsuo et al., 2012).

3.4 Discussion

Hemocyanin is mainly known as oxygen transporter (van Holde & Miller, 1995) but also functions in many other aspects like osmotic regulation (Seidl et al., 2002) and anti–fungal defense factor (Destoumieux–Garzon et al., 2001). The hemocyanin is

synthesized mainly in tissues like hepatopancreas and hemolymph, then released into other tissues including epithelium (van Holde & Miller, 1995; Destoumieux–Garzon et al., 2001; Kronstadt et al., 2013). However, our results found that the hemocyanin which was transported into the shell does not work as an oxygen transporter but a pigment–binding function and involved into *L. vannamei* shell color change (Chapter 2). The possible explanation is the function of a protein is correlated with the organ or tissue where it exists. Hemocyanins that were reported with oxygen transportation function, innate immune function were isolated from hepatopancreas, hemolymph or blood (van Holde & Miller, 1995; Destoumieux–Garzon et al., 2001; Seidl et al., 2002). All these tissues or organs are mainly correlated with the respiration or immune functions during shrimp life history. There is no need to transport any oxygen or display any immune function in non–cell tissue like the shell. In nature status, the main function of shrimp shell is protection: calcification is known to play a major role in making the skeleton, while the organismal coloration is mainly served as communication and camouflage (Kronstadt et al., 2013). According to this principle, the hemocyanin which was transferred to the exoskeleton may active as the color change function.

PMF analysis provided a limited match of peptide fragments between LvPBP75 and hemocyanin (Fig. 2–5B). Based on the obtained peptide fragments, nucleotide sequence of LvPBP75 was determined by cDNA cloning. Typical hemocyanin characteristics including, landmark peptides of arthropod hemocyanin and a putative tyrosinase cooper–binding domain were detected in the deduced protein sequence (Fig. 3–6). A significantly high sequence similarity (~80%) is also observed between LvPBP75 and the hemocyanin or its subunits (Fig. 3–7). The results determined by PMF analysis and cDNA cloning strongly suggest that the LvPBP75 belongs to hemocyanin family.

Secondary structure contents obtained in Fig. 3–7 and Table 3–2 showed about 30% difference. The possible explanations are 1) different ways to get data. The secondary structure content of LvPBP75 was determined using the CDSSTR program

of the CDPro package. CDSSTR is a modification of singular value decomposition with variable selection (VARSLC program). In CDSSTR program, an initial data base of proteins with known spectra and secondary structures is selected and used on all of the reduced data sets to evaluate the conformation of the unknown protein. This method gives an excellent evaluation of protein conformation in solution (Greedfield, 1996; Sreerama & Woody, 2000). However, the secondary structure consensus prediction methods displayed a consensus results of the selected calculation methods. Slight differences will be produced with different calculation methods, even using the same origin data. 2) Composition of LvPBP75 itself. As reported in chapter 2, LvPBP75 is consisted of hemocyanin and astaxanthin. The prediction results were calculated based on the deduced amino acids which was not bound with any pigments. However, CD spectra showed an intact far–UV spectrum of LvPBP75, which means the pigment was tightly bound with hemocyanin. As reported, carotenoids are combined with proteins via hydrophobic sites, and association of a carotenoid pigment with a protein may result in two profound effects: change the pigment to become water–soluble and change the color of the pigment (Shahidi & Brown, 1998). In the experiment of reconstruction of crustacyanin, crustacyanin subunits–astaxanthin complex showed a bathochromic shift compared with natural curstacyanin subunits (Ferrari et al., 2012). These changes may bring structural differences to LvPBP75 without binding pigments and intact LvPBP75.

At the secondary structure level, protein denaturation is a process of losing its regular structure conformation (α–helix, β–sheet, and β–turn) and generating irregular configurations (random coil) (Greenfield, 1996; Wang, 2007). Protein is able to withstand heat treatment at a certain temperature due to the increasing of its solubility promoted by low salt concentrations. Meanwhile, the denatured proteins can protect the undenatured part from heating before the temperature reaches a critical point (Wang, 2007). In the condition of high NaCl concentrations (> 0.1 M), the Na^+ competitively bind water molecules on the surface of LvPBP75, destroying the hydration film and making proteins aggregate and precipitate under hydrophobic

interactions (Wang, 2007). These precipitated proteins are extremely sensitive to heat treatments. Besides, LvPBP75 was reported be a thermal sensitive pigment–binding protein (Chapter 2). Ionic bond, which is resulted from the neutralization of an acid and amine on side chains, is sensitive to any combination of the various acidic or alkaline pHs. Denaturation occurred by disruption of the ionic bonds is irreversible. Hydrogen bond occurs between amide groups can be disrupted by the addition of alcohols. New hydrogen bonds will be formed instead between the alcohol molecules and the protein side chains. In addition, LvPBP75 is consist of astaxanthin, a fat–soluble substance, is readily soluble in organic solvents such as acetone, alcohol, and chloroform.

In conclusion, LvPBP75 was identified as hemocyanin by cDNA cloning and PMF analysis. Our results strongly suggest a novel function of hemocyanin as binding with pigment and its involvement in *L. vannamei* shell color change. Bioinformatic analysis revealed that there were some structural differences between LvPBP75 and the hemocyanins derived from the hepatopancreas of *L. vannamei*. LvPBP75 showed significant red color change after being subjected to conditions of heat with high concentration of NaCl (> 0.1 M), acidic (< 5) or alkaline (> 9) pH, and alcohols. However, understanding on the pigment–binding ability and hemocyanin–astaxanthin interaction on LvPBP75 is limited. In next chapter, further studies are focused on the elucidation of pigment–binding ability of the hemocyanin derived from shrimp shell and its interaction with astaxanthin.

```
L.vannamei          - - - - - M R V L V V L G L V A A A A - - - - - - F Q V A S A D - - - V Q Q Q K D V L Y L L N K I  Y  36
P.monodon           M G T V N M K V L L L F A L V A A A A A W P N F G F Q S D A G G A A D A Q K Q H D V N F L L H K I  Y  50
F.chinensis         - - - - - M K V L V V L A F V A T A A A R P N L G F Q A D A A D V S D A Q K Q H D I N F L L H K I  Y  45
F.merguiensis       - - - - - M R V L V V L G L I A A A A - - - - - - F Q V V S A D - - - V Q K Q K D V L Y L L H R I  Y  36
M.japonicus subunit L - - - - - M K V L V L F A L V A A A A A W P S F G F Q S D A G G V S D A Q K Q H D I N F L L H K I  Y  45
M.japonicus subunit Y - - - - - M K V L V V L G L V A A A A - - - - - - F Q V V G A D D - - V Q K Q K D I L Y L V H K I  Y  37
                                * : * * : : : : : * : * *             * *     . . .         . * : * : *   : * : : * *

L.vannamei          G D I Q D G D L L A T A N S F D P V G N L G S Y S D G G A A V Q K L V Q D L N D G K L L E Q K H W F  86
P.monodon           G D I R D S N L K G K A D S F D P E A N L S H Y S D G G K A V Q K L M R D L K D N R L L Q Q R H W F 100
F.chinensis         G E I R D P N L K G K A D S F D P E A D L S H Y S D S G E A V H K L I R D L K D H R L L E Q N H W F  95
F.merguiensis       G D I Q D A D L L A T A N S F D P A G - - G S Y S D G G A A V Q R L L K G L N D G R L L E Q K H W F  84
M.japonicus subunit L G D I R D D A L K A K A D S F D P E A D L S H Y S D D G E A V H T L I R D L K D D R L L Q Q K H W F  95
M.japonicus subunit Y G D I Q D A D L K A T A N S F D P V A D L G I Y S D G G A A A Q R L V K D L N D G K L L Q Q K H W F  87
                      * : * :   *     . .   * : * * * *   .     .   * * * . *   * . :   * : : . * : *   : * * : * . * * *

L.vannamei          S L F N T R H R N E A L M L F D V L I H C K D W A S F V G N A A Y F R Q K M N E G E F V Y A L Y V A 136
P.monodon           S L F N P R Q R E E A L M L F D V L I H C K D W D T F V S N A A Y F R Q I M N E G E F V Y A L Y V A 150
F.chinensis         S L L S P R Q R H E A L M L F D V L I R C K D W D T F V S N A A Y F R Q R M N E G E F V Y A L Y V A 145
F.merguiensis       S L F N T R H R N E A L L L F D V L I H S S D W A T F V G N A A F F R Q K I N E G E F V Y A L Y V A 134
M.japonicus subunit L S L F N S R Q R H E A L M L F D V L I H C K D W D T F V S N A A Y F R Q R M N E G E F V N A L Y V A 145
M.japonicus subunit Y S L F N T R H R H E A L L L F D V L I H C N D W A G F V G N A A Y F R Q K M N E G E F V Y A V Y V A 137
                      * * : . . * : * . * * * : * * * * * * : . . * *     * * . * * * : * * *   : * * * * * *   * : * * *

L.vannamei          V I H S S L A E H V V L P P L Y E V T P H L F T N S E V I E E A Y R A K Q K Q T P G K F K S S F T G 186
P.monodon           V I H S P L S E H V V L P P L Y E V T P H L F T N S E V I E A A Y R A K Q T Q K P G K F K S S F T G 200
F.chinensis         V I H S P L A E H V V L P P L Y E V A P H L F T N S E D I E A A Y R A K Q T Q T P G K F Q S S F T G 195
F.merguiensis       V I H S P L T E D V V L P P L Y E I T P H L F T N S E V I E A A Y R A K Q K Q T P G K F E S T F T G 184
M.japonicus subunit L V I H S S L A E Y V V L P P L Y E V T P H L F T N S E V I E A A Y R A K Q T Q K P G K F K S S F T G 195
M.japonicus subunit Y V I H S P L A E H V V L P P L Y E I T P H P F T N S E V I E E A Y R A K Q T Q T P G K F K S T F T G 187
                      * * * . * : *   * * * * * * * * : : * *   * * * * *   * *   * * * * * * . * . * * * * : * : * * *

L.vannamei          T K K N P E Q R V A Y F G E D I G L N T H H V T W H M E F P F W W N D A Y G H H L D R K G E N F F W 236
P.monodon           T K K N P E Q R V A Y F G E D I G M N T H H V T W H M E F P F W W D D K Y S H H L D R K G E N F F W 250
F.chinensis         T K K N P E Q R V A Y F G E D I G M N T H H V T W H M E F P F W W Q D E Y S H H L D R K G E S F F W 245
F.merguiensis       T K K N P E Q R V A Y F G E D I G L N T H H V T W H M E F P F W W D D E Y G H H L D R K G E N F F W 234
M.japonicus subunit L T K K N P E Q R V A Y F G E D I G M N T H H V T W H M E F P F W W Q D K Y S H H L D R K G E N F F W 245
M.japonicus subunit Y T K K N P E Q R V A Y F G E D I G L N T H H V T W H M E F P F W W D D K Y G H H L D R K G E N F F W 237
                      * * * * * * * * * * * * * : * * * * * * * * * * * * * * : *   *   . * * * * * * * * . * * *

L.vannamei          I H H Q L T V R F D A E R L S N Y L D P V G E L Q W N K P I V D G F A P H T T Y K Y G G Q F P A R P 286
P.monodon           V H H Q L T V R F D A E R L S N Y L D P V D E L H W E K P I V Q G F A P H T T Y K Y G G Q F P S R P 300
F.chinensis         V H H H L A V R F D A E R L S N Y L D P V D E L H W E K P I V Q G F A P H T T Y K Y G G Q F P S R P 295
F.merguiensis       V H H Q L T V R F D A E R L S N Y L D P V G E L H W Y K P I V D G F A P H T T Y K Y G G Q F P A R P 284
M.japonicus subunit L V H H Q L T V R F D A E R L S N Y L D P V D E L H W E K P I V Q G F A P H T T Y K Y G G Q F P S R P 295
M.japonicus subunit Y V H H Q L T V R F D A E R L S N Y L D P V G E L Q W H K E I V E G F A P H T T Y K Y G G Q F P T R P 287
                      : * * : * : * * * * * * * * * * * * * * . * * : *   *   * * : * * * * * * * * * * * * * : * *

L.vannamei          D N V K F E D V D D V A R I R D M V I V E S R I R D A I A H G Y I V D S E G K H I D I S N E K G I D 336
P.monodon           D N V D F E D V D G V A R I R D L L I V E S R I R D A I A H G Y I V D R A G N H I D I M N E R G I D 350
F.chinensis         D N V N F E D V D G V A R I R D L L I V E S R I R D A I A H G Y I I D K Q G N R I D I M N E R G I D 345
F.merguiensis       D N V K F E D V D D V A R I R D M V I V E S R I R D A I A H G Y I I D S H G K Q I D I S N E K G I D 334
M.japonicus subunit L D N A R F E D V D G V A R I R D L L I V E S R I R D A I A H G Y I V D R E G K H I D I M N E R G I D 345
M.japonicus subunit Y D N V N F E D V D G V A R I R D M T I I E S R I R D A I A H G Y I V D S H G K H I D I N N E R G I D 337
                      * *   * * * * * . * * * * * *   * : * * * * * * * * * * * * * : *     * : : * * *   * * : * * *

L.vannamei          I L G D I I E S S L Y S P N V Q Y Y G A L H N T A H I V L G R Q G D P H G K F D L P P G V L E H F E 386
P.monodon           V L G D V I E S S L Y S P N V Q Y Y G A L H N T A H I V L G R Q S D P H G K Y D L P P G V L E H F E 400
F.chinensis         I L G D I I E S S M Y S P N V Q Y Y G A L H N T A H I V L G R Q A D P H G K Y A L P P G V L E H F E 395
F.merguiensis       I L G D V I E S S L Y S P N V Q Y Y G A L H N T A H I V L G R Q G D P H G K F D L P P G V L E H F E 384
M.japonicus subunit L V L G D I I E S S L Y S P N V Q Y Y G A L H N T A H I V L G R Q S D P H G K Y D L P P G V L E H F E 395
M.japonicus subunit Y I L G D I I E S S L Y S P N V Q Y Y G A L H N T A H I V L G R Q A D P H G K Y D L P P G V L E H F E 387
                      : * * * : * * * * : * * * * * * * * * * * * * * * * * * * * * * . * * * * *   * * * * * * * * * * *

L.vannamei          T A T R D P S F F R L H K Y M D N I F K E H K D N L P P Y T K A D L E F S G V S V T E L A V V G E L 436
P.monodon           T A T R D P S F F R L H K Y M D N I F K E H K D S L P P Y T V E E L T F A G V S V D N V A I E G E L 450
F.chinensis         T A T R D P S F F R L H K Y M D N I F K E H K D S L P P Y S K E E L T F T G V N V E N L S V D G E L 445
F.merguiensis       T A T R D P S F F R L H K Y M D N I F K E H K D S L P P Y T K A D L E F S G V S I S E V N V V G E L 434
M.japonicus subunit L T A T R D P S F F R L H K Y M D N I F K E H K D T L P P Y T A E E L T F A G V S V D S I A I E G A L 445
M.japonicus subunit Y T A T R D P S F F R L H K Y M D N I F K E H K D T L T P Y T K A D L E F A G V S I D N V A V E G E L 437
                      * * * * * * * * * * * * * * * * * * * * * * * * . * . * *   :   * * : * * . : . : : * *

L.vannamei          E T Y F E D F E Y S L I N A V D D A E G I P D V E I S T Y V P R L N H K E F T F R I D V E N G - G A 485
P.monodon           E T F F E D F E Y N L I N A V D D T E Q I P D V E I S T Y V P R L N H K D F K I K I D V S N N K G Q 500
F.chinensis         E T F F E D Y E Y S L I N A V D D T E E I A D V E I S T Y V P R L N H K D F A Y N I E V T N N N G K 495
F.merguiensis       E T Y F E D F E Y N L I N A V D D A E G I P D V D I S T Y V P R L N H K E F T F K I D I E N G - G S 483
M.japonicus subunit L E T Y F E D F E Y N L I N A V D D T E Q I P D V E I S T Y V P R L N H K D F A F K I G V S N N K G E 495
M.japonicus subunit Y E T Y F E D F E Y S L I N A V D D A E G I Q D V A I S T Y V P R L N H K E F T I K L D V K S - - D A 485
                      * : * * * : * * . * * * * * * : *   *   * *   * * * * * * * * * * : * . : :   . . .

L.vannamei          E R L A T V R I F A W P H K D N N G I E Y T F D E G R W N A I E L D K F W V S L K G G K T S I E R K 535
P.monodon           E V L A T V R I F A W P H L D N N G I E F T F D E G R W N A I E L D K F W V K L P A G T H H F E R K 550
F.chinensis         E V L T T V R I F A W P H R D N N G I E Y T F D E G R W N A I E L D K F W V K L S P G S N H I V R K 545
F.merguiensis       P R L A T V R I F A W P H K D N N G I E F T F D E G R W N A I E L D K F W V S L A G G K N S I E R K 533
M.japonicus subunit L E T L A T V R I F A W P H L D N N G I E F S F D E G R W H A I E L D K F W V K L G T G V T E I T R K 545
M.japonicus subunit Y A R L A T V R I F A W P H K D N N G I E Y T F D E G R W N A I E L D K F W V S L S S G S N A I E R K 535
                        * : * * * * * * * *   * * * * * * : : * * * * * : * * * * * * * * . *     *       :   * *
```

(Continued)

```
L.vannamei            S T E S S V T V P D V P S I H D L F A E A E A G G - - - - A G L A K F E S A T G L P N R F L L P K G 581
P.monodon             S S E S A V T V P D V P S F A T L F E K T K E A L A G A D S G L T D F E S A T G I P N R F L L P K G 600
F.chinensis           S S E S A V T V P D V P S F D T L F K K A E A A L G G G D A G L T E F E S A T G I P N R F L L P K G 595
F.merguiensis         S T E S S V T V P D V P S I D T L F A K T A A G G - - - - D G L S E F A S A T G L P N R F L L P K G 579
M.japonicus subunit L C S E S A V T V P D V P S F A T L F E K T K A A L G G A D S G L T D F E S A T G I P N R F L L P K G 595
M.japonicus subunit Y S T E S G V T V P D V P S I Q T L F D K A A A G G - - - - A G L T E Y E S A T G L P N R F L L P K G 581
                       . : * * . * * * * * * * : * * : : . * * : . : * * * * : * * * * * * * *

L.vannamei            N D R G L E F D L V V A V T D G D A D S A V P N L H E N T E Y N H Y G S H G V Y P D K R P H G Y P L 631
P.monodon             N E Q G L E F D L V V A V T D G A A D A A V D G L H E N T E F N H Y G S H G K Y P D N R P H G Y P L 650
F.chinensis           N E Q G L E F D L V V A V T D G E A D A A V E G L H D N T D F I H Y G S H G K Y P D N R P H G Y P L 645
F.merguiensis         N D K G L E F D L V V A V T D G D A D A A V P D L H L N T K Y N H Y G A N G V Y P D K R P H G Y P L 629
M.japonicus subunit L N E Q G L E F D L V V A V T D G D A D A A V A D L H Q N T D Y N H Y G A H G V Y P D K K P H G Y P L 631
M.japonicus subunit Y N E K G L E F D L V V A V T D G A A D A A V D G L H E N T E F N H Y G A Y G K Y P D N R P H G Y P L 645
                       * : : * * * * * * * * * * * * * * : * * . * * . * * . : * * * : * * * * : : * * * * * *

L.vannamei            D R K V P D E R V F E D L P N F K H I Q V K V F N H G E H I H - -                                 662
P.monodon             D R K V P D E R V F E D L P N F G H I Q V K V F N H G E Y I Q H D                                 683
F.chinensis           D R K V P D D R V F E V L P N F K H I Q V K V F N H G E H I H H H                                 678
F.merguiensis         D R R V P D E R V F E E L P N F K H I Q V K V F N H G E H I H S -                                 661
M.japonicus subunit L D R S V P D E R V F E D L P N F G H I Q V K V F N H G E H I H H D                                 678
M.japonicus subunit Y D R K V P D E R V F E E L S N F K R I Q V K V F N H G V H I E H S                                 664
                       * *   * * * : * * * *   * . * *   : * * * * * * * *   : * .
```

Figure 3–1 Alignment of the amino acid sequences of hemocyanin from different shrimp species. The peptides of LvPBP75 obtained from MALDI–TOF–MS were highlighted with bold red. The primer regions were framed. Multiple sequence alignments were performed using Clustal W. Accession numbers were (GenBank protein sequence databases): *L. vannamei*, AHN85635; *P. monodon*, AEB77775; *F. chinensis*, ACM61982; *F. merguiensis*, AGT20779; *M. japonicus* subunit L, ABR14693; *M. japonicus* subunit Y, ABR14694.

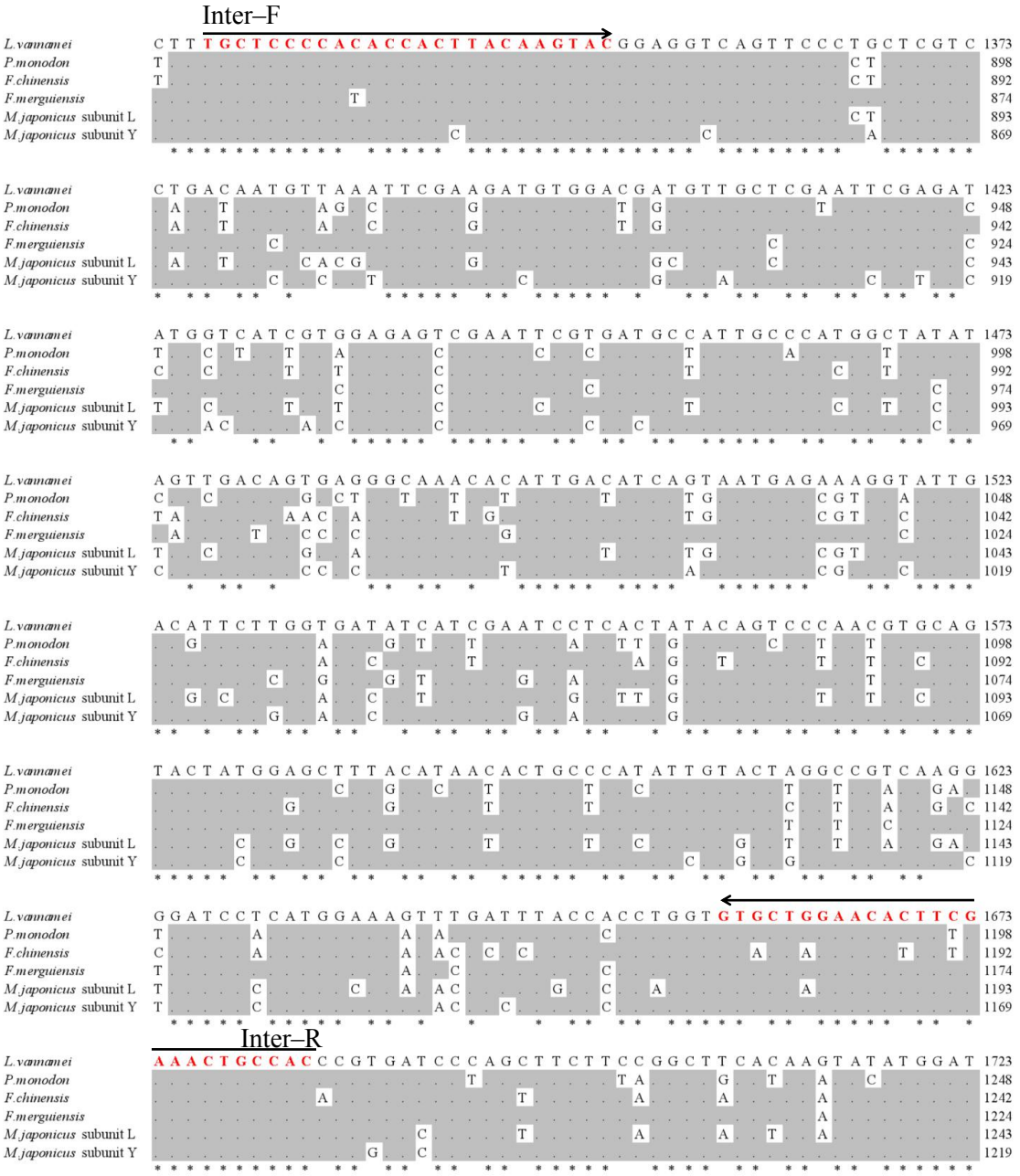

Figure 3–2 Multiple sequence alignment of nucleotide sequences of hemocyanin from different shrimp species. Multiple sequence alignments were performed using Clustal W. The positions of internal amplification primers were marked with red. Accession numbers were (GenBank nucleotide sequence databases): *L. vannamei* (X82502), *P. monodon* (JF357966), *F. chinensis* (FJ594414), *F. merguiensis* (KC920897), *M. japonicus* subunit L (EF375711) and subunit Y (EF375712).

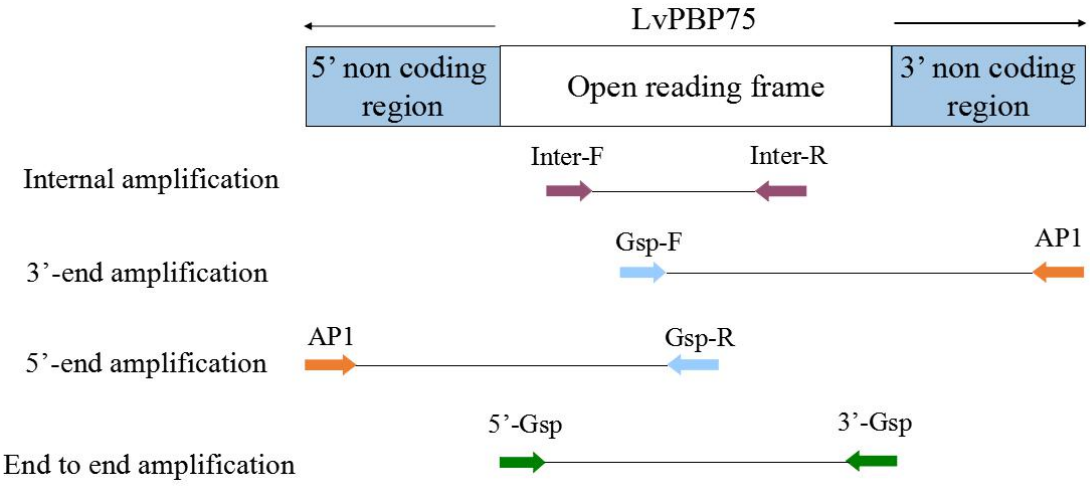

Figure 3–3 Strategy for the cDNA cloning of LvPBP75 derived from the shell of *L. vannamei* (Meaning of letters: Inter, internal amplification primer; Gsp, gene–specific primer; F, forward primer; R, reverse primer).

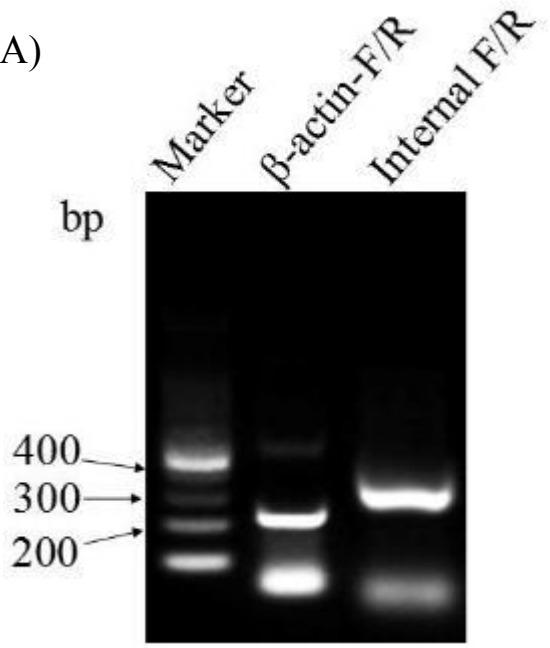

```
Query     1 T G C T C C C C A C A C C A C T T A C A A G T A C G G A G G T C A G T T C C C T G C T C G T C C T G A C A A T G T T A A   60
Sbjct  1106 . . . . . . . . . . . . . . . . . . . . . . . . T . . . . . . . . . . . . . . . . . . . . . . . . . . . . . . . . . . . 1165
            * * * * * * * * * * * * * * * * * * * * * * * *   * * * * * * * * * * * * * * * * * * * * * * * * * * * * * * * * * *

Query    61 A T T C G A A G A T G T G G A C G A T G T T G C T C G A A T T C G A G A T A T G G T C A T C G T G G A G A G T C G A A T  120
Sbjct  1166 . . . . . . . . . . . . . . . . . . . . . . . . . . . . . . . . . . . . . . . . . . . . . . . . . . . . . . . . . . . . 1225
            * * * * * * * * * * * * * * * * * * * * * * * * * * * * * * * * * * * * * * * * * * * * * * * * * * * * * * * * * * *

Query   121 T C G T G A T G C C A T T G C C C A T G G C T A T A T A G T T G A C A G T G A G G G C A A A C A C A T T G A C A T C A G  180
Sbjct  1226 . . . . . . . . . . . . . . . . . . . . . . . . . . . . . . . . . . . . . . . . . . . . . . . . . . . . . . . . . . . . 1285
            * * * * * * * * * * * * * * * * * * * * * * * * * * * * * * * * * * * * * * * * * * * * * * * * * * * * * * * * * * *

Query   181 T A A T G A G A A A G G T A T T G A C A T T C T T G G T G A T A T C A T C G A A T C C T C A C T A T A C A G T C C C A A  240
Sbjct  1286 . . . . . . . . . . . . . . . . . . . . . . . . . . . . . . . . . . . . . . . . . . . . . . . . . . . . . . . . . . . . 1345
            * * * * * * * * * * * * * * * * * * * * * * * * * * * * * * * * * * * * * * * * * * * * * * * * * * * * * * * * * * *

Query   241 C G T G C A G T A C T A T G G A G C T T T A C A T A A C A C T G C C C A T A T T G T A C T A G G C C G T C A A G G G G A  300
Sbjct  1346 . . . . . . . . . . . . . . . . . . . . . . . . . . . . . . . . . . . . . . . . . . . . . . . . . . . . . . . . . . . . 1405
            * * * * * * * * * * * * * * * * * * * * * * * * * * * * * * * * * * * * * * * * * * * * * * * * * * * * * * * * * * *

Query   301 T C C T C A T G G A A A G T T T G A T T T A C C A C C T G G T G T G C T G G A A C A C T T C G A A A C T G C C A C        357
Sbjct  1406 . . . . . . . . . . . . . . . . . . . . . . . . . . . . . . . . . . . . . . . . . . . . . . . . . . . . . . . .       1462
            * * * * * * * * * * * * * * * * * * * * * * * * * * * * * * * * * * * * * * * * * * * * * * * * * * * * * * *
```

Figure 3–4 (A) 1.2% agarose gel electropherogram of amplified internal region (M: 100 bp DNA ladder). (B) Nucleotide sequence alignment of internal fragment and hepatopancreas derived hemocyanin (Accession No.: KJ151291). The identical residues are shown by dots.

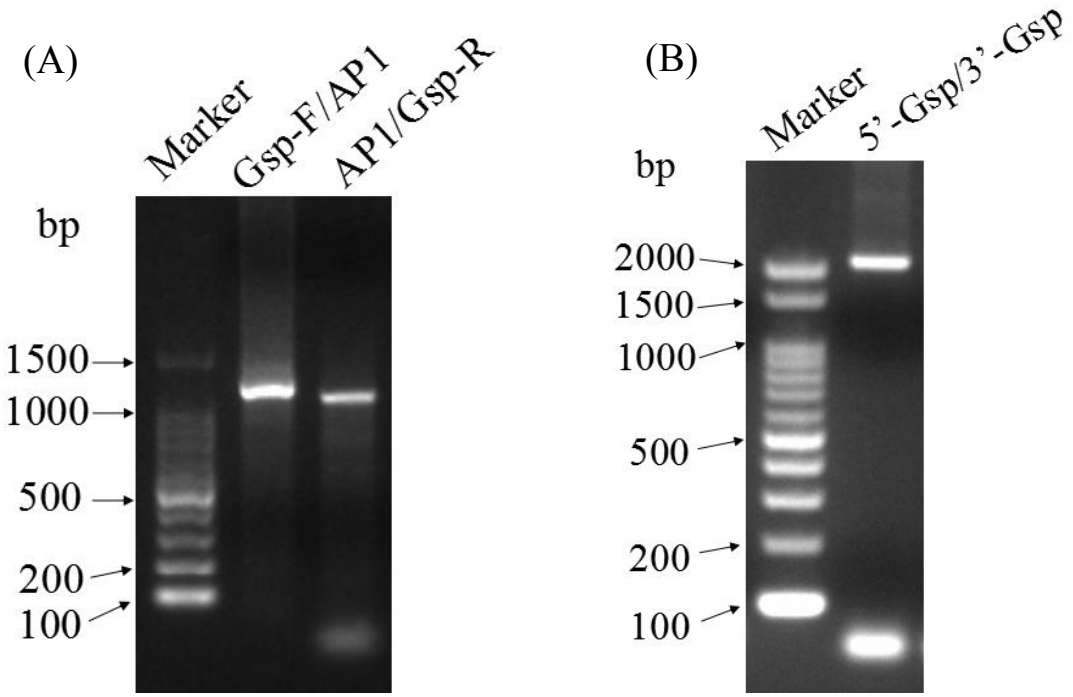

Figure 3–5 1.2% agarose gel electrophoregram of 3'–end/5'–end products (A) and end to end amplification products (B) (M: 100 bp DNA ladder).

```
1    a a a t g g g a a t t t t c a g a a t g a t a a t a a c a a g g g a a t a a c c a t a a g t t g c t g a a g t t c a c c
61   a t c a g c a c c a t g a g g g t c t t a g t g g t t c t t g g g c t t g t c g c t g c t g c c g c c t t t c g g g t g
1                        M   R   V   L   V   V   L   G   L   V   A   A   A   A   F   R   V
121  g c c a g t g c a g a t g t t c a g c a g c a g a a a g a c g t c c t t t a t c t c c t g a a c a a a a t c t a t g g a
18    A   S   A   D   V   Q   Q   Q   K   D   V   L   Y   L   L   N   K   I   Y   G
181  g a c a t t c a g g a c g g a g a c c t g c t g g c t a c t g c c a a t t c c t t t g a t c c c g t t g g a a a c t t a
38    D   I   Q   D   G   D   L   L   A   T   A   N   S   F   D   P   V   G   N   L
241  g g c a g c t a c a g t g a t g g t g g t g c a g c c g t g c a a a a a c t g g t g c a g g a c c t t a a t g a c g g c
58    G   S   Y   S   D   G   G   A   A   V   Q   K   L   V   Q   D   L   N   D   G
301  a a a c t c t t g g a g c a g a a a c a c t g g t t c t c c c t t t t c a a t a c a a g g c a t c g t a a t g a g g c a
78    K   L   L   E   Q   K   H   W   F   S   L   F   N   T   R   H   R   N   E   A
361  c t c a t g c t t t t c g a c g t c c t c a t c c a c t g c a a a g a c t g g g c a t c c t t t g t c g g c a a t g c a
98    L   M   L   F   D   V   L   I   H   C   K   D   W   A   S   F   V   G   N   A
421  g c c t a c t t c c g t c a g a a a a t g a a t g a a g g a g a g t t t g t t t a t g c c t t g t a t g t t g c c g t g
118   A   Y   F   R   Q   K   M   N   E   G   E   F   V   Y   A   L   Y   V   A   V
481  a t c c a c t c g t c t t t g g c t g a a g a c g t g g t g c t c c c t c c c c t c t a t g a g g t c a c a c c g c a c
138   I   H   S   S   L   A   E   D   V   V   L   P   P   L   Y   E   V   T   P   H
541  c t c t t c a c c a a c a g t g a a g t t a t c g a a g a a g c t t a t c g t g c c a a a c a g a a g c a g a c g c c t
158   L   F   T   N   S   E   V   I   E   E   A   Y   R   A   K   Q   K   Q   T   P
601  g g c a a a t t c a a g t c c t c c t t t a c g g g a a c c a a g a a a a a c c c t g a a c a g a g a g t g g c a t a t
178   G   K   F   K   S   S   F   T   G   T   K   K   N   P   E   Q   R   V   A   Y
661  t t c g g t g a a g a t a t c g g c t t g a a t a c c c a t c a c g t t a c c t g g c a t a t g g a a t t c c c c t t c
198   F   G   E   D   I   G   L   N   T   H   H   V   T   W   H   M   E   F   P   F
721  t g g t g g a a t g a t g c t t a c g g c c a t c a t c t g g a t c g c a a a g g a g a a a a c t t c t t c t g g a t t
218   W   W   N   D   A   Y   G   H   H   L   D   R   K   G   E   N   F   F   W   I
781  c a t c a c c a a c t t g c c g t c c g a t t t g a t g c t g a a c g t c t g t c c a a t t a t c t g g a t c c a g t a
238   H   H   Q   L   A   V   R   F   D   A   E   R   L   S   N   Y   L   D   P   V
841  g g t g a a c t c c a g t g g a a c a a g c c c a t t g t a g a t g g c t t c g c t c c c c a c a c c a c t t a c a a g
258   G   E   L   Q   W   N   K   P   I   V   D   G   F   A   P   H   T   T   Y   K
901  t a t g g a g g t c a g t t c c c t g c t c g t c c t g a c a a t g t t a a a t t c g a a g a t g t g g a c g a t g t t
278   Y   G   G   Q   F   P   A   R   P   D   N   V   K   F   E   D   V   D   D   V
961  g c t c g a a t t c g a g a t a t g g t c a t c g t g g a g a g t c g a a t t c g t g a t g c c a t t g c c c a t g g c
298   A   R   I   R   D   M   V   I   V   E   S   R   I   R   D   A   I   A   H   G
1021 t a t a t a g t t g a c a g t g a g g g c a a a c a c a t t g a c a t c a g t a a t g a g a a a g g t a t t g a c a t t
318   Y   I   V   D   S   E   G   K   H   I   D   I   S   N   E   K   G   I   D   I
1081 c t t g g t g a t a t c a t c g a a t c c t c a c t a t a c a g t c c c a a c g t g c a g t a c t a t g g a g c t t t a
338   L   G   D   I   I   E   S   S   L   Y   S   P   N   V   Q   Y   Y   G   A   L
1141 c a t a a c a c t g c c c a t a t t g t a c t a g g c c g t c a a g g g g a t c c t c a t g g a a a g t t t g a t t t a
358   H   N   T   A   H   I   V   L   G   R   Q   G   G   D   P   H   G   K   F   D   L
1201 c c a c c t g g t g t g c t g g a a c a c t t c g a a a c t g c c a c c c g t g a t c c c a g c t t c t t c c g g c t t
378   P   P   G   V   L   E   H   F   E   T   A   T   R   D   P   S   F   F   R   L
1261 c a c a a g t a t a t g g a t a a g a t t t t c a a a g a a c a c a a g g a c a a c c t a c c c c c a t a c a c c a a a
398   H   K   Y   M   D   K   I   F   K   E   H   K   D   N   L   P   P   Y   T   K
1321 g c c g a t t t g g a a t t c t c t g g c g t g t c t g t c a c a g a g c t a g c c g t t g t a g g t g a a c t g g a g
418   A   D   L   E   F   S   G   V   S   V   T   E   L   A   V   V   G   E   L   E
1381 a c c t a c t t t g a a g a t t t c g a a t a c a g t c t t a t c a a c g c a g t t g a t g a t g c t g a a g g a a t c
438   T   Y   F   E   D   F   E   Y   S   L   I   N   A   V   D   D   A   E   G   I
1441 c c a g a t g t g g a a a t c a g c a c a t a t g t g c c t c g t c t t a a c c a c a a a g a g t t c a c t t t t a g g
458   P   D   V   E   I   S   T   Y   V   P   R   L   N   H   K   E   F   T   F   R
1501 a t t g a t g t a g a g a a t g g a g g t g c t g a g a g a t t g g c t a c a g t t c g t a t c t t t g c c t g g c c t
478   I   D   V   E   N   G   G   A   E   R   L   A   T   V   R   I   F   A   W   P
1561 c a t a a a g a c a a c a a c g g a a t c g a g t a t a c a t t t g a c g a a g g t c g c t g g a a t g c c a t c g a g
498   H   K   D   N   N   G   I   E   Y   T   F   D   E   G   R   W   N   A   I   E
1621 t t g g a t a a g t t c t g g g t a t c t t t g a a g g g t g g a a a a a c t t c a a t t g a a c g c a a g t c c a c g
518   L   D   K   F   W   V   S   L   K   G   G   K   T   S   I   E   R   K   S   T
1681 g a a t c t t c a g t a a c t g t a c c g g a c g t g c c a a g c a t a c a t g a c c t g t t t g c a g a a g c c g a g
538   E   S   S   V   T   V   P   D   V   P   S   I   H   D   L   F   A   E   A   E
1741 g c a g g c g g c g c t g g c c t t g c c a a a t t c g a g a g t g c a a c a g g c c t a c c a a a c a g g t t c c t t
558   A   G   G   A   G   L   A   K   F   E   S   A   T   G   L   P   N   R   F   L
1801 c t c c c c a a g g g c a a c g a t a g a g g c c t g g a a t t c g a c c t t g t g g t g g c g g t g a c t g a t g g t
578   L   P   K   G   N   D   R   G   L   E   F   D   L   V   V   A   V   T   D   G
1861 g a t g c c g a c t c a g c a g t g c c g a a c c t t c a t g a g a a t a c c g a g t a c a a t c a c t a c g g t t c c
598   D   A   D   S   A   V   P   N   L   H   E   N   T   E   Y   N   H   Y   G   S
1921 c a t g g c g t g t a c c c c c g a t a a g c g t c c t c a t g g t t a t c c t c t g g a c c g c a a a g t t c c a g a t
618   H   G   V   Y   P   D   K   R   P   H   G   Y   P   L   D   R   K   V   P   D
1981 g a g c g c g t g t t t g a a g a t c t t c c t a a c t t t a a g c a c a t c c a a g t t a a g g t c t t c a a t c a t
638   E   R   V   F   E   D   L   P   N   F   K   H   I   Q   V   K   V   F   N   H
2041 g g g g a a c a c a t t c a t t a g t g a t t c a a g c t t a c a a c t c t t t c a t a t g a a a t a t g c g a t g a a
658   G   E   H   I   H   *   *
2101 a a a a a t t g t t c t c t t t g a a t t t t t t t c c c c c c a a a a t a a a a a t a t t g c g g g a a a a a a a a a a
2161 a a a a a a a a a a a a a a a a a a a a a a a a
```

Figure 3–6 Nucleotide sequence and deduced amino acid sequence of LvPBP75. The initial methionine codon is at position 70 and indicated with bold, whereas the stop codon is at position 2,056 of the nucleotide sequence and indicated with an asterisk. The polyadenylation signal is in italics. The landmark peptides of arthropod hemocyanin are indicated with frame. Transmembrane domains are in bold and italics, tyrosinase copper binding domain is double underlined. N– and C–terminals are shadowed.

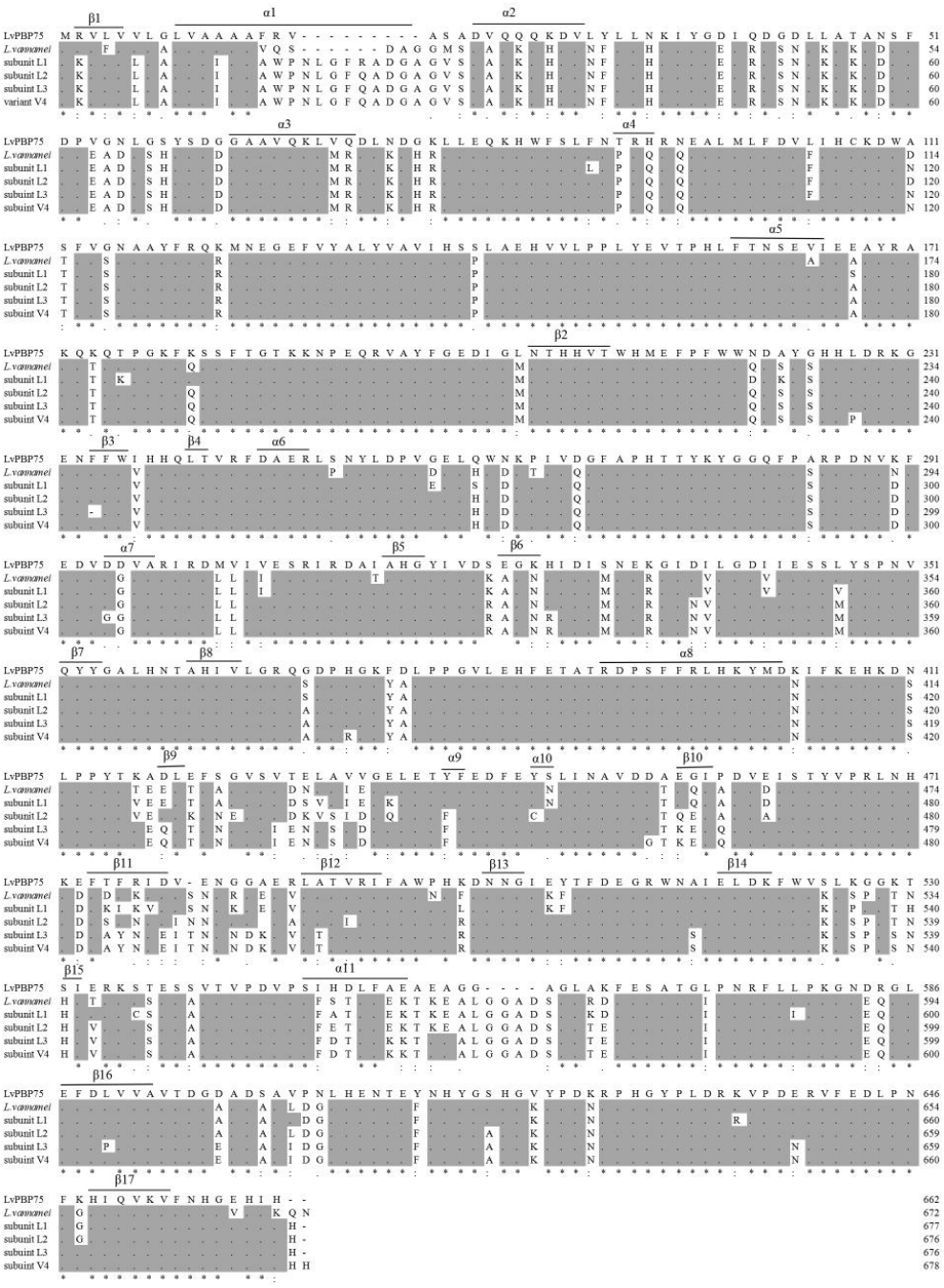

Figure 3–7 Multiple sequence alignment of deduced amino acid sequence of LvPBP75 with other known hemocyanins and their subunits derived from the hepatopancreas of *L. vannamei*. Sequence similarity is delineated as identical (asterisk), strongly similar (colon), and weakly similar (dot). The predicted secondary structure is indicated by α or β (α, α–helices; β, β–strands). Accession numbers (DDBJ/EMBL/GenBank amino acid sequence databases): hemocyanin, AIN41163; subunit L1, AHY86475; subunit L2, AHY86476; subunit L3, AHY86477; subunit V4, AKI81624.

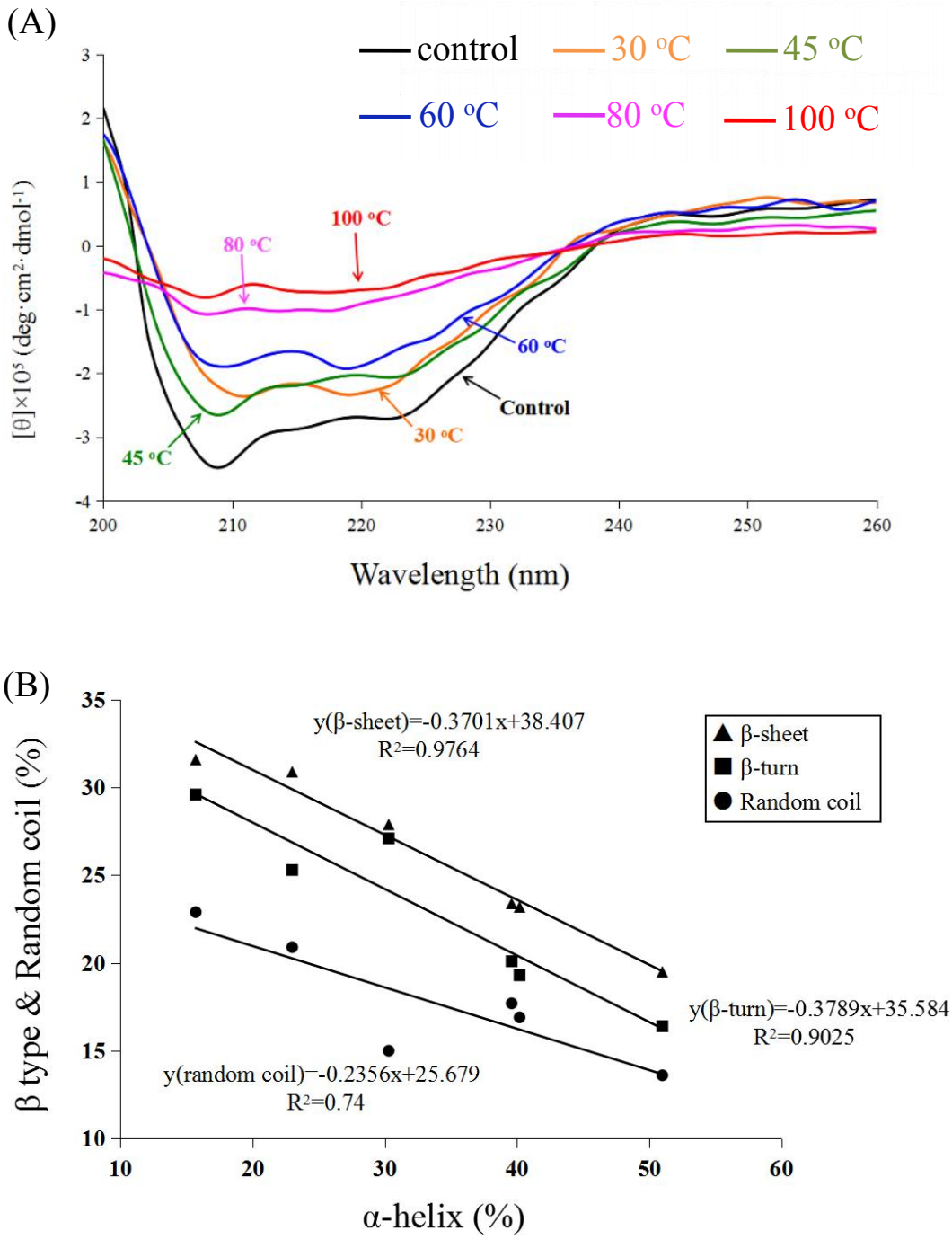

Figure 3–8 Circular dichroism spectra analysis. (A) Changes of CD spectra in LvPBP75 induced by different heating temperatures. Colored spectra refer to the native state (black), heated at 30 ºC (orange), 45 ºC (green), 60 ºC (blue), 80 ºC (pink) and 100 ºC (red). (B) Plots of the β–sheet (▲), turn (■) and random coil structure (●) contents against the α–helix content for heat–treated LvPBP75.

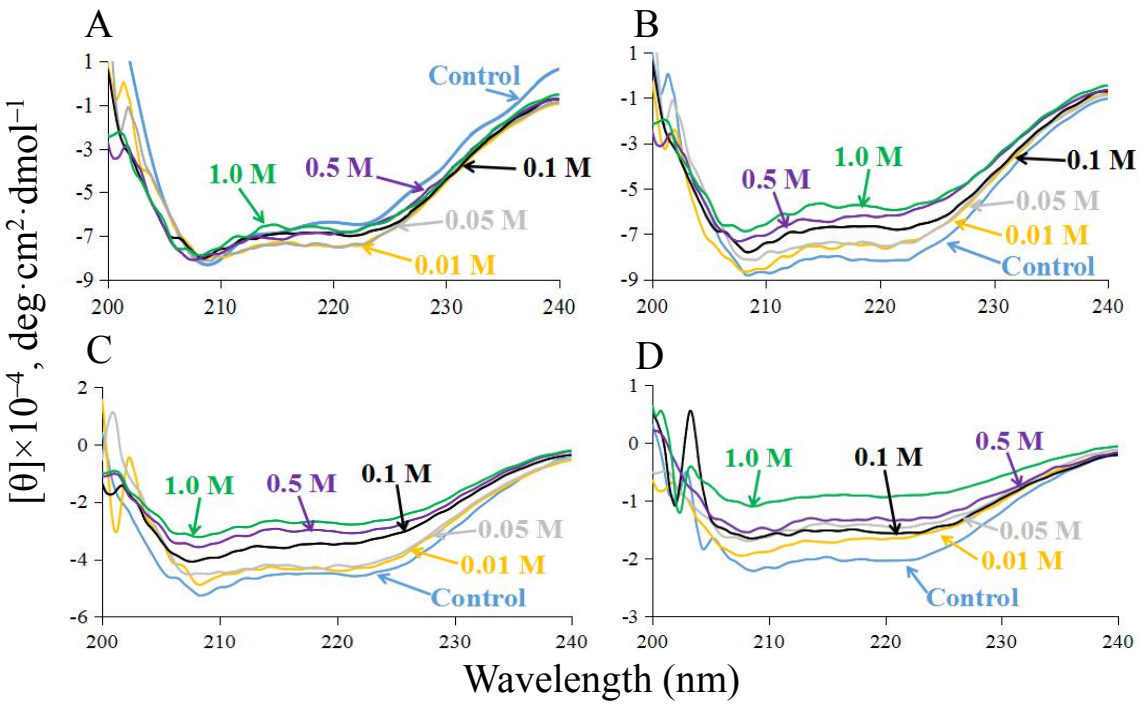

Figure 3–9 Changes of CD spectra in LvPBP75 induced by different concentrations of NaCl at different heating temperatures. (A) room temperature, (B) 30 °C, (C) 60 °C and (D) 100 °C. Colored spectra refer to the unheated (blue), NaCl concentration at 0.01 M (yellow), 0.05 M (gray), 0.1 M (black), 0.5 M (purple) and 1.0 M (green).

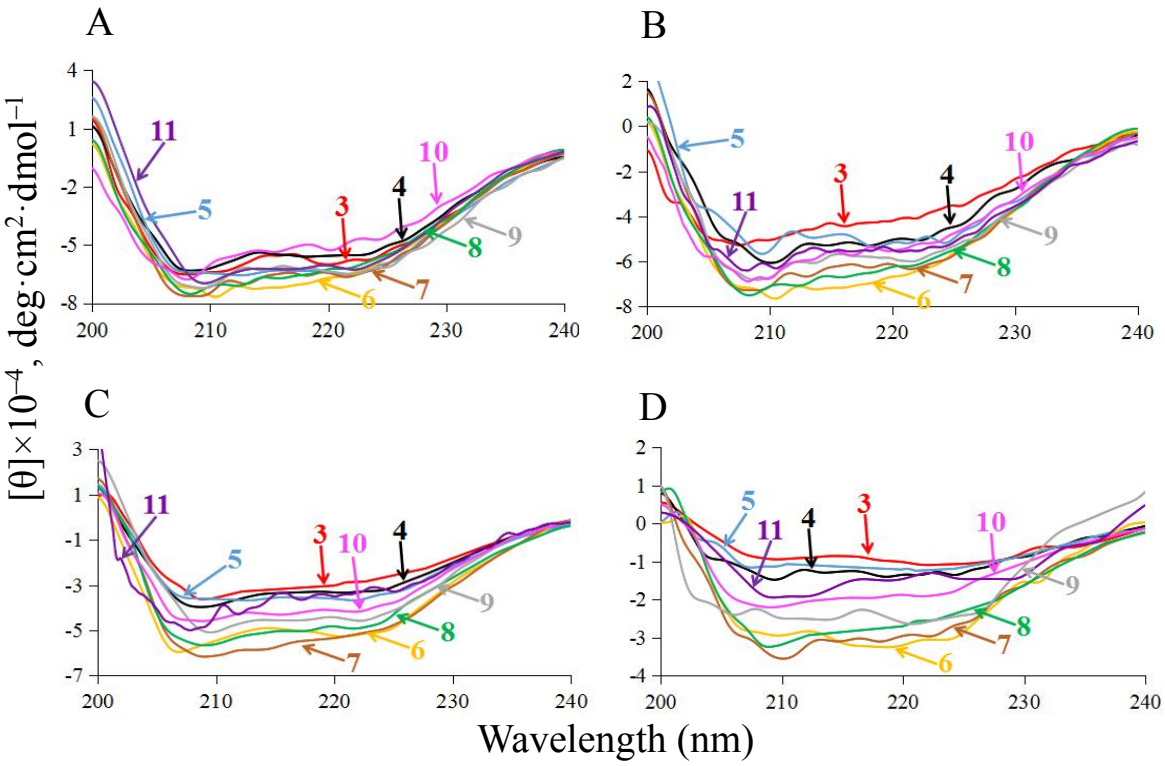

Figure 3–10 Changes of CD spectra in LvPBP75 induced by different pHs at different heating temperatures. (A) room temperature, (B) 30 ºC, (C) 60 ºC and (D) 100 ºC. Colored spectra refer to pH 3–red, pH 4–black, pH 5–blue, pH 6–yellow, pH 7–brown, pH 8–green, pH 9–gray, pH 10–pink, pH 11–purple.

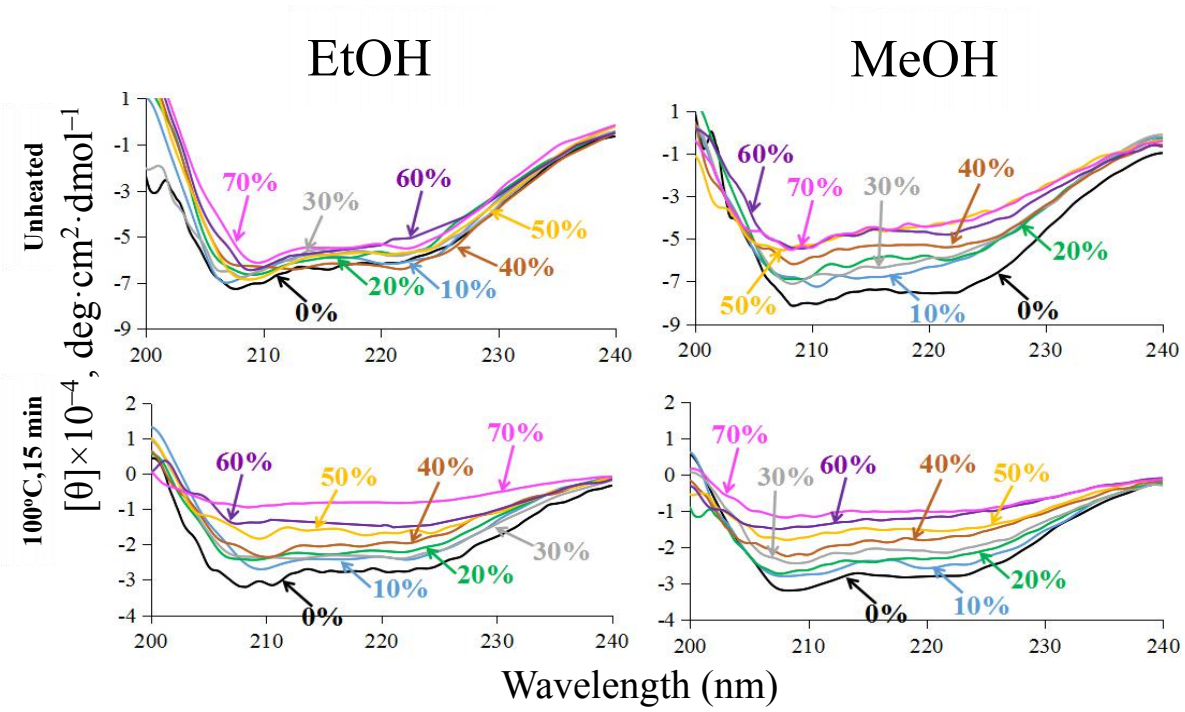

Figure 3–11 Changes of CD spectra in LvPBP75 induced by different alcohols at different heating temperatures. Colored spectra refer to the native state–black and alcohol concentration of 10%–blue, 20%–green, 30%–gray, 40%–brown, 50%–yellow, 60%–purple and 70%–pink.

Table 3–1 List of primers for LvPBP75 cDNA amplification

Name*	Sequence (5' to 3')	Objective	GC Content (%)	Annealing Temperature (°C)
Inter–F	TGCTCCCCCACACCACTTACAAGTAC	Internal amplification	52	59.3
Inter–R	GTGGCAGTTTCRAAGTGTTCYAGCAC		46–54	58–61.1
Gsp–R	GCAATGGCATCACGAATTCG	5'–end amplification	50	51.8
Gsp–F	TCCCAACGTGCAGTACTATG	3'–end amplification	50	51.8
5'–Gsp	GCACCATGAGGGTCTTAGTGGTTC	ORF amplification	54	59.1
3'–Gsp	TCACTAATGAATGTGTTCCCCATG		42	54.0
β–F	GACTTCGAGCAGGAGATGAC	Template confirmation	55	53.8
β–R	AGGGCAGTGATTTCCTTCTGC		52	54.4

(* Meaning of letters: Inter, internal amplification primer; Gsp, gene–specific primer; β, beta–actin primer; F, forward primer; R, reverse primer)

Table 3–2 Secondary structure contents of LvPBP75 under different heat treatments

	α–helix (%)*	β–sheet (%)	β–turn (%)	Random coil (%)
Control	51.0 ± 0.216[a]	19.5 ± 0.262[a]	16.4 ± 0.216[a]	13.6 ± 0.245[a]
30 ºC	40.2 ± 0.330[b]	23.2 ± 0.330[b]	19.3 ± 0.330[b]	16.9 ± 0.327[b]
45 ºC	39.6 ± 0.377[b]	23.4 ± 0.356[b]	20.1 ± 0.356[c]	17.7 ± 0.330[c]
60 ºC	30.3 ± 0.287[c]	27.9 ± 0.294[c]	27.1 ± 0.205[d]	15.0 ± 0.249[d]
80 ºC	23.0 ± 0.249[d]	30.9 ± 0.236[d]	25.3 ± 0.262[e]	20.9 ± 0.245[e]
100 ºC	15.7 ± 0.262[e]	31.6 ± 0.249[e]	29.6 ± 0.249[f]	22.9 ± 0.236[f]

(* Means followed by different small letters within the same column differ significantly at $p = 0.05$ compared with unheated samples. Data expressed as means ± standard deviation, n=3)

Table 3–3 Color measurement of LvPBP75 heated with different concentrations of NaCl at different heating temperatures

		NaCl concentration					
		0 M	0.01 M	0.05 M	0.1 M	0.5 M	1.0 M
Room Temp.	L*	6.74±0.009[a]	6.80±0.014[b]	6.66±0.008[c]	6.84±0.005[d]	6.75±0.005[a]	6.63±0.005[e]
	a*	–0.57±0.009[a]	–0.64±0.009[b]	–0.58±0.012[ac]	–0.62±0.017[b]	–0.60±0.009[cd]	–0.61±0.014[bd]
	b*	0.91±0.016[ab]	0.90±0.009[b]	0.93±0.012[a]	0.93±0.014[a]	0.96±0.009[c]	0.91±0.017[ab]
30 °C	L*	5.82±0.005[a]	5.62±0.009[b]	5.59±0.005[bc]	5.39±0.009[d]	5.30±0.005[e]	5.24±0.009[f]
	a*	–0.37±0.009[a]	–0.34±0.012[b]	–0.36±0.009[ab]	–0.15±0.012[c]	–0.10±0.009[d]	–0.06±0.005[e]
	b*	2.02±0.014[a]	1.95±0.009[b]	1.99±0.014[bc]	2.13±0.012[d]	2.23±0.009[e]	2.19±0.012[f]
60 °C	L*	4.36±0.009[a]	4.28±0.005[b]	3.88±0.012[c]	3.67±0.012[d]	3.63±0.009[e]	3.39±0.016[f]
	a*	1.15±0.012[a]	1.19±0.005[b]	1.24±0.009[c]	1.57±0.012[d]	1.78±0.009[e]	1.83±0.009[f]
	b*	3.16±0.009[a]	3.20±0.008[b]	3.58±0.005[c]	4.02±0.009[d]	4.37±0.005[e]	4.43±0.014[f]
100 °C	L*	3.21±0.012[a]	2.87±0.009[b]	2.71±0.012[c]	2.39±0.016[d]	2.06±0.014[e]	1.86±0.014[f]
	a*	2.38±0.009[a]	2.54±0.009[b]	2.71±0.012[c]	3.00±0.009[d]	3.23±0.017[e]	3.20±0.009[e]
	b*	3.86±0.014[a]	3.99±0.016[b]	4.29±0.008[c]	4.57±0.016[d]	4.78±0.009[e]	4.91±0.012[f]

(Means followed by different lower–case letters within the same column differ significantly at $p < 0.05$ versus the control. Data are expressed as mean ± standard deviation, n = 3)

Table 3–4 Color measurement of LvPBP75 heated with different pHs at different heating temperatures (RT: room temperature: 30, 60, and 100 mean heated at 30, 60, and 100 ^{o}C, respectively)

		pH								
		3	4	5	6	7	8	9	10	11
Room Temp.	L*	5.72±0.009^{a}	6.02±0.014^{b}	6.13±0.042^{c}	6.83±0.014^{d}	6.80±0.005^{d}	6.67±0.012^{e}	6.55±0.022^{f}	6.02±0.042^{b}	5.82±0.005^{g}
	a*	–0.24±0.012^{a}	–0.26±0.009^{ab}	–0.27±0.009^{c}	–0.38±0.005^{d}	–0.37±0.005^{c}	–0.38±0.008^{c}	–0.30±0.022^{d}	–0.27±0.012^{ab}	–0.27±0.009^{b}
	b*	1.46±0.021^{a}	1.29±0.012^{b}	1.22±0.005^{c}	1.18±0.005^{d}	1.18±0.008^{d}	1.22±0.022^{c}	1.24±0.025^{c}	1.32±0.008^{e}	1.43±0.012^{f}
30 ^{o}C	L*	5.59±0.005^{a}	5.86±0.021^{b}	5.82±0.005^{c}	6.72±0.022^{d}	6.76±0.014^{e}	6.48±0.009^{f}	6.47±0.012^{f}	6.06±0.008^{g}	5.86±0.017^{b}
	a*	0.16±0.009^{a}	–0.14±0.009^{b}	–0.24±0.009^{cd}	–0.30±0.008^{e}	–0.28±0.017^{ef}	–0.22±0.019^{c}	–0.26±0.017^{df}	–0.17±0.017^{g}	–0.11±0.012^{h}
	b*	2.07±0.017^{a}	2.00±0.014^{b}	2.02±0.014^{b}	1.25±0.014^{c}	1.22±0.024^{c}	1.40±0.014^{d}	1.57±0.014^{e}	1.77±0.014^{f}	1.96±0.022^{a}
60 ^{o}C	L*	3.60±0.009^{a}	3.86±0.021^{b}	4.82±0.005^{c}	6.40±0.008^{d}	5.58±0.024^{e}	5.53±0.033^{f}	5.17±0.012^{g}	5.04±0.022^{h}	4.66±0.017^{i}
	a*	0.92±0.025^{a}	0.13±0.012^{b}	–0.04±0.005^{c}	–0.24±0.017^{d}	–0.15±0.009^{e}	–0.12±0.009^{c}	–0.05±0.017^{c}	0.11±0.012^{b}	0.31±0.012^{f}
	b*	2.63±0.017^{a}	2.32±0.031^{b}	2.20±0.026^{c}	1.54±0.024^{d}	1.55±0.008^{d}	1.61±0.019^{e}	1.80±0.019^{f}	2.08±0.012^{g}	2.19±0.009^{c}
100 ^{o}C	L*	2.04±0.036^{a}	3.31±0.021^{b}	4.21±0.017^{c}	5.07±0.017^{d}	5.04±0.036^{d}	4.86±0.025^{e}	4.24±0.008^{c}	3.84±0.022^{f}	3.15±0.008^{g}
	a*	2.16±0.036^{a}	1.26±0.008^{b}	1.16±0.012^{c}	0.90±0.022^{d}	0.80±0.012^{e}	0.99±0.012^{f}	1.05±0.017^{g}	1.11±0.012^{h}	1.82±0.019^{i}
	b*	4.37±0.037^{a}	3.22±0.022^{b}	2.81±0.008^{c}	2.59±0.021^{d}	2.60±0.009^{d}	2.61±0.017^{d}	2.71±0.019^{e}	2.93±0.026^{f}	3.50±0.036^{g}

(Means followed by different lower–case letters within the same column differ significantly at $p < 0.05$ versus the control. Data are expressed as mean ± standard deviation, n = 3)

Table 3–5 Color measurement of LvPBP75 heated with different alcohols at 100 °C, 15 min (Upper, EtOH; Lower, MeOH)

	Concentration	L*		a*		b*	
	(%)	Unheated	100°C,15 min	Unheated	100°C,15 min	Unheated	100°C,15 min
EtOH	0	6.73±0.014[a]	3.40±0.009[a]	–0.56±0.05[a]	1.26±0.016[a]	0.89±0.017[a]	3.39±0.012[a]
	10	6.70±0.009[b]	6.23±0.012[b]	–0.51±0.012[b]	0.41±0.012[b]	1.01±0.012[b]	1.41±0.012[b]
	20	6.52±0.025[c]	6.37±0.017[c]	–0.45±0.008[c]	0.25±0.017[c]	0.86±0.022[a]	1.26±0.008[c]
	30	6.49±0.016[c]	6.42±0.029[d]	–0.19±0.021[d]	0.44±0.025[b]	0.89±0.016[a]	1.09±0.022[d]
	40	6.71±0.021[b]	6.36±0.008[c]	0.35±0.021[e]	0.67±0.008[d]	1.08±0.016[c]	1.20±0.009[e]
	50	6.40±0.008[d]	6.17±0.017[e]	0.54±0.014[f]	0.90±0.022[e]	1.15±0.012[d]	1.39±0.021[b]
	60	6.35±0.031[e]	6.19±0.024[be]	1.04±0.034[g]	1.16±0.012[f]	1.55±0.028[e]	1.80±0.021[f]
	70	6.24±0.008[f]	6.04±0.036[f]	1.05±0.017[g]	1.21±0.020[g]	1.75±0.029[f]	2.30±0.017[g]
MeOH	0	6.73±0.017[a]	3.25±0.024[a]	–0.56±0.009[a]	1.19±0.012[a]	0.89±0.009[a]	3.34±0.021[a]
	10	6.74±0.009[bc]	6.13±0.042[b]	–0.57±0.009[b]	0.37±0.009[b]	0.91±0.016[ab]	1.31±0.014[b]
	20	6.43±0.012[d]	6.48±0.009[c]	–0.44±0.012[c]	0.22±0.019[c]	1.05±0.008[c]	1.40±0.014[c]
	30	6.66±0.005[e]	6.55±0.022[d]	0.58±0.012[d]	0.72±0.017[d]	0.93±0.012[b]	1.11±0.016[d]
	40	6.63±0.005[f]	6.31±0.021[e]	0.61±0.014[d]	0.75±0.016[d]	1.03±0.014[c]	1.26±0.017[e]
	50	6.48±0.009[g]	6.36±0.009[ef]	0.72±0.012[e]	0.91±0.012[e]	1.08±0.009[d]	1.16±0.009[f]
	60	6.72±0.022[c]	6.28±0.005[f]	0.71±0.016[e]	1.06±0.022[f]	1.25±0.014[e]	1.60±0.029[g]
	70	6.76±0.008[b]	6.48±0.009[c]	0.96±0.041[f]	1.28±0.025[g]	1.73±0.017[f]	1.95±0.016[h]

(Means followed by different lower–case letters within the same column differ significantly at $p < 0.05$ versus the control. Data are expressed as mean ± standard deviation, n = 3)

Chapter 4 Gene distribution and functional expression of red color–related protein LvPBP

4.1 Introduction

Even though the red color change on crustacean shell surface is correlated with the release of pigment, the accumulation and interaction of pigment–binding proteins in crustaceans is depended upon many factors. It was reported that black tiger prawn (*Penaeus monodon*) shell color is affected by the background color of the tanks in which the prawns were growing (Tume et al., 2009). The prawns fed in black background showed a much more orange color compared with those grown in white background after cooking. This was due to the accumulation of pigment–binding protein was higher in black background groups than white background ones. Different accumulation of pigment–binding protein is correlated with the interaction between pigment and protein. Briefly, the prawns cultured in black tanks need to synthesize more pigment–binding protein to dark their shell color, while the ones grown in white tanks lightened themselves via reducing the formation of pigment–binding protein. Background color not only affects the prawns but also determines the shell color change on crabs (Hemmi et al., 2006; Kronstadt et al., 2013). However, the experiment on color change in American lobster (*Homarus americanus*) in response to background color and ultraviolet light revealed that American lobster shell color change is mainly affected by ultraviolet light. In the absence of ultraviolet light, lobster shell color trends to match the background color after 60 days of exposure (Michael et al., 2009). The interaction of pigment–binding proteins derived from lobster shell was more sensitive against ultraviolet light than background color. In addition, study on the effects of background and temperature on body color of fiddler crab (*Uca panacea*) revealed that its shell color is correlated with sex (Kronstadt et al., 2013). The surface color of male crabs showed a more sensitive response to the environment change than females, suggesting the interactions in pigment–binding proteins showed differences

even though these proteins were derived from the same species. Furthermore, crustacean shell colors are also influenced by daily diet, mainly the feeding amount of astaxanthin (ATX), habitat, life history, and water quality (Palma & Steneck, 2001; Melville–Smith et al., 2003). Studies on crustacean coloration suggested a wide distribution, accumulation, and interaction mechanisms in pigment–binding proteins.

Yet despite the increase in the knowledge of crustaceans, there has been very little progress in defining the pigment–binding ability of the red color–related proteins derived from crustacean shell. In chapter 2, a novel red color–related protein, LvPBP75, was purified from the shell of *L. vannamei*. It had closely corresponded with *L. vannamei* shell color change and was identified as hemocyanin, which could bind with ATX (Chapter 3). However, understanding of the LvPBP75 gene distribution and pigment–binding ability is lacking. In view of these circumstances, this chapter reported 1) distribution of LvPBP75 gene, 2) expression and purification of recombinant LvPBP75, 3) reconstruction and structural properties of artificial LvPBP75.

4.2 Materials and Methods

4.2.1 Shrimp and tissue collection

The shrimp samples were collected as described in 3.2.1. Eight target tissues including muscle, epithelium, intestine, hepatopancreas, eyestalk, hemolymph, heart, and nerve were collected from alive individuals and were used immediately for RNA isolation.

4.2.2 RNA extraction and cDNA synthesis

Extraction of RNA and synthesis of double–strand cDNA was performed followed with the description in 3.2.3. Single–strand cDNA was synthesized from 1 μg of total RNA by PrimerScript™ RT Master Mix (Perfect Real Time, Takara, Otsu,

Japan) following the protocol of the manufacturer.

4.2.3 Semi–quantitative and quantitative real time PCR

Semi–quantitative real time PCR reactions were carried out using Ex Taq polymerase (Takara, Otsu, Japan) according to the manufacturer's introductions. The β–actin primers, β–actin–F and β–actin–R, were designed based on *L. vannamei* β–actin sequence (GenBank accession No. AF300705) to amplify a β–actin gene fragment of 295 bp. The PCR products were analyzed using 1.2% agarose gel electrophoresis.

The quantitative real time PCR amplifications were carried out using SYBR® Premix EX TaqTM II (Tli RNaseH Plus) Kit (Takara, Shuzo, Japan) and ABI 7300 Real Time PCR System (Applied Biosystems, Foster City, CA, USA) in total volume of 20 μL containing 10 μL of 2 × SYBR® Premix EX Taq, 2 μL aliquot of single–strand cDNA, 0.4 μM of each primer, and 0.4 μL of 50 × ROX reference dye. Two gene specific primers, qLvPBP–F and qLvPBP–R, were designed to amplify a PCR product of 138 bp. The thermal profile for LvPBP75 real time PCR was: 95 ^{o}C for 30 s, 40 cycles of 94 ^{o}C for 5 s and 60 ^{o}C for 31 s. Dissociation curve analysis of the amplification products was performed at the end of each PCR reaction to confirm that only one PCR product was amplified and detected. The quantitative real time PCR of β–actin followed almost the same conditions described earlier using the primers qLvPBP–F and qLvPBP–R, while the annealing temperature was changed to 64 ^{o}C. After the PCR program, data were analyzed with the ABI 7300 SDS software (Applied Biosystems, Foster City, CA, USA), and the baseline was set automatically by the software to maintain consistency. Relative quantification of each gene expression level was generated using the $2^{-\triangle\triangle Ct}$ method (Schmittgen & Livak, 2001) and data were expressed as means of triplicate measurements.

4.2.4 Expression and purification of recombinant LvPBP (rLvPBP)

Red color–related protein, LvPBP75 was expressed in *Escherichia coli* as a His–tagged protein using a pET–44a vector system (Promega, Madison, WI, USA) (Fig. 4–1). The cDNA region encoding the mature protein of LvPBP75 was amplified with specific primers LvPBP–*Pst*I and LvPBP–*Sal*I (Table 4–1). Two restriction sites, *Pst*I and *Sal*I, were added to the 5' end of the primers, respectively. PCR reaction was performed using Ex Taq DNA polymerase (Takara Bio, Otsu, Japan) in a 25 μL volume under the following conditions: 94 ^{o}C for 5 min, 35 cycles of 94 ^{o}C for 30 s, 60 ^{o}C for 30 s and 72 ^{o}C for 4 min, and final extension at 72 ^{o}C for 3 min. The amplified product and the pET–44a vector were individually digested with *Pst*I and *Sal*I and then ligated with each other using a DNA Ligation Kit (Takara Bio, Japan) at 4 ^{o}C overnight. *E. coli* JM 109 was transformed with the ligated product and cultured on LB agar containing 0.005% ampicillin at 37 ^{o}C overnight. Single colonies were selected for the plasmid extraction, and then screened by colony PCR using pET upstream and Colidown primers (Table 4–1).

The LvPBP–pET44a plasmid was transformed into the Rosetta–gami B (DE3) pLysS expression host cell and plated on LB agar containing 25 μg/mL kanamycin, 34 μg/mL chloramphenicol, and 12.5 μg/mL tetracycline. After overnight incubation at 37 ^{o}C, 5 independent colonies were selected for the insert confirmation by colony PCR and nucleotide sequencing.

A single colony of successfully transformed *E. coli* was selected and grown in 200 mL of LB medium containing 25 μg/mL kanamycin, 34 μg/mL chloramphenicol, and 12.5 μg/mL tetracycline at 37 ^{o}C until the absorbance at 600 nm reached 0.7. The culture was then added with IPTG (isopropyl–β–D–1–thiogalactoside) at a concentration of 1.0 mM and further incubated for 2 h at 37 ^{o}C. Bacteria were harvested by centrifugation at 6,000 × *g* for 10 min at 4 ^{o}C, and then resuspended in lysis buffer (10 mM Tris–HCl (pH 7.0), 10% Glycerol, 0.5 M NaCl, 0.1% NP–40, 5 mM 2–Mercaptoethanol, 1 mM PMSF (Phenylmethylsulfonyl fluoride)). After sonication and centrifugation, the precipitate which containing rLvPBP75 was dialyzed against 20 mM phosphate buffer (pH 7.0) before applied to affinity HPLC on

a HisTrap^{TM} HP column (1 × 1 mL, GE Healthcare Biosciences, Uppsala, Sweden) that was equilibrated with binding buffer (20 mM phosphate buffer, 0.5 M NaCl, 20 mM imidazole, pH 7.0) and washed with elution buffer (20 mM phosphate buffer, 0.5 M NaCl, 250 mM imidazole, pH 7.0) at a flow rate of 0.7 mL/min. Finally, the rLvPBP75 was dialyzed against 20 mM sodium phosphate buffer (pH 7.0) twice to remove the NaCl and imidazole. Subsequently, the purified protein was analyzed by 12% SDS–APGE and the protein concentration was estimated by the Lowry method (Lowry et al., 1951) using DC Protein Assay kit (Bio–Rad Laboratories, Hercules, CA, USA).

4.2.5 Identical analysis between LvPBP and rLvPBP

The insert confirmation of LvPBP–pET44a plasmid DNA was performed by colony PCR using pET upstream and Colidown primers (Table 4–1) and nucleotide sequencing using a BigDye Terminator v3.1 Cycle Sequencing Kit and an ABI 3130 Genetic Analyzer (Applied Biosystems, Foster City, CA, USA).

Investigation of the secondary structure of rLvPBP75 was performed by using a circular dichroism (CD) spectropolarimeter (J–725, JASCO, Japan) followed with the description in 3.2.6.

4.2.6 Construction of artificial LvPBP

The artificial LvPBP75 was constructed as described by Zagalsky (1985) and Ferrari (Ferrari et al., 2012) using rLvPBP75 and ATX with some modifications. The purified rLvPBP75 (10 mg) was first dialyzed in a mixture of equal volumes of 40 mM Tris–HCl pH 7.0, 200 mM ammonium sulfate and acetone at 4 ^{o}C overnight, then mixed with ATX (1 mg) which was dissolved in acetone. The mixture was incubated overnight at 4 ^{o}C in the dark against phosphate buffer (20 mM, pH 7.0). The free astaxanthin was removed by using a 3K Amicon Ultra Centrifugal Device (MWCO 3000). The hemocyanins derived from keyhole limpet (*Megathura crenulata*) and

Atlantic horseshoe crab (*Limulus polyphemus*) hemolymph (Sigma–Aldrich, St. Louis, MO, USA) were used as control. The UV–visible absorption spectra of recombinant complexes were determined by a micro–volume spectrophotometer from 220 to 800 nm (BioSpec–nano, Shimadzu, Kyoto, Japan).

4.2.7 Structural analysis of artificial LvPBP

The artificial LvPBP75 solution with a final concentration of 0.5 mg/mL were subjected at temperatures of 30, 45, 60, 80, and 100 °C for 10 min, and unheated sample was set as control. The supernatant of each sample was collected by centrifugation before subjected to the secondary structure analysis. Investigation on the changes of secondary structure of artificial LvPBP75 was performed by using a circular dichroism (CD) spectropolarimeter (J–725, JASCO, Japan) followed with the description in 3.2.6.

4.2.8 Statistical analysis

Statistical analysis of all data were followed with the description in 2.2.6.

4.3 Results

4.3.1 Tissue distribution of LvPBP

Tissue distribution of LvPBP75 mRNA in *L. vannamei* was analyzed by both of semi–quantitative and quantitative real time PCR. As determined by semi–quantitative real time PCR analysis, LvPBP75 expression was robust in the hepatopancreas, hemolymph, and heart, medium in epithelium, low in muscle, intestine, and nerve, and absent from eyestalk (Fig. 4–2A). From the quantitative real time PCR, the mRNA of LvPBP75 could be detected in all the tissues examined. The relative expression levels of LvPBP75 in other tissues were normalized to that in muscle, which was set as baseline (1.0). The results showed that, LvPBP75 has the highest expression level in

hepatopancreas, mediate level in heart and hemolymph, followed with epithelium and intestine, and the lowest in eyestalk, nerve, and muscle. A high expression level of LvPBP75 was detected in epithelium, which was 4.64–fold over that in muscle (Fig. 4B).

4.3.2 Expression and purification of rLvPBP

The preparation of restriction enzymes digested pET–44a vector (7,298 bp) and amplification of mature LvPBP75 with restriction enzyme sites (2,051 bp) are shown in Fig. 4–3. After agarose gel purification, two DNA fragments were ligated together using T4 DNA ligase kit (Takara Bio, Japan) followed with the manufacturer's instruction. The LvPBP75 recombinant expression vector was designated as LvPBP–pET44a. It was first transformed into the non–expression host cell (*E. coli* JM 109) for the insert check. The digested LvPBP–pET44a showed two obvious bands at 7,300 bp and 2,100 bp, respectively (Fig. 4–4A). Colony PCR products showed clear bands around 2,100 bp (Fig. 4–4B). The positive colony with correct insert LvPBP75 sequence was then inoculated with LB medium containing 0.005% ampicillin to make the LvPBP–pET44a plasmid DNA.

Different incubation conditions were conducted to induce the target recombinant LvPBP75. The target 75 kDa band was better induced at 37 ^{o}C than 30 ^{o}C. At 37 ^{o}C, the target protein was induced much more under 1.0 mM IPTG than 0.5 mM IPTG. The strongest expression of target protein began at 2 hours and barely no changes within the increasing of incubation time (Fig. 4–5).

The His–tagged recombinant LvPBP75 was eventually purified by affinity chromatography (Fig. 4–6A). As analyzed by SDS–PAGE, a prominent 75 kDa protein band corresponding to His–tagged rLvPBP75 was observed in the precipitate fraction of IPTG–induced bacteria (lane 4 in Fig. 4–6B). Following affinity chromatography on a HisTrap Chelating HP column, rLvPBP75 was obtained in an electrophoretically pure state (lane 5 in Fig. 4–6B). In a typical experiment, 200 mL of the culture

medium yielded about 5 mg rLvPBP75.

4.3.3 Identical analysis between LvPBP and rLvPBP

The LvPBP–pET44a plasmid DNA was then subjected to sequencing procedure. Alignment analysis revealed that the plasmid DNA was 100% similar to the LvPBP75 nucleotide sequence (Data not shown). This result suggested that the target DNA of LvPBP75 was successfully ligated with pET–44a expression vector. The molecular weight of purified rLvPBP75 was around 75 kDa (Fig. 4–6B, lane 5), which was matched with the molecular weight of LvPBP75 (Fig. 2–4 C).

As illustrated in Fig. 4–7B, the rLvPBP75 showed two negative bands at 223 and 208 nm, consistent with those of the LvPBP75 (Fig.3–8A control). The α–helix content of rLvPBP75 was calculated to be 53.3 ± 0.262% using the CDSSTR program of the CDpro package, which was also in accordance with LvPBP75 (Table 3–2).

Results of alignment of nucleotide sequence, molecular weight, and secondary structure analysis demonstrate that the rLvPBP75 produced in this study was identical with LvPBP75 purified from the shell of *L. vannamei*, and can be used as an alternative of LvPBP75 in the further study.

4.3.4 Construction and structural analysis of artificial LvPBP

The rLvPBP75 showed a single peak at 267 nm in Tris–Acetone buffer (pH 7.0), and ATX also showed a single peak at 472 nm before combined (Data not shown). After overnight incubation at 4 ^{o}C, the artificial LvPBP75 complex showed two peaks at 272 and 450 nm simultaneously (Fig. 4–7A), suggesting that the rLvPBP75 was successfully combined with ATX. It was notable that the typical ATX peak (~ 480 nm in acetone) was not found in the *Megathura crenulata* and *Limulus polyphemus* hemolymph derived hemocyanin binding experiment (Fig. 4–7A), indicating that the pigment–binding ability of hemocyanins has species–specificity. It may correlated with the structural differences among hemocyanins. Due to the slight bathochromic

shift of ATX in the artificial LvPBP75, the mixture itself showed a slight pink color.

The structural differences among hemocyanins were illuminated in two parts, first part is effect of astaxanthin on structure of LvPBP75. CD spectra of LvPBP75 showed a slight loss compared with rLvPBP75 (Fig. 4–7A). The absorption spectra may slightly change due to the influences of protein concentration, buffer system, temperature of measurement and instrument differences. After considering these factors, the changes of CD spectra probably reflects the increase in conformational flexibility of hemocyanin when bound with ATX. The binding ratio of rLvPBP75 and ATX was calculated to be 0.346 based on their molar mass, which means that 1 ATX could bound with 26 kDa protein, which was in accordance with the previous study on crustacyanin subunit. 1 molar ATX was combined with 22 kDa protein (Palma & Steneck 2001; Elizabeth et al., 2009).

In another part, to understand the effects of hemocyanin on structure of LvPBP75, three–dimensional structure models of LvPBP75 monomer and *L. vannamei* hepatopancreas derived hemocyanin (Genbank accession number: AIN41163) monomer were built by using SWISS–MODEL online tool (http://www.swissmodel.expasy.org). As shown in Fig. 4–8B, no red color regions were found, which means the quality of built models were acceptable for further analysis. The LvPBP75 shares 80% sequence identity with the hemocyanin and its subunits that derived from the hepatopancreas of *L. vannamei* (Chapter 3). It is therefore highly likely that the LvPBP75 and hemocyanins monomer adopt the similar three–dimensional structure. Interestingly, total four different regions were found between these two hemocyanin monomers, one is spatial difference of α–helix, one is β–sheet changed to α–helix, the remaining two are α–helix changed to β–sheet. Protein function is determined by its structural properties, even though LvPBP75 shares 80% sequence identity with hemocyanins. But LvPBP75 monomer possesses a different spatial structure compared with other hemocyanin monomer, and these unique structure differences may correlate with the pigment–binding function and red color change on shrimp surface.

4.4 Discussion

CD spectra have been extensively used to estimate and monitor the structural changes of the proteins due to temperature, denaturants, or binding interactions for decades (Dreon et al., 2007; Lakshminarayanan et al., 2010; Clarke, 2012; Matsuo et al., 2012). The changes of CD spectra between LvPBP75 and rLvPBP75 probably reflects the conformational flexibility of hemocyanin gained by the hydrophobic residues associated to ATX binding. The binding ratio of rLvPBP75 and ATX was 0.346, which means that 1 ATX could bound with 26 kDa protein. The reported ATX content in crustacyanin is 1 ATX per 22 kDa apoprotein (Palma & Steneck 2001; Elizabeth et al., 2009). The pigment–binding protein found in the egg of golden apple snail has 1 ATX per 30 kDa protein chromophore. ATX was tightly bound to the protein but it did not make any substantial contribution to the structural changes of pigment–binding complex (Dreon et al., 2007). According to these results, the protein can be expected to dominate the CD spectra of pigment–binding complex. However, Ferrari et al. (2012) reported the reconstitution of crustacyanin using astaxanthin and crustacyanin subunits that derived from the shell of American lobster (*Homarus americanus*). The recombinant crustacyanin subunit H_1 and H_2 with astaxanthin produced a bathochromic shift of 85–95 nm compared with natural crustacyanin subunits from *H. americanus* in complex with astaxanthin. All these results suggest that, ATX could bound to shell derived hemocyanin, but unlike the reconstruction of crustacyanin subunits, it does not bring any structural changes to the pigment–binding complex.

Hemocyanin is mainly known as oxygen transporter (van Hodle & Miller, 1995), but also functions in many other aspects like osmotic regulation (Seidl et al., 2002) and anti–fungal defense factor (Destoumieux–Garzón et al., 2001). As shown in Fig. 4–2A, hepatopancreas, hemolymph, and heart involved abundant mRNA expression for hemocyanin, indicating that the hemocyanin is synthesized mainly in these organs, then released into other tissues including epithelium. However, according to our

previous study, the hemocyanin that purified from shrimp shell does not work as an oxygen transporter but a pigment–binding function and involved into *L. vannamei* shell color change. The possible explanation is the function of a protein is correlated with the organ or tissue where it exists. Hemocyanins that were reported with oxygen transportation function and innate immune function were isolated from hepatopancreas, hemolymph or blood (van Hodle & Miller, 1995; Destoumieux–Garzón et al., 2001; Seidl et al., 2002) All these tissues or organs are mainly correlated with the respiration or immune functions during shrimp life history. There is no need to transport any oxygen or display any immune function in non–cell tissue like the shell. In nature status the main function of shrimp shell is protection: calcification is known to play a major role in making the skeleton, while the organismal coloration is mainly served as communication and camouflage (Hemmi et al., 2006; Tume et al., 2009; Kronstadt et al., 2013). According to this principle, the hemocyanin which was transferred to the exoskeleton may active as the color change function.

In protein, the covalent bond is one of the main chemical bonds to maintain its conformational stability, including Van der Waal's force, hydrogen bond, ionic bond etc. When the reconstructed pigment–binding complex was heated, the covalent bond that linked hemocyanin to ATX has been destroyed due to the denaturation of complex. At the low heating temperature range (30–45 ^{o}C), denaturation of reconstructed binding protein was significant (Table 4–2) compared with natural LvPBP75 (Table 3–2). This may be due to the interaction of artificial LvPBP75 is weaker than the natural LvPBP75. Thus, the artificial complex was much more sensitive to the low heating temperatures compared with the natural binding complex. A continuous high temperature (> 60 ^{o}C) may break this balance and brought another significant denaturation to the complex. The inter–transformation among secondary structures may explained to be the hydrogen bonds between amide groups can be promoted by temperatures, which stabilized the β types as well as the α–helical structure rather than random coil (Thomas & Dill, 1993).

Conclusively, our results revealed that ATX could bound to hemocyanin and this

pigment–binding complex had closely corresponded to *L. vannamei* shell color change. But unlike crustacyanin, ATX does not bring any structural changes to the pigment–binding complex. Pigment–binding ability of the hemocyanin that derived from shrimp shell has species– or tissue–specificity and their unique structural features play an important role during binding. Further research is needed to better understand the interaction of hemocyanin–ATX and its physiological functionality. However, previous studies on American lobster (*Homarus americanus*) shell revealed that, the red color–related pigment–binding protein was consist of 22 kDa apo protein and ATX. Thus, in next chapter, studies are mainly focused on to clarify 1) whether the low molecular weight proteins (< 40 kDa) in *L. vannamei* shell are correlated with the shrimp shell color change, 2) whether the hemocyanin–ATX binding protein (LvPBP75) is unique in *L. vannamei* or not.

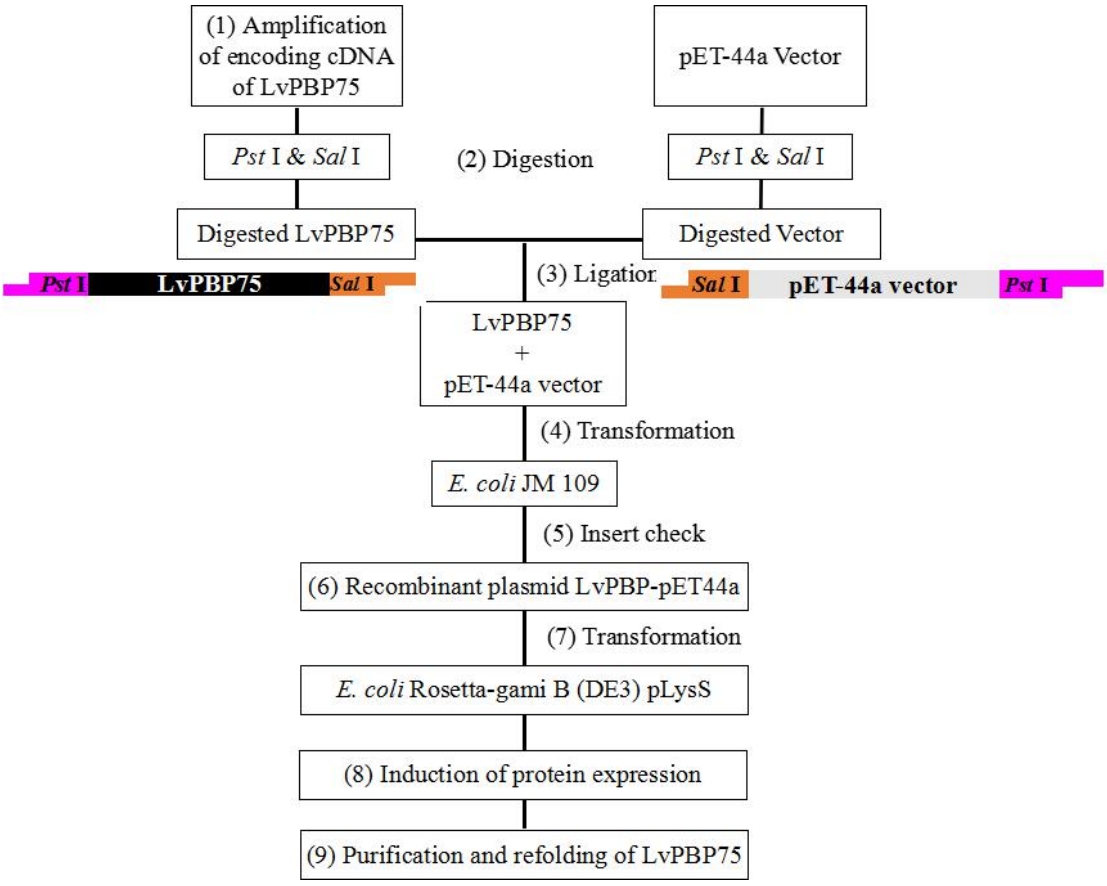

Figure 4–1 Procedure for expression of recombinant LvPBP75 (rLvPBP75).

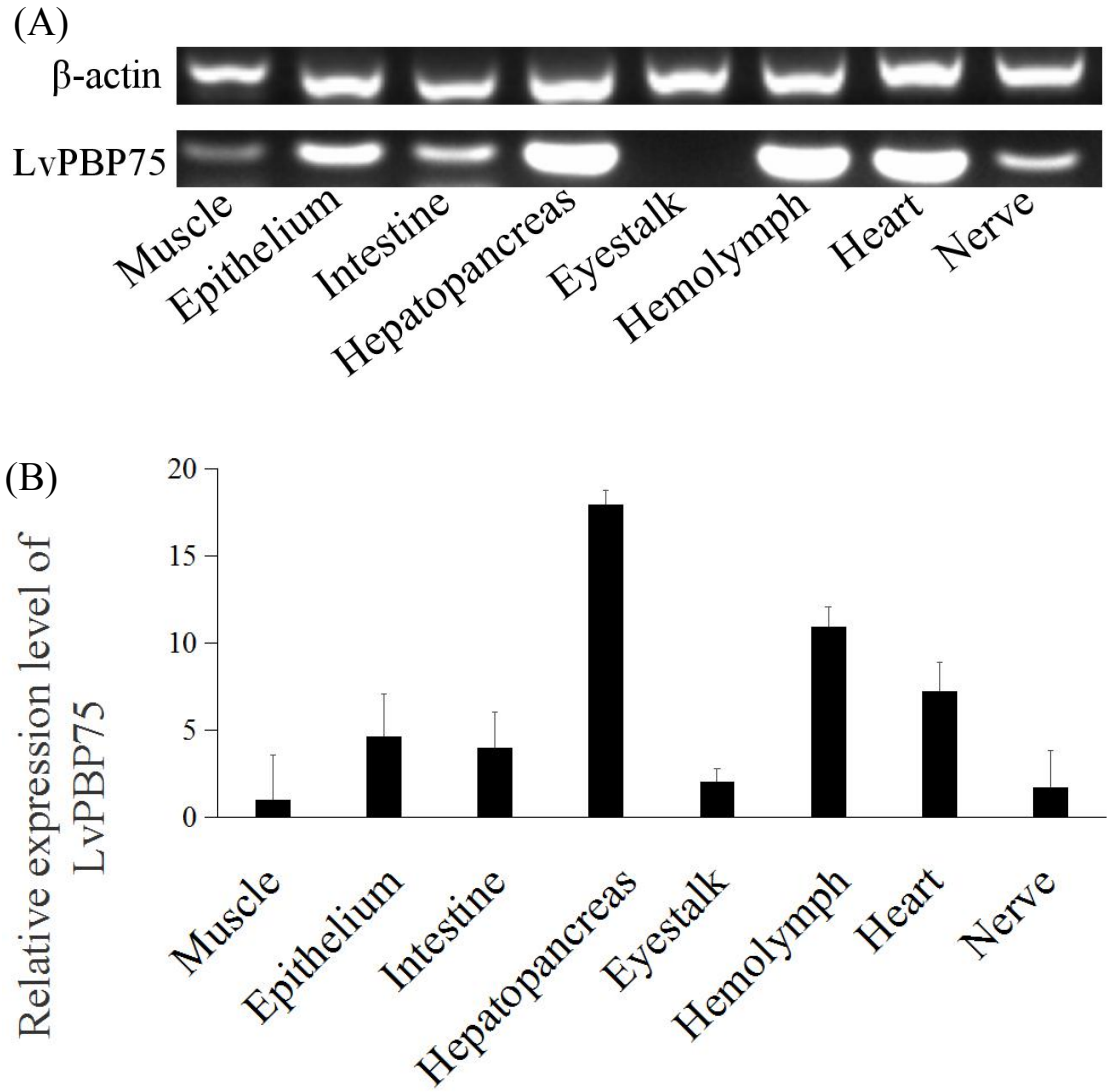

Figure 4–2 Tissue distribution of LvPBP75 mRNA in *L. vannamei*, as determined by semi–quantitative real–time PCR (A) and quantitative real–time PCR (B). LvPBP75 expression was normalized to β–actin expression. Bars represent the mean of triplicate tissue samples ± SD.

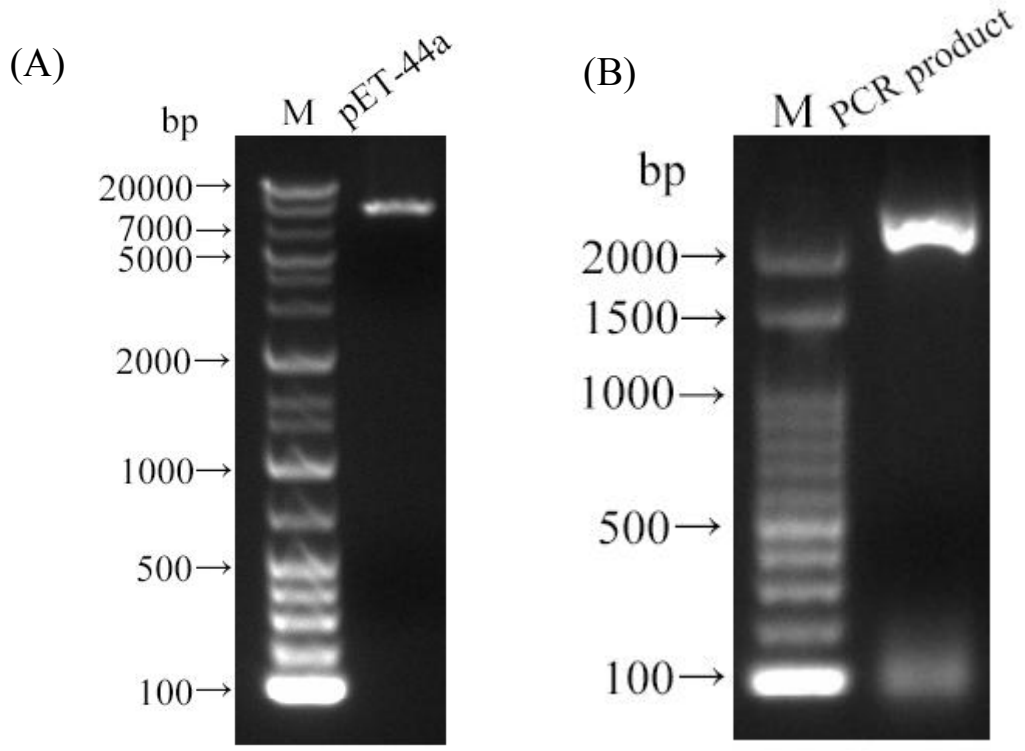

Figure 4–3 1.2% agarose gel electrophoresis of restriction enzymes digested pET–44a vector (A) and amplification of mature LvPBP75 with restriction enzyme sites (B).

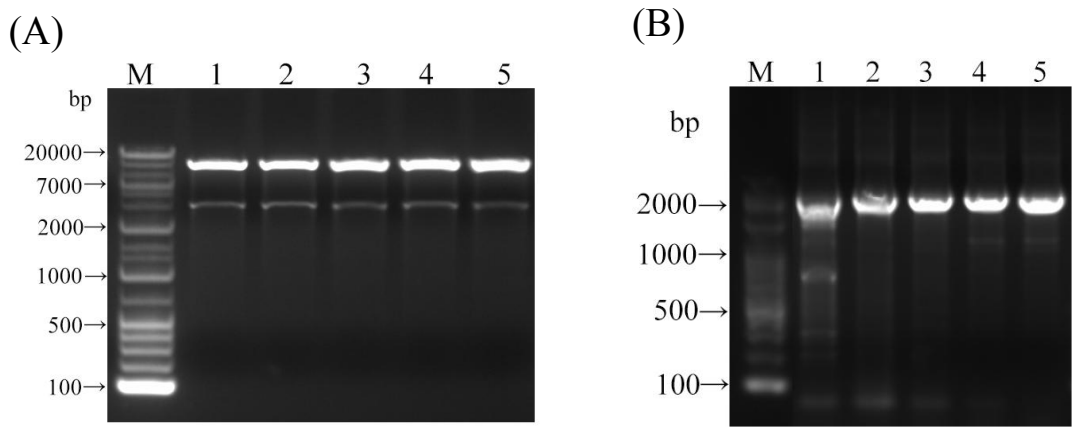

Figure 4–4 Insert check of recombinant expression vector LvPBP–pET44a. (A) LvPBP–pET44a digested by two restriction enzymes; (B) Colony PCR screening of LvPBP–pET44a using pET upstream and Colidown primers (Lane numbers mean different positive single colonies).

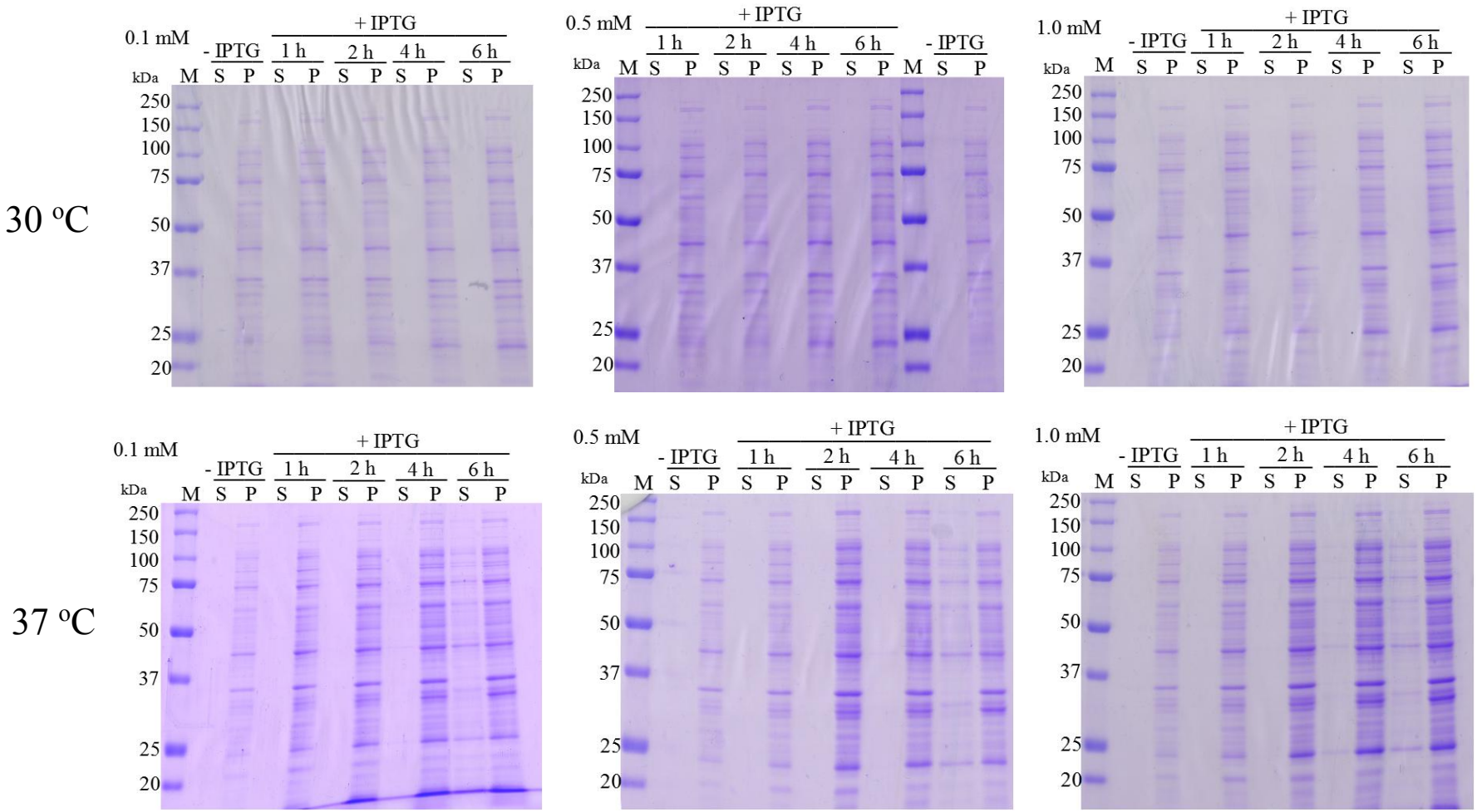

Figure 4–5 SDS–PAGE analysis of different incubation conditions: temperature (30 and 37 °C), induction time (1, 2, 4 and 6 h) and IPTG concentration (0.1, 0.5 and 1.0 mM).

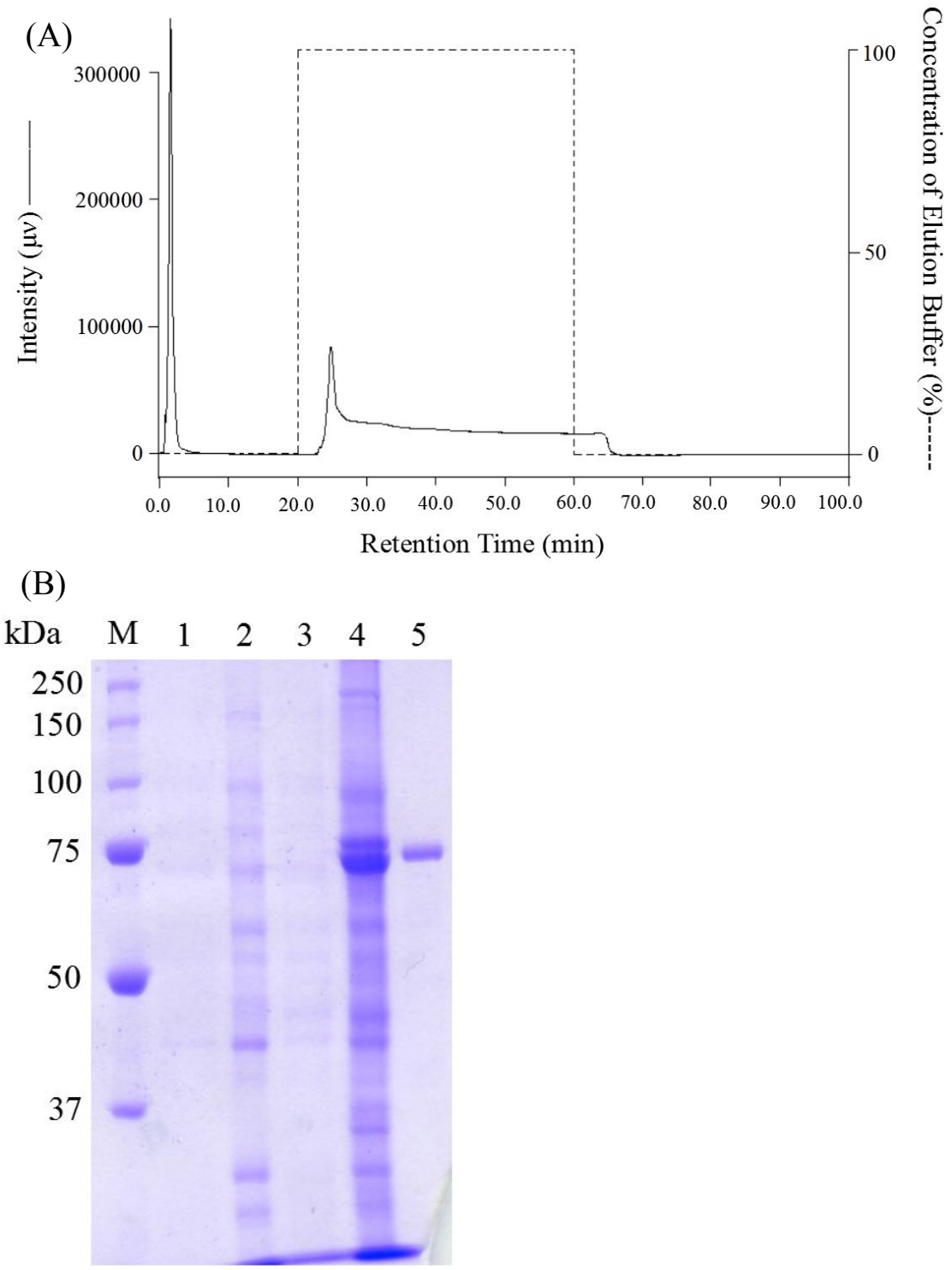

Figure 4–6 (A) Purification of rLvPBP75 on the affinity chromatography. (B) Analysis of expression and purification of rLvPBP75 by SDS–PAGE. Lanes: M, protein marker; 1, soluble fraction from non–induced *E. coli*; 2, unsoluble fraction from non–induced *E. coli*; 3, soluble fraction from IPTG–induced *E. coli*; 4, unsoluble fraction from IPTG–induced *E. coli*; 5, purified rLvPBP75.

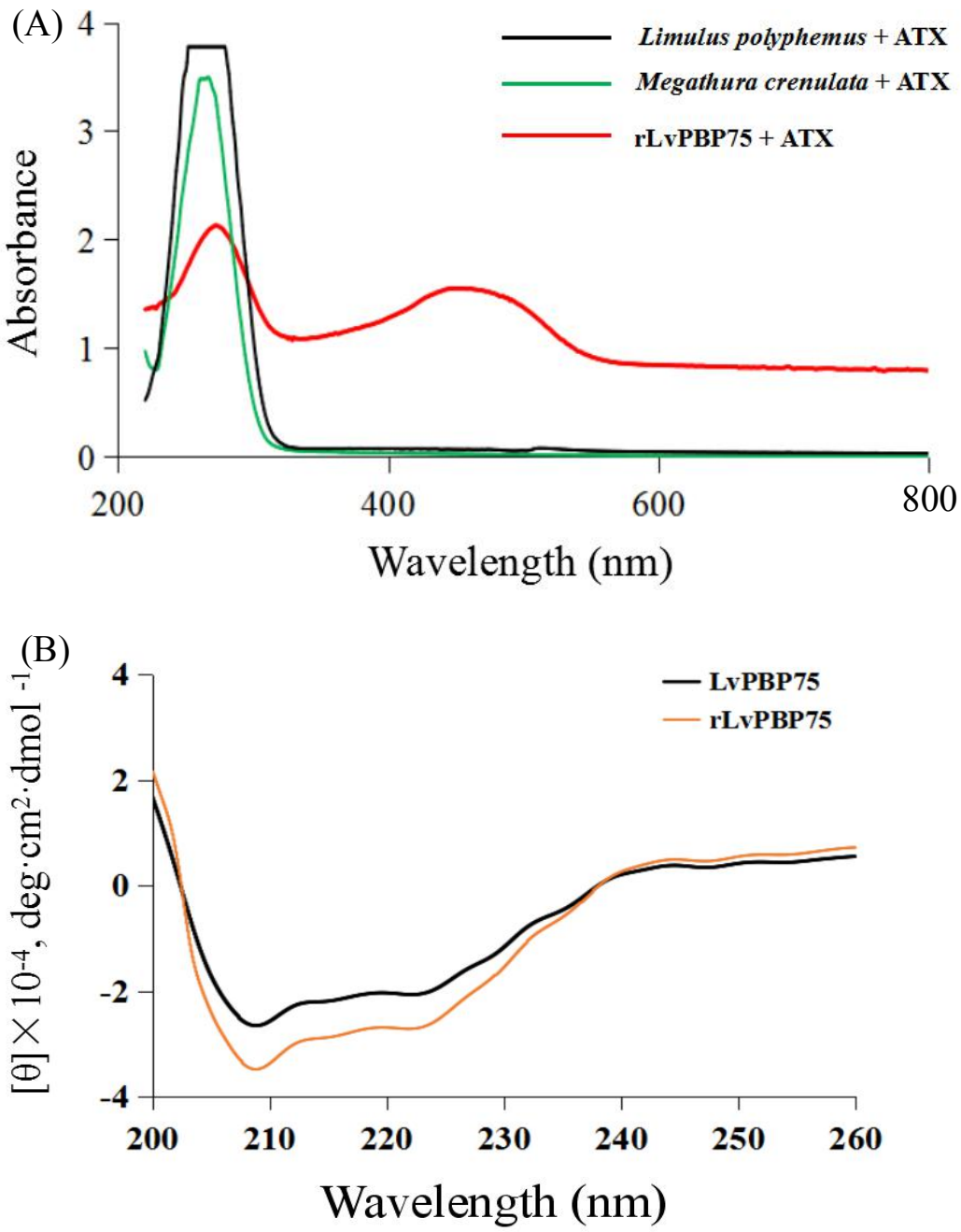

Figure 4–7 (A) The absorption spectra of hemocyanin astaxanthin binding complexes (——— *Limulus polyphemus* derived hemocyanin, ····· *Megathura crenulata* derived hemcoyanin, – · – · – recombinant LvPBP75). (B) CD spectra of LvPBP75 (▪▪▪▪) and rLvPBP75 (▬) in 20 mM phosphate buffer (pH 7.0) at room temperature.

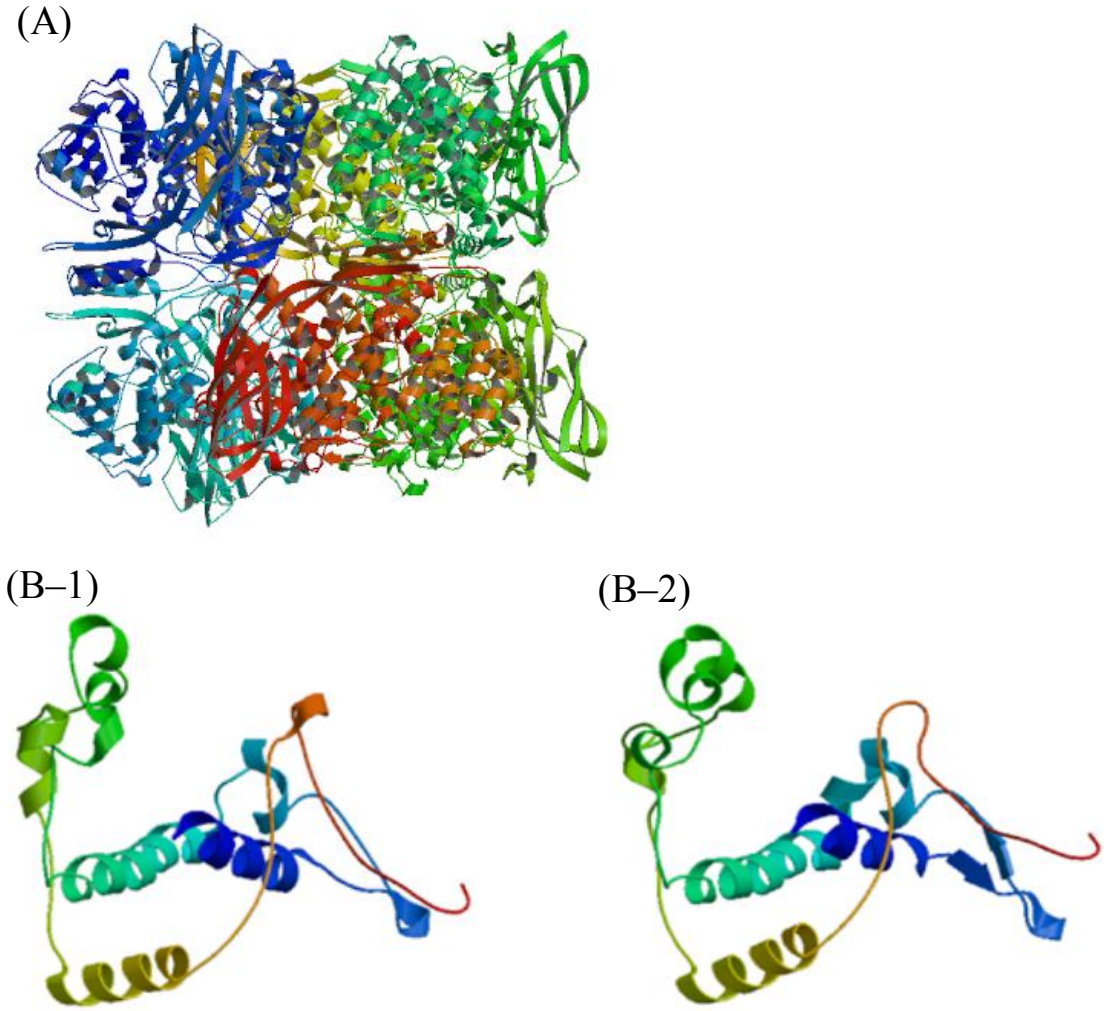

Figure 4–8 (A) 3D model of red color–related pigment–binding protein derived from the shell of *L. vannamei*, LvPBP75. (B) Ribbon diagram of LvPBP75 monomer (B–1) and *L. vannamei* hepatopancreas derived hemcoyanin monomer (B–2).

Table 4–1 Nucleotide sequences of primers used in this chapter

Primer*	Sequence (5'–3')	Objective
LvPBP–*Pst*I	AACTGCAGGGCAGATGAGGGTCTTAGTGGTTC	Mature protein amplification
LvPBP–*Sal*I	CGCGTCGACTCACTAATGAATGTGTTCCCCATG	
pET upstream	ATGCGTCCGGCGTAGA	Sequencing
Colidown	TTCACTTCTGAGTTCGGCATG	
qLvPBP–F	CGAATTCGTGATGCCATTGC	Real time PCR
qLvPBP–R	CATAGTACTGCACGTTGGGA	
β–actin–F	GACTTCGAGCAGGAGATGAC	
β–actin–R	AGGGCAGTGATTTCCTTCTGC	

(* Meaning of letters: LvPBP, LvPBP75 mature peptide amplification primer; qLvPBP, gene–specific primer for quantitative real time PCR; F, forward primer; R, reverse primer. Restriction sites (*Pst*I & *Sal*I) were underlined)

Table 4–2 Secondary structure contents of rLvPBP75–ATX under different heat treatments

	α–helix (%)*	β–sheet (%)	β–turn (%)	Random coil (%)
Control	53.3 ± 0.262[a]	18.6 ± 0.262[a]	14.4 ± 0.216[a]	14.9 ± 0.287[a]
30 ºC	40.5 ± 0.330[b]	23.1 ± 0.330[b]	20.9 ± 0.327[b]	16.7 ± 0.327[b]
45 ºC	38.5 ± 0.309[c]	25.3 ± 0.309[c]	18.4 ± 0.330[c]	18.5 ± 0.330[c]
60 ºC	29.4 ± 0.340[d]	28.5 ± 0.327[d]	27.8 ± 0.356[d]	14.9 ± 0.330[d]
80 ºC	22.9 ± 0.262[e]	31.8 ± 0.294[e]	25.3 ± 0.262[e]	20.2 ± 0.309[e]
100 ºC	14.6 ± 0.330[f]	30.3 ± 0.327[f]	28.4 ± 0.330[f]	27.0 ± 0.330[f]

(* Means followed by different small letters within the same column differ significantly at p = 0.05 compared with unheated samples. Data expressed as means ± standard deviation, n=3)

Chapter 5 Specificity analysis of red color–related protein LvPBP

5.1 Introduction

Crustaceans like shrimps and crabs have a remarkable red color change during cooking. In addition to reflecting the freshness of crustaceans, the red color change also plays a significant role in consumer acceptability of commercial crustacean species. Studies on crustacean shell color change were mainly focused on lobsters like American lobster (*Homarus americnaus*), European lobster (*H. gammarus*), and Western Australia lobster (*Panulirus cygnus*). Pioneering study on lobster shell revealed that this well–known red color change is due to the release of pigments from denatured PBPs, named crustacyanin (Wald & Nathanson, 1948; Zagalsky, 1985; Chayen et al., 2003; Durbeej & Eriksson, 2003; Elizabeth et al., 2009; Wade et al., 2009). Crustacyanin extracted from a lobster shell comprises apoproteins and astaxanthin (Wald & Nathanson, 1948). The predominant PBP in the lobster shell is α–crustacyanin (λmax: 632 nm, ~320 kDa), which contains 16 protein subunits and 16 astaxanthin molecules (Zagalsky, 1985; Chayen et al., 2003). After irreversible dissociation, β–crustacyanin (λmax: 585 nm, ~40 kDa) appears; eight units of β–crustacyanin can form one unit of α–crustacyanin. Both α– and β–crustacyanin can easily dissociate into apoproteins (~20 kDa) under experimental conditions (Elizabeth et al., 2009). Wade et al. (2012) reported that the red color–related proteins found in *P. monodon* were ranged from 21–100 kDa. However, Cremades et al., (2003) separated two different types of red color–related proteins, carotenoprotein–1 and carotenoprotein–2 from crayfish byproducts. Both proteins showed various molecular weights. Klomklao et al. (2009) extracted two different pigment–binding proteins with molecular weight around 211 and 45 kDa, respectively from *P. monodon*.

However, in the previous chapters, a novel red color–related pigment–binding protein, LvPBP75 was purified from the shell of *L. vannamei*. It was identified as hemocyanin–ATX complex but not the reported crustacyanins. Yet despite the increase

in the knowledge of PBPs in crustaceans, there has been few progress in the specificity analysis of the red color–related PBPs among shrimp species. Thus, the aim of this chapter was to demonstrate: 1) the relationship between small molecular weight proteins (< 40 kDa) and the red color change in *L. vannamei*, 2) specificity of LvPBP75 among some shrimp species.

5.2 Materials and Methods

5.2.1 Materials

All samples were collected in frozen status directly from aquaculture farm. After species confirmation by using 16s rRNA sequencing method, the shells were treated as described in 2.2.1. The crude red color–related proteins were collected for further purification.

5.2.2 Relationship between small molecular weight proteins and red color change in *L. vannamei* shrimp

The crude water–soluble proteins derived from *L. vannamei* shell was separated into two parts: larger and smaller than 50 kDa, by using a 50K Amicon Ultra Centrifugal Device (Merck Millipore Ltd., Tullagreen, Carrigtwohill Co. CORK, Ireland). The low molecular weight fraction (< 50 kDa) was subjected (0.5 ml with a concentration of 4.03 mg/ml) to ion exchange HPLC on an IEC QA–825 column (8 × 75 mm, Showadenko, Tokyo, Japan), the column was equilibrated with 20 mM phosphate buffer (pH 7.0) and developed by a linear gradient of NaCl (0–1 M over 70 min) in 20 mM phosphate buffer (pH 7.0) at a flow rate of 0.5 ml/min.

5.2.3 Purification of red color–related PBP from the shell of kuruma shrimp, American lobster, and Japanese spiny lobster

Purification of red color–related PBP from the shell of kuruma shrimp

(*Marsupenaeus japonicus*), American lobster (*Homarus americanus*), and Japanese spiny lobster (*Panulirus japonicus*) was followed as described in 2.2.2 with slight changes. In *M. japonicus*, the crude water–soluble proteins were applied to gel filtration HPLC on a Superdex 75 GL column (1 × 30 cm, GE Healthcare Biosciences, UK) that was equilibrated and washed with 0.15 M NaCl/20 mM phosphate buffer (pH 7.0) at a flow rate of 0.5 mL/min. The red color–related fraction No. 1 was collected for the further purification using ion exchange HPLC on an IEC QA–825 column (8 × 75 mm, Showadenko, Japan), the column was equilibrated with 20 mM phosphate buffer (pH 7.0) and developed by a linear gradient of NaCl (0–1 M over 70 min) in 20 mM phosphate buffer (pH 7.0) at a flow rate of 0.5 ml/min.

The crude water–soluble fraction derived from *H. americanus* shell was directly subjected to HPLC on an IEC QA–825 column (8 × 75 mm, Showadenko, Japan), the column was equilibrated with 20 mM phosphate buffer (pH 7.0) and developed by a linear gradient of NaCl (0–1 M over 65 min) in 20 mM phosphate buffer (pH 7.0) at a flow rate of 0.5 ml/min.

In the condition of *P. japonicus*, the crude water–soluble proteins were applied to gel filtration HPLC on a Superdex 200 GL column (1 × 30 cm, GE Healthcare Biosciences, UK) that was equilibrated and washed with 0.15 M NaCl/20 mM phosphate buffer (pH 7.0) at a flow rate of 0.7 mL/min. The red color–related fraction No. 4 was collected for the further purification using ion exchange HPLC on an IEC QA–825 column (8 × 75 mm, Showadenko, Japan), the column was equilibrated with 20 mM phosphate buffer (pH 7.0) and developed by a linear gradient of NaCl (0–1 M over 70 min) in 20 mM phosphate buffer (pH 7.0) at a flow rate of 0.7 ml/min.

5.2.4 Electrophoretic analysis of shell derived PBPs

Protein pattern was analyzed by SDS–PAGE on a 5–20% precast gel (Atto, Tokyo, Japan) with a WSE–1025 cPAGE Ace Twin (Atto, Japan) compact PAGE system. Before SDS–PAGE, the proteins were mixed with an equal volume of 0.125 M

Tris–HCl buffer (pH 6.8) containing 4% SDS and 10% 2–mercaptoethanol and heated in a boiling water bath for 5 min. After being run, the gel was stained with a Rapid Coomassie Brilliant Blue (CBB) R–250 (Kanto Chemical, Japan), and Precision Plus Protein Standards (Bio–Rad Laboratories, USA) were used as a reference.

5.2.5 Analysis of protein color change

Investigation of the color changes were performed by heating at temperatures of 100 °C for 10 min. Unheated samples were set as controls. Temperatures and color changes were monitored and recorded. Color changes were investigated by using the colorimeter (CLR–7100F, Shimadzu, Japan). The results are expressed as L* (brightness), a* (+a red, –a green), and b* (+b yellow, –b blue).

5.2.6 Statistical analysis

Statistical analysis of all data were followed with the description in 2.2.6.

5.3 Results

5.3.1 Relationship between small molecular weight proteins and red color change in *L. vannamei* srhimp

After centrifugation, > 50 kDa fraction showed a dark blue color, while the flow through (< 50 kDa) showed a transparent color (Data not shown). No significant red color change could be detected in < 50 kDa fraction after heating at 100 ^{o}C for 10 min (Table 5–1). As shown in Fig. 5–1 total 5 peaks were obtained and a clear band with molecular weight around 30 kDa was found in peak 1 & 3. However, after heat treatment, no significant red color change could be detected (Data not shown). The results suggested that, red color change was not correlated with small molecule protein in *L. vannamei*.

5.3.2 Purification of red color–related proteins derived from kuruma shrimp, American lobster, and Japanese spiny lobster

As shown in Fig. 5–2A, the proteins larger than 50 kDa were disappeared within the red color change in kuruma shrimp.The crude water soluble proteins were first applied to gel filtration HPLC on a Superdex 75 column, total 5 fractions were collected (Fig. 5–3). Fraction No.1 showed a significant red color change and then subjected to the further purification using ion exchange chromatography. As shown in Fig. 5–4A, 7 fractions were obtained, only peak 4 and 6 showed detectable red color change. And one clear band with molecular weight around 75 kDa was found in peak 4, which was in accordance with results obtained from *L. vannamei*. In red color changed fraction No. 6, except the 75 kDa band, two other proteins were found, 250 and 37 kDa. The 250 kDa complex may correspond to the aggregates of myofibrillar–like proteins. Thus, it shows no relationship with red color change. To understand whether the 35 kDa protein was correlated with the red color change, gel filtration fraction No. 2 was subjected to ion exchange purification and the results were showed in Fig. 5–4B. Total 8 fractions were obtained and the pure 35 kDa protein was obtained in fraction No. 3, but it showed no color change ability (Data not shown). These results suggested that, in kuruma shrimp, the red color change was correlated with the 75 kDa protein.

The red color–related proteins were purified from American lobster shell using ion exchange chromatography, total 8 fractions were obtained (Fig. 5–5A). After heat treatment, fraction No. 1, 2, 3, and 5 showed significant red color change (Table 5–2). SDS–PAGE analysis revealed that lane 3 showed a clear band with molecular mass around 22 kDa, it matches the previous description of β–crustacyanin (Fig. 5–5B). α–crustacyanin was confirmed in the crude proteins (molecular mass around 180 kDa). The unexplained bands showed in lane 1 suggest the dissociation of α–crustacyanins had occurred under the experimental conditions. It was notable that the 75 kDa protein was also found in the red color changed fraction No.1.

To understand whether the 75 kDa protein is correlated with red color change in

American lobster shell or not. The fraction No. 1 was divided into two parts, larger and smaller than 50 kDa by using a 50K Amicon Ultra Centrifugal Device (Merk Millipore, Ireland). After heat treatment, red color change could only be detected in lower than 50 kDa fraction (Data not shown). As shown in Fig. 5–5C, β–crustacyanin band could not be found in < 50 kDa fraction, which means the dissociation of β–crustacyanin had occurred under the experimental conditions. The results suggesting that, in American lobster, the red color change was not correlated with 75 kDa protein and crustacyanins could dissociated under the experimental conditions.

Finally, the red color-related proteins were purified from Japanese spiny lobster. As shown in Fig. 5–6A, total 4 peaks were obtained from gel filtration HPLC. Only fraction No. 4 which was eluted between the retention time of 70 to 100 min showed a significant red color change (Data not shown). Then it was concentrated and subjected to the ion exchange HPLC. As shown in Fig. 5–6B, two main peaks were obtained and only fraction No.1 showed a significant red color change after heat treatment. SDS–PAGE analysis revealed that only one protein band with molecular weight around 75 kDa was found (Fig. 5–6B insert). All the results indicated that, in Japanese spiny lobster, the red color change was correlated with 75 kDa protein.

5.4 Discussion

The pigment–binding protein complex, called crustacyanin, were originally identified from the European lobster (*Homarus gammarus*) and were grouped into the broad classes based on amino acid composition, electrophoretic mobility and peptide mapping (Cheesman et al., 1967; Quarmby et al., 1977; Budd et al., 2017). The native crustacyanin, α–crustacyanin, has a molecular weight of about 320 kDa, which is a multi–macromolecular complex consist of eight β–crustacyanin (Chayen et al., 2003). As shown in Fig. 2–3, slight changes were detected in the proteins located less than 45 kDa when heated at 100 ^{o}C for 10 min. These proteins might correspond to some free amino acids oligopepetides or dissociations of large–sized proteins (Cremades et al.,

2003; Elizabeth et al., 2003; Gamiz–Hernandez et al., 2015). Meanwhile, the < 50 kDa fraction showed no red color change (Table 5–1) and the purified small molecular weight proteins showed no relationship with red color change (Fig. 5–1).

Pigment–binding proteins derived from different crustaceans possess various molecular weights. As reported in lobster shell, they were ranged from 40–90 kDa (Simpson et al., 1993). Wade et al., (2012) found that the red color–related proteins in black tiger shrimp (*Penaeus monodon*) were located from 21–100 kDa. The red color–related protein purified from kuruma shrimp and Japanese spiny lobster showed same molecular weight around 75 kDa (Fig. 5–4 & 5–6), which was in accordance with the results obtained from *L. vannamei*. Meanwhile, the small molecular weigh proteins showed no relationships with red color change on these shrimp. However, the red color–related protein with molecular weight around 22 kDa was purified from the shell of American lobster (Fig. 5–5). Interestingly, the protein with molecular weight around 75 kDa showed no red color change ability in American lobster shell.

Among crustacean species, the functional properties of proteins are correlated with their structural features. A putative tertiary structure of β–crustacyanin was proposed by Keen (Keen et al., 1991a, b) as a molecular model based on the coordinated from the solved crystal structures of retinol–binding protein (Newcomer et al., 1984), β–lactoglobulin (Papiz et al., 1986) and bilin–binding proteins (Huber et al., 1987; Holden et al., 1987). The predicted structures have a β–barrel structure typical of the lipocalins and consisting of eight antiparallel β–strands arranged in two orthogonal β–sheets to form a calyx. The β–crustacyanin model also suggested that it could bound with two ATXs.

Chemical reconstitution studies revealed that both 4 and 4' keto groups are essential for the formation of β–crustaycanin–type complex: they are likely to be conjugated with the polyene chain (Chayen et al., 2003). While the hydroxy groups at these positions are not effective and they are not involved in the spectral shift phenomenon, but the increased polarity make it easier for the end groups to be positioned correctly in the binding site (Castillo et al., 2013, Chayen et al., 2003).

The ^{13}C MAS NMR together with Stark spectroscopy results suggested and essentially symmetrical polarization of the ATX in crustaycanin with some asymmetry superimposed on the two halves of the chromophore (Chayen et al., 2003). The bathochromic shift of crustacaynins was attributed to perturbation of the ground–state electronic structure of the pigment caused and this effect is quantitatively different correlated with the binding ATXs (Chayen et al., 2003).

Arthropod hemocyanins are built as multiples of hexamers, each hexamer made of monomers of about 75 kDa (van Holde et al., 2001). Sequence analysis revealed that arthropod hemocyanin may contain several variants of the common monomer sequence (Voit et al., 2000), each variant occupying a specific position in the intact molecule. The sequences are sufficiently similar to each other and all arthropod hemocyanin subunits may have a similar tertiary structure (van Holde et al., 2001).

However, molluscan hemocyanins are built on an entirely different way (van Holde et al., 2001). The polypeptide chains are about 350–450 kDa, which consists of seven or eight globular peptide strands (Miller et al., 1998; Lieb et al., 2000). In the blood of cephalopod molluscs, like squids, the circulating hemocyanin shows decamers. While in some other molluscs (mainly gastropods), dimers or higher oligomers of these decamers could be detected (Miller et al., 1998; Lieb et al., 2000). It was notable that, the hemocyanin unit derived from arthropod and molluscan have a quite different tertiary structure (van Holde et al., 2001). The molluscan subunit is smaller than the one derived from arthropod. A highly rich helical domain and largely b–sheet structure could be detected in molluscan derived hemocyanin subunit (van Holde et al., 2001).

In conclusion, the *L. vannamei* shell color change was not correlated with < 50 kDa proteins. The 75 kDa protein was correlated with the red color change on the surface of *L. vannamei*, *M. japonicus*, and *P. japonicus*, while the 22 kDa protein was correlated with the red color change on *H. americanus*. The red color change on shrimp surface was not found to be associated with these two proteins simultaneously. The red color–related pigment–binding protein LvPBP75 is not species–specific,

further investigation is necessary to understand the red color–related proteins among a variety of crustacean species.

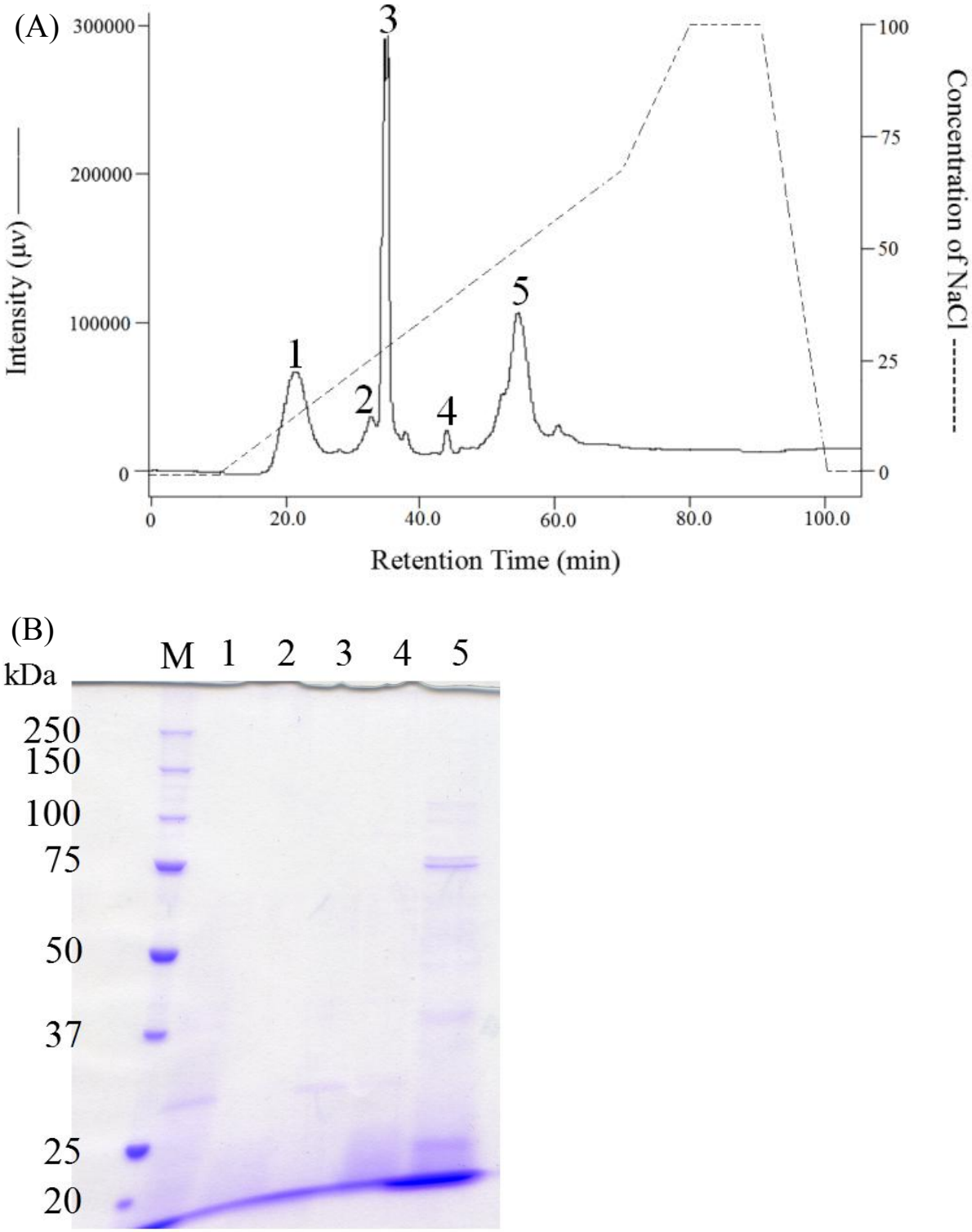

Figure 5–1 Purification (A) and protein pattern (B) of small molecule weight proteins derived from the shell of *L. vananmei* using ion exchange HPLC on IEC QA–825 column.

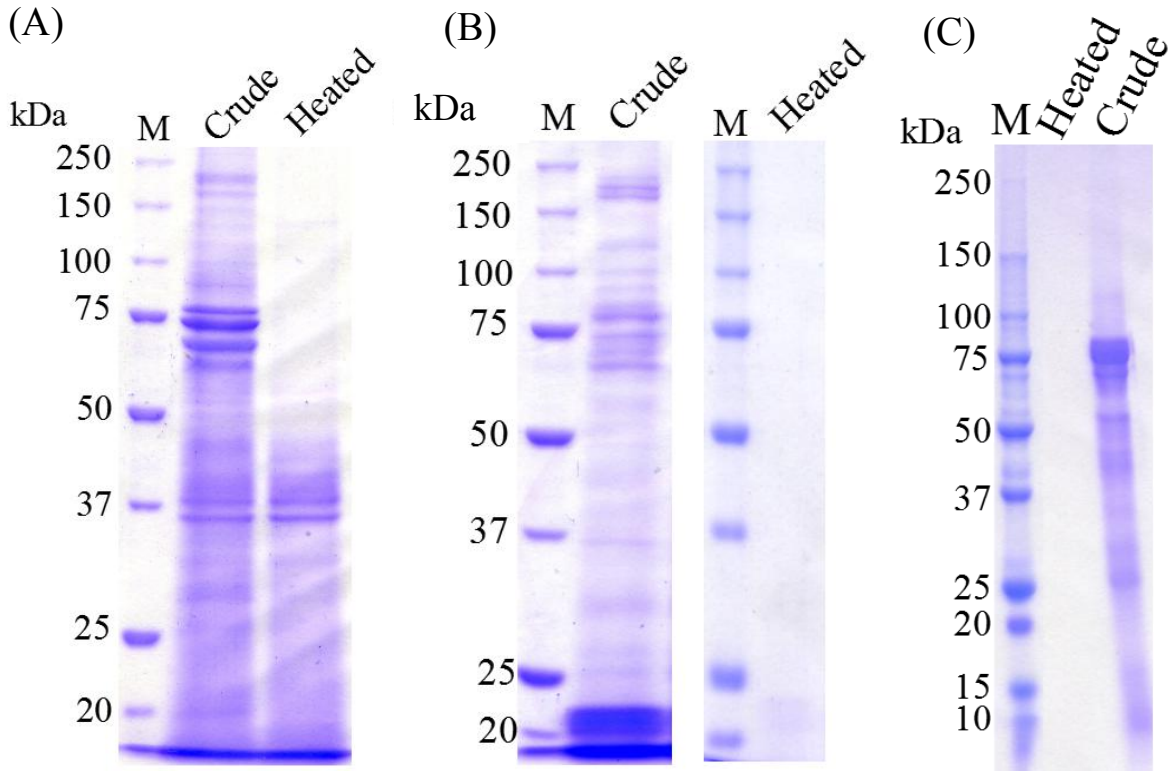

Figure 5–2 Protein files of crude water soluble proteins derived from kuruma shrimp (A), American lobster (B) and Japanese spiny lobster (C) after heated at 100 ^{o}C, 10 min (Lane M: marker).

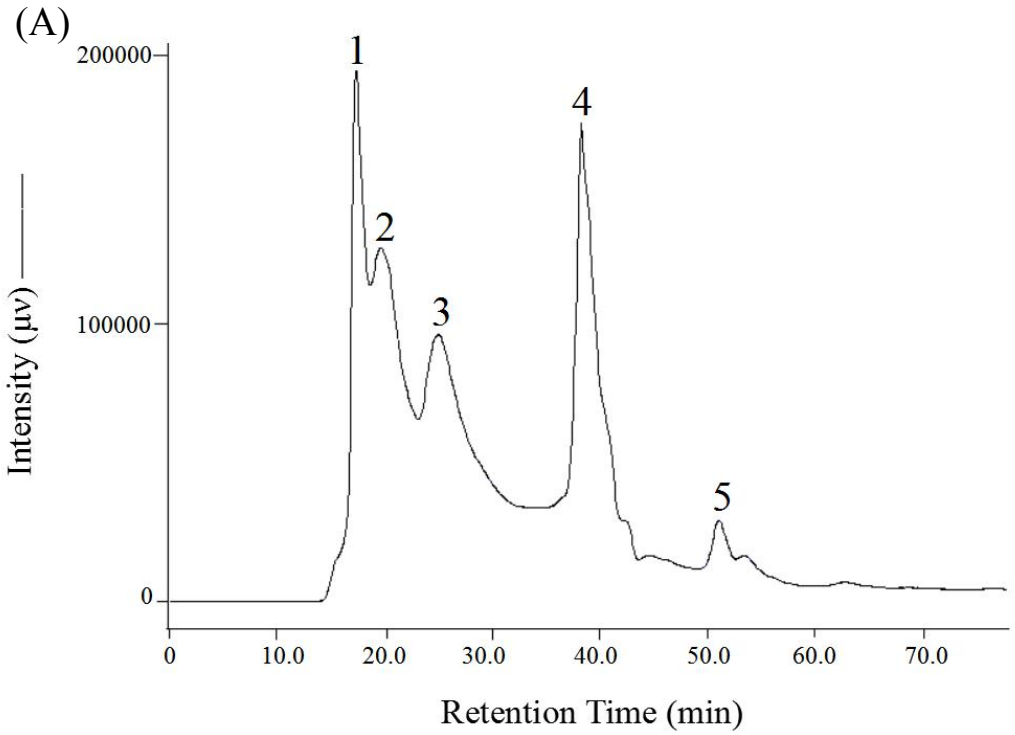

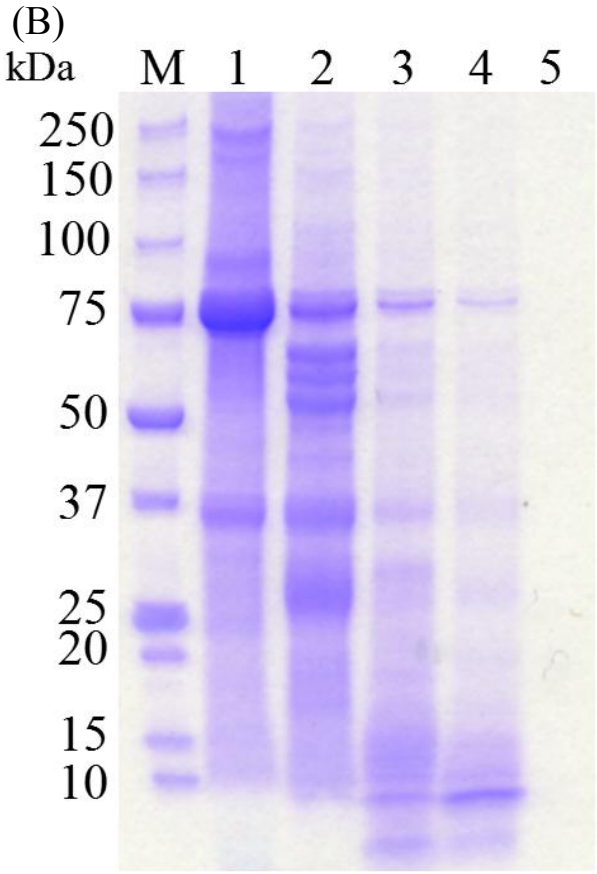

Figure 5–3 Purification (A) and protein pattern (B) of red color–related protein derived from kuruma shrimp shell by using Superdex 75 gel filtration column.

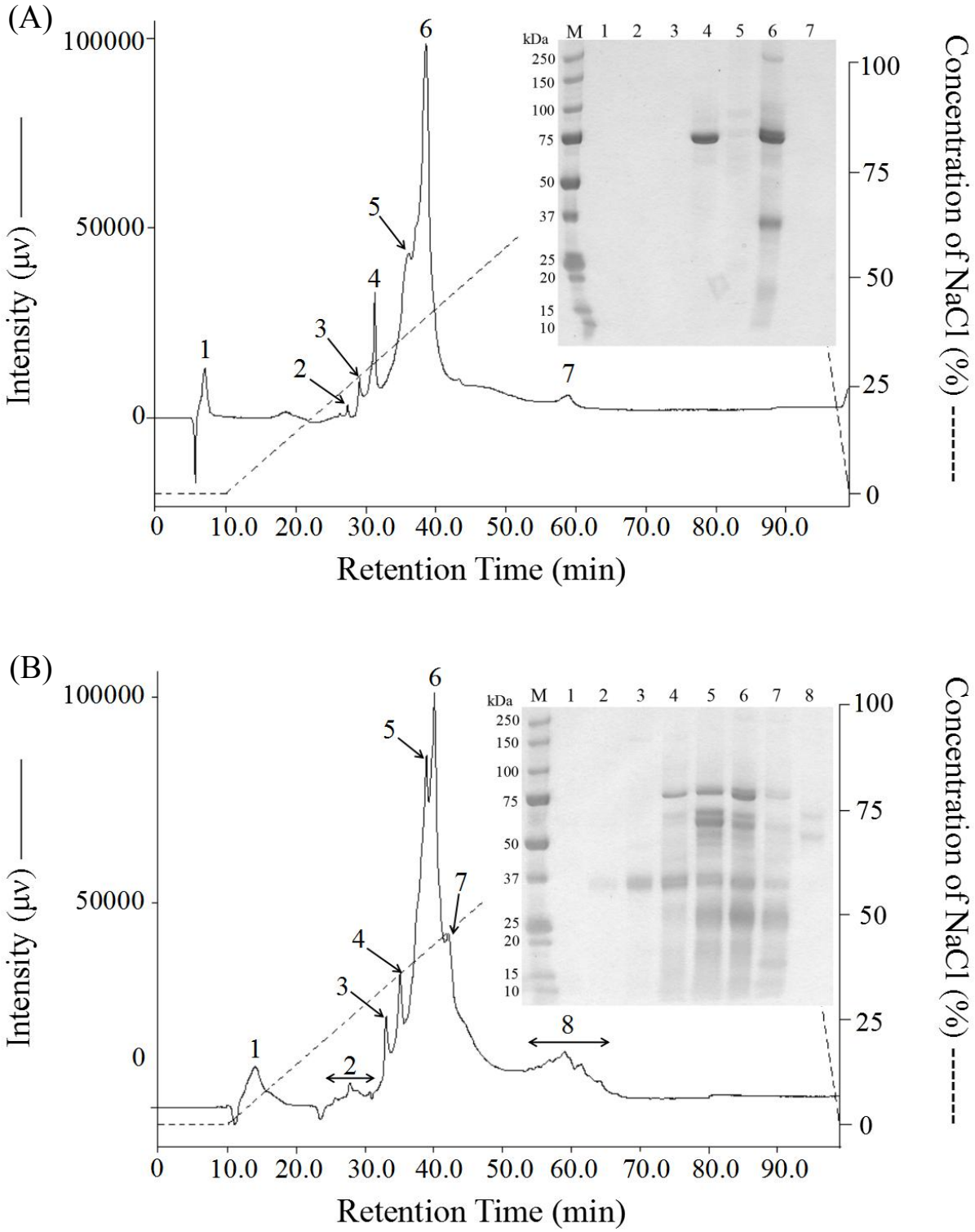

Figure 5–4 Purification of gel filtration derived fraction No.1 (A) and fraction No.2 (B) using ion–exchange HPLC on IEC QA–825 column. The inserts were protein patterns of purified fractions.

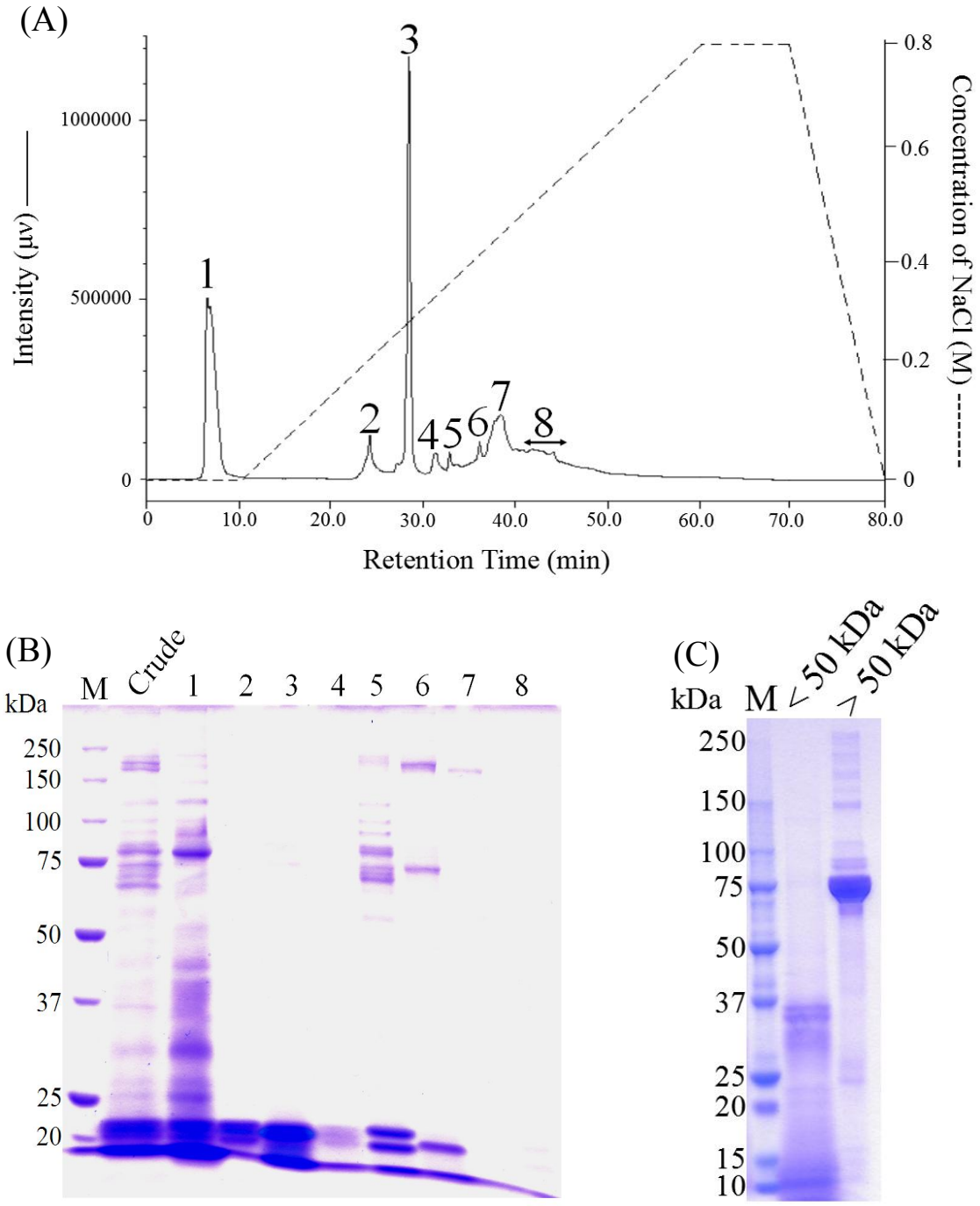

Figure 5–5 Purification (A) and SDS–PAGE analysis (B) of red color–related proteins derived from American lobster shell using ion–exchange HPLC on an IEC QA–825 column. (C) Protein files of ultracentrifugation fractions of fraction No. 1 which was collected from ion exchange HPLC.

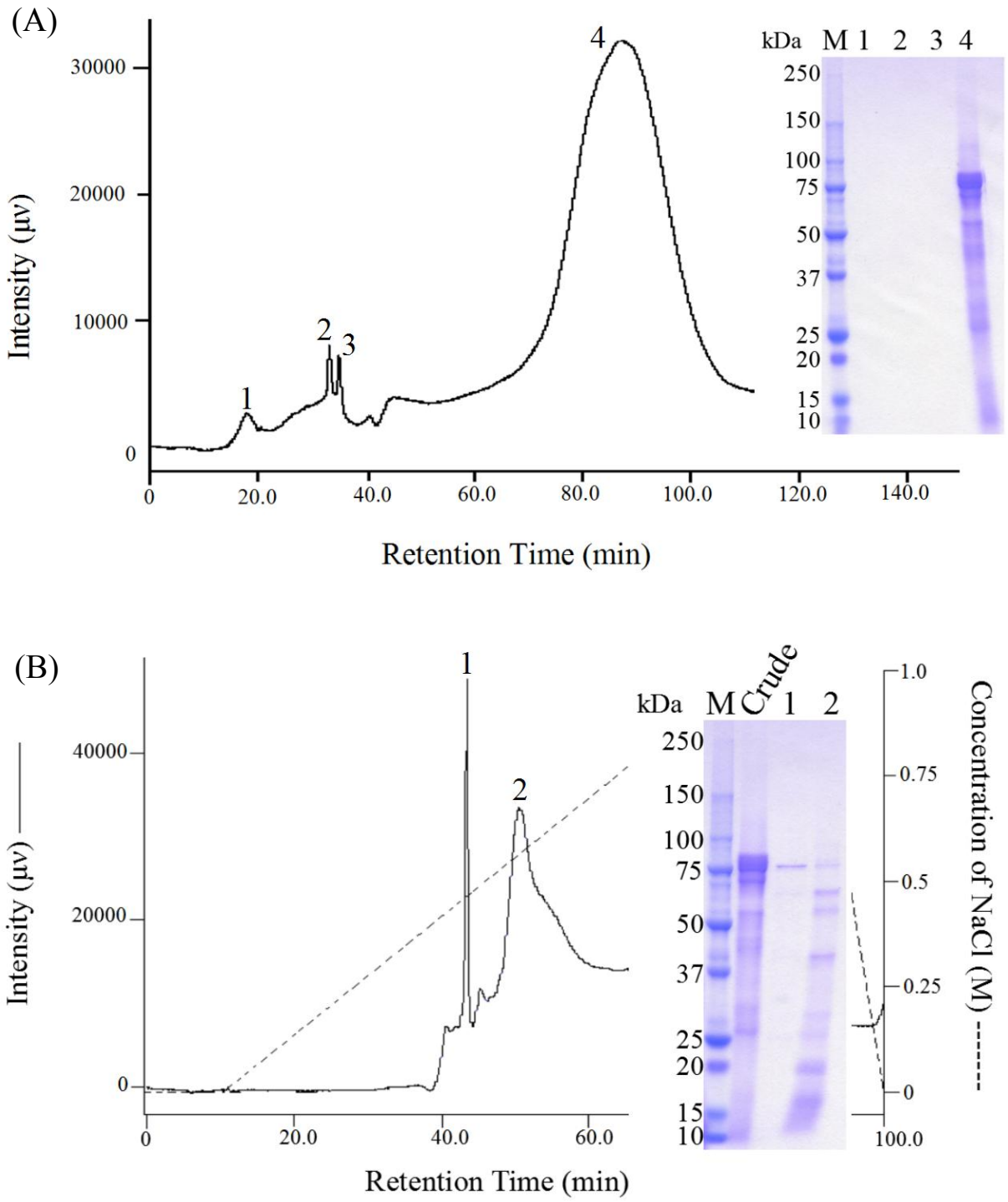

Figure 5–6 Purification of the red color–related proteins derived from Japanese spiny lobster shell using gel filtration HPLC on a Superdex 200 column (A) and ion–exchange HPLC on an IEC QA–825 column (B). The inserts were protein patterns of purified fractions.

Table 5–1 Color changes of different fractions (</> 50 kDa) derived from the crude water–soluble proteins of *L. vannamei*

	> 50 kDa		< 50 kDa	
	Before	After	Before	After
L*	5.87±0.009	3.66±0.005	5.54±0.005	5.68±0.009
a*	–0.27±0.009	0.44±0.009	–0.16±0.005	–0.17±0.009
b*	0.28±0.012	1.36±0.005	1.32±0.017	1.34±0.005

Table 5–2 Color changes of fractions purified from American lobster by using IEC QA–825 column (Upper: before heat treatment, Lower: 100 ^{o}C, 10 min. 1–8: fraction numbers)

	1	**2**	**3**	**4**	**5**	**6**	**7**	**8**
L*	4.87±0.009	5.66±0.005	5.54±0.005	5.68±0.009	5.14±0.009	5.23±0.008	4.12±0.016	5.34±0.009
a*	–0.27±0.009	–0.24±0.009	–0.16±0.005	–0.17±0.009	–0.17±0.009	–0.15±0.009	–0.59±0.012	–0.23±0.012
b*	0.28±0.012	1.36±0.005	1.32±0.017	1.34±0.005	1.33±0.021	1.24±0.005	0.38±0.008	1.49±0.012

	1	**2**	**3**	**4**	**5**	**6**	**7**	**8**
L*	4.87±0.012	4.37±0.005	4.56±0.009	5.96±0.014	4.14±0.014	3.73±0.005	3.64±0.012	4.97±0.005
a*	0.11±0.012	0.15±0.009	0.03±0.012	–0.20±0.014	–0.14±0.005	–0.17±0.014	0.04±0.009	–0.10±0.009
b*	1.72±0.009	1.53±0.014	1.55±0.014	1.40±0.019	1.25±0.014	0.93±0.014	1.06±0.024	1.12±0.005

Chapter 6 Summary of main finding and discussion

6.1 Summary

1) A novel red color–related protein was purified from the shell of *L. vannamei* using ammonium sulfate precipitation, gel filtration, and anion exchange HPLC. Gel filtration HPLC and SDS–PAGE analysis demonstrated that the pure protein has a molecular mass of ~75 kDa. It was a homogenous monomer with purity more than 90%. It was identified as a combined complex of hemocyanin and astaxanthin, but not the previous described crustacyanin in lobster shell.

2) On the basis of the partial amino acid sequences determined by peptide mass fingerprinting, a full–length cDNA of 2,183 bp including an ORF of 1,986 by that encodes 662 amino acid residues was cloned. A blast analysis revealed that it shares nearly 80% similarity with hemocyanins derived from *L. vannamei*. Circular dichroism analysis illuminated that it is a protein rich in α–helix conformation. This red color–related protein was a thermal sensitive protein, color changes of this protein can be promoted after being subjected to conditions of high concentrations of NaCl, acidic or alkaline pH, and high concentrations of alcohols. The results suggested a novel function of hemocyanin as binding with pigment and involved in *L. vannamei* shell color change.

3) Tissue distribution revealed that LvPBP75 has the highest expression level in hepatopancreas, mediate level in heart, hemolymph, epithelium, and intestine, and the lowest in eyestalk, nerve, and muscle. Reconstruction and structural analysis revealed that astaxanthin could bound to the hemcoyanin derived from the shell of *L. vannamei*, but not the hemocyanins derived from hepatopancreas or hemolymph from other invertebrates. The results suggested that the pigment–binding ability of hemocyanins has tissue– or species–specificity and their unique structural features play an important role during binding.

4) The small molecular weight proteins (< 40 kDa) were not correlated with the shell color change in *L. vannamei*. The 75 kDa protein was correlated with the red

color change on the surface of *L. vannamei*, *M. japonicus*, and *P. japonicus*, while the 22 kDa protein was correlated with the red color change on *H. americanus*. The results suggested that the red color change on *L. vannamei* surface is mainly correlated with LvPBP75 and it is not specific in *L. vannamei*.

6.2 Discussion

Crustaceans like shrimps and crabs have a remarkable red color change during cooking. In addition to reflecting the freshness of crustaceans, the red color change also plays a significant role in consumer acceptability of commercial crustacean species.

Pigment–binding proteins derived from different crustacean species show different relationships with the red color change. In the lobster shell, they ranged from 40–90 kDa (Buchwald & Jencks, 1968; Simpson et al., 1993). However, Wade et al. (2012) reported that the proteins found in black tiger shrimp *(P. monodon*) ranged from 21–100 kDa. Cremades et al. (2003) separated two different types of pigment–binding proteins, carotenoprotein–1 and carotenoprotein–2, from crayfish (*Procambarus clarkii*) by–products by using a solid filtration method. Carotenoprotein–1 has molecular mass from less than 10 kDa to more than 400 kDa. Meanwhile, carotenoprotein–2 comprises two main proteins weighing 40 and 22 kDa, respectively, followed by a series of proteins with small molecular masses. Elizabeth et al. (2009) found two main pigment–binding proteins with molecular masses around 40 and 300 kDa from *J. lalandii* shell, respectively. In this study, a novel red color–related protein with the molecular weight around 75 kDa was found in the shell of *L. vannamei*.

LvPBP75 was identified as hemocyanin by peptide mass finerprinting and cDNA analysis, which could bound with pigment. Hemocyanin is mainly known as oxygen transporter (van Holde & Miller, 1995; van Holde et al., 2000) but also functions in many other aspects like osmotic regulation (Seidl et al., 2002) and anti–fungal defense factor (Destoumieux–Garzon et al., 2001). However, in this study, the hemocyanin

derived from the shell of *L. vananmei* does not work as an oxygen transporter but a pigment–binding function and involved into shrimp shell color change. This might be correlated with the organ or tissue where hemocyanins exist. Hemocyanins that were reported with oxygen transportation function, innate immune function were isolated from hepatopancreas, hemolymph or blood (van Holde & Miller, 1995; Destoumieux–Garzon et al., 2001; Seidl et al., 2002). All these tissues or organs are mainly correlated with the respiration or immune functions during shrimp life history. There is no need to transport any oxygen or display any immune function in non–cell tissue like the shell. In nature status the main function of shrimp shell is protection: calcification is known to play a major role in making the skeleton, while the organismal coloration is mainly served as communication and camouflage (Kronstadt et al., 2013). According to this principle, the hemocyanin which was transferred to the exoskeleton may active as the color change function.

Changes of CD spectra between LvPBP75 and rLvPBP75 probably reflects the increase in conformational flexibility of hemocyanin gained by the hydrophobic residues associated to ATX binding. The binding ratio of rLvPBP75 and ATX was calculated to be 0.346 based on their molar mass, which means that 1 ATX could bound with 26 kDa protein. The reported ATX content in crustacyanin is about 1 ATX per 22 kDa apoprotein (Palma & Steneck 2001; Elizabeth et al., 2009). Similar situation was found in the pigment–binding protein derived from the egg of golden apple snail, which has 1 ATX per 30 kDa protein chromophore. ATX was tightly bound to the protein but it did not make any substantial contribution to the structural changes of pigment–binding complex (Dreon et al., 2007). According to these results, the protein can be expected to dominate the CD spectra of pigment–binding complex. However, Ferrari et al. (2012) reported the reconstitution of crustacyanin using astaxanthin and crustacyanin subunits that derived from the shell of American lobster (*H. americanus*). The recombinant crustacyanin subunit H_1 and H_2 with astaxanthin produced a bathochromic shift of 85–95 nm compared with natural crustacyanin subunits from *H. americanus* in complex with astaxanthin. Our results suggest that,

ATX could bound to hemocyanin and this pigment–binding complex had closely corresponded to *L. vannamei* shell color change. But unlike crustacyanin, ATX does not bring any structural changes to the pigment–binding complex.

Based on the above results and discussion, a novel red color–related pigment–binding protein, LvPBP75 was purified from the shell of *L. vannamei* by using ammonium sulfate precipitation, gel filtration, and anion exchange HPLC. It had closely corresponded to *L. vannamei* shell color change under heat treatment and was identified as hemocyanin which could bind with ATX. The pigment–binding ability of hemocyanins has tissue– or species–specificity. Meantime, this red color–related hemocyanin–ATX binding complex was not specific among shrimp species.

6.3 Prospect for future study

Further research should be carried out based on the current findings in this study, e.g., to further investigate the red color–related proteins among other crustacean species, to characterize the binding site and structural properties of LvPBP75 and to clarify the transportation and pigment–binding mechanisms of hemocyanin in *L. vannmei*. It is anticipated that further studies could lead to promising understanding and application of crustacean PBPs in food processing industry.

Acknowledgements

First of all, I would like to thank the Ministry of Education, Culture, Sports, Science and Technology in Japan, for supporting my study in Japan, and the Sasakawa Scientific Research Grant from the Japan Sciences Society for funding partial of this work.

I am grateful to my supervisor Professor Shoichiro Ishizaki, Laboratory of Marine Biomaterial & Functional Biochemistry, Graduate School of Marine Science and Technology, Tokyo University of Marine Science and Technology, for the precious guidance and encouragement throughout this study. I would like to thank Professor Yuji Nagashima, Faculty of Agro–Food Science, Niigata Agro–Food University, for his valuable suggestions and comments in this study.

I would also like to thank members of my dissertation committee, Drs. Tomoyuki Koyama, Tomoaki Hagiwara, and Hidehiro Kondo for their useful advises and kind considerations on this thesis.

I am grateful to all my lab members and friends for their suggestions and help during my past three years. Especially Dr. Wu Haiyun, Laboratory of Ocean Science, Tokyo University of Marine Science and Technology, and Mr. Gao Wei, Laboratory of Food Hygiene, Nagasaki University, for their valuable suggestions and kind assistance.

Finally, I'd like to thank my father Pan Yougen, my mother Wang Jinfeng and my girlfriend Ma Jingrong for their mental and financial supports during my overseas study.

References

Ando, M., Fukai, T., Kawasaki, K., Itoh, T., & Tsukamasa, Y. (2014). Improvement of red color development on the surface of kuruma prawn *Marsupenaeus japonicus* under various conditions. Journal of Food Science, 79, E202–207.

Babu, C. M., Chakrabarti, R., & Sambasivarao, R. S. (2008). Enzymatic isolation of carotenoid–protein complex from shrimp head waste and its use as a source of carotenoids. LWT–Food Science and Technology, 41, 227–235.

Begum, S., Cianci, M., Durbeej, B., Falklöf, O., Hädener, A., Helliwell, J. R., Helliwell, M., Regan, A. C., & Ian, F. W. C. (2015). On the origin and variation of colors in lobster carapace. Physical Chemistry Chemical Physics, 17, 16723–16732.

Bhosale, P., & Bernstein, P. S. (2007). Vertebrate and invertebrate carotenoid–binding proteins. Archives of Biochemistry and Biophysics, 458, 121–127.

Brookmire, L., Mallikarjunan, P., Jahncke, M., & Grisso, R. (2013). Optimum cooking conditions for shrimp and Atlantic salmon. Journal of Food Science, 78, S303–313.

Buchwald, M., & Jencks, W. P. (1968). Properties of the crustacyanins and the yellow lobster shell pigment. Biochemistry, 7, 844–859.

Budd, A. M., Hinton, T. M., Tonks, M., Cheers, S., & Wade, N. M. (2017). Rapid expansion of pigmentation genes in Penaeid shrimp with absolute preservation of function. Journal of Experimental Biology, 220, 4109–4118.

Casariego, A. M., Luppi, T., & Iribarne, O. (2011). Differential coloration patterns in the intertidal crab *Neohelice* (=*Chasmagnathus*) *granulata*. Journal of the Marine Biological Association of the United Kingdom, 91, 1041–1047.

Castillo, R., Nègre–Sadargues, G., & Lenel, R. (2013). General Survey of the Carotenoids in Crustacea, in Carotenoid Chrmistry & Biochemistry, ed. by Britton G & Goodwin T. Pergamon, Oxford, pp. 211–224.

Chayen, N. E., Cianci, M., Grossmann, J. G., Habash, J., Helliwell, J. R., Nneji, G. A., Raftery, J., Rizkallah, P. J., & Zagalsky, P. F. (2003). Unravelling the structural chemistry of the colouration mechanism in lobster shell. Acta crystallographica. Section D: Biological crystallography, 59, 2072–2082.

Cheesman, D. F., Zagalsky, P. F., & Ceccaldi, H. J. (1967). Purification and properties of crustacyanin. Proceedings of the Royal Society B: Biological Sciences, 164, 130–151.

Cianci, M., Rizkallah, P. J., Olczak, A., Raftery, J., Chayen, N. E., Zagalksy, P. F., & Helliwell, J. R. (2002). The molecular basis of the coloration mechanism in lobster shell, β–crustacyanin at 3.2–Å resolution. Proceedings of the National Academy of Science of the United States of America, 99, 9795–9800.

Clarke, D.T. (2012). Circular dichroism in protein folding studies. Current Protocols in Protein Science, 28.3, 1–17.

Cremades, O., Parrado, J., Alvarez–Ossorio, M. C., Jover, M., Collantes, de Teran, L., Gutierrez, J. F., & Bautista, J. (2003). Isolation and characterization of carotenoproteins from crayfish (*Procambarus clarkii*). Food Chemistry, 82, 559–566.

Crothers, L., Gering, E., & Cummings, M. (2011). Aposematic signal variation predicts male–male interactions in a polymorphic poison frog. Evolution, 65, 599–605.

Crozier, G. F. (1970). Tissue carotenoids in prespawning and spawning sockeye salmon (*Oncorhynchus nerka*). Journal of the Fisheries Research Board of Canada, 27, 973–975.

Cuthill, I. C., Stevens, M., Sheppard, J., Maddocks, T., Parraga, C. A., & Troscianko, T. S. (2005). Disruptive coloration and background pattern matching. Nature, 434, 72–74.

Destoumieux–Garzón, D., Saulnier, D., Garnier, J., Jouffrey, C., Bulet, P., & Bachère, E. (2001). Crustacean Immunity. Antifungal peptides are generated from the c terminus of shrimp hemocyanin in response to microbial challenge. Journal of

Biological Chemistry, 276, 47070–47077.

Detto, T., Backwell, P. R. Y., Hemmi, J. M., & Zeil, J. (2006). Visually mediated species and neighbour recognition in fiddler crabs (*Uca mjoebergi* and *Uca capricomis*). Proceedings of the Royal Society B–Biological Sciences, 273, 1661–1666.

Dreon, M. S., Ceolin, M., & Heras, H. (2007). Astaxanthin binding and structural stability of the apple snail carotenoprotein ovorubin. Archives of Biochemistry and Biophysics, 460, 107–112.

Durbeej, B., & Eriksson, L. A. (2003). On the bathochromic shift of the absorption by astaxanthin in crustacyanin, a quantum chemical study. Chemical Physics Letters, 375, 30–38.

Elizabeth, T., David, W., & Andrew, B. (2009). Characterisation of the carotenoprotein found in carapace shells of *Jasus lalandii*. Comparative Biochemistry and Physiology, Part B, 153, 39–42.

Erickson, M. C., Bulgarelil, M. A., Resurreccion, A. V. A., Vendetti, R. A., & Gates, K. A. (2007). Consumer differentiation, acceptance, & demographic patterns to consumption of six varieties of shrimp. Journal of Aquatic Food Product Technology, 15, 35–51.

Ertl, N. G., Elizur, A., Brooks, P., Kuballa, A. V., Anderson, T. A., & Knibb, W. R. (2013). Molecular characterisation of colour formation in the prawn *Fenneropenaeus merguiensis*. PLoS One, 8, e56920, 1–17.

Fernlund, P., & Josefsson, L. (1968). Chromactivating hormones of *Pandalus Borealis*. Isolation and purification of the 'red–pigment–concentrating hormone'. Biochimica et Biophysica Acta, 158, 262–273.

Ferrari, M., Folli, C., Pincolini, E., McClintock, T. S., Rössle, M., Berni, R., & Cianci, M. (2012). Structural characterization of recombinant crustacyanin subunits from the lobster *Homarus americanus*. Acta Crystallographica Section F, 68, 846–853.

Gamiz–Hernandez, A. P., Angelova, I. N., Send, R., Sundholm, D., & Kaila, V. R. I. (2015). Protein–induced color shift of carotenoids in β–crustacyanin. Angewandte

Chemie International Edition, 54, 11564–11566.

Ghidalia, W. (1985). Structural and biological aspects of pigments, in The Biology of Crustacea, Vol. 9, Bliss, D. E. and Mantel, L. H., Eds., Academic Press, New York, 301.

Goncalves, A. A., & Menezes de Oliveira, A. R. (2016). Melanosis in crustaceans: A review. LWT–Food Science and Technology, 65, 791–799.

Greene, C. M., Waters, D., Clark, R. M., Contois, J. H., & Fernandez, M. L. (2006). Plasma LDL and HDL characteristics and carotenoid content are positively influenced by egg consumption in an elderly population. Nutrition & Metabolism, 3, 6.

Greenfield, N. J. (1996). Methods to estimate the conformation of proteins and polypeptides from circular dichroism data. Analytical Biochemistry, 235, 1–10.

Gross, J. (1991). Pigments in vegetables: Chlorophylls and Carotenoids, Van Nostrand Reinhold, New York.

Hemmi, J. M., Marshall, J., Pix, W., Vorobyev, M., & Zeil, J. (2006). The variable colours of the fiddler crab *Uca vomeris* and their relation to background and predation. Journal of Experimental Biology, 209, 4140–4153.

Herring, P. J. (1969). Pigmentation and carotenoid metabolism of the marine isopoda *Idotea metallica*. Journal of the Marine Biological Association of the United Kingdom, 49, 767–779.

Holden, H. M., Rypniewski, W. R., Law, J. H., & Rayment, I. (1987). The molecular structure of insecticyanin from the tobacco hornworm *Manduca sexta* L. at 2.6 A resolution. EMBO Journal, 6, 1565–1570.

Huang, Y. R., Mirtala, F. G. Z., & Shiau, C. Y. (2016). Changes in biochemical compositions and quality of white shrimp (*Litopenaeus vannamei*) during storage. Journal of Aquatic Food Product Technology, 25, 35–45.

Huber, R., Schneider, M., Epp, O., Mayr, I., Messerschmidt, A., Pflugrath, J., & Kayser, H. (1987). Crystallization, crystal structure analysis and preliminary molecular model of the bilin binding protein from the insect *Pieris brassicae*.

Journal of Molecular Biology, 195, 423–434.

Jouni, Z. E., & Wells, M. A. (1996). Purification and partial characterization of a lutein–binding protein from the midgut of the silkworm *Bombyx mori*. Journal of Biological Chemistry, 271, 14722–14726.

Keen, J. N., Caceres, I., Eliopoulos, E. E., Zagalsky, P. F., & Findlay, J. B. C. (1991a). Complete sequence and model for the A2 subunit of the carotenoid pigment complex, crustacyanin. European Journal of Biochemistry, 197, 407–417.

Keen, J. N., Caceres, I., Eliopoulos, E. E., Zagalsky, P. F., & Findlay, J. B. C. (1991b). Complete sequence and model for the C1 subunit of the carotenoprotein, crustacaynin, and model for the dimer, beta–crustacaynin, formed from the C1 and A2 subunits with astaxanthin. European Journal of Biochemistry, 202, 31–40.

Kelly, S. M., Jess, T. J., & Price, N. C. (2005). How to study proteins by circular dichroism. BBA Proteins and Proteomics, 1751, 119–139.

Kitahara, T. (1984). Carotenoids in the pacific salmon during the marine period. Comparative Biochemistry and Physiology Part B: Comparative Biochemistry, 78, 859–862.

Klomklao, S., Benjakul, S., Visessanguan, W., Kishimura, H., & Simpson, B. K. (2009). Extraction of carotenoprotein from black tiger shrimp shells with the aid of bluefish trypsin. Journal of Food Biochemistry, 33, 201–217.

Kronstadt, S. M., Darnell, M. Z., & Munguia, P. (2013). Background and temperature effects on *Uca panacea* color change. Marine Biology, 160, 1373–1381.

Lakshman, M. R., & Okoh, C. (1993). Carotenoid–protein complexes. Methods In Enzymology, 214, 74–86.

Lakshminarayanan, R., Bromley, K. M., Lei, Y. P., Snead, M. L., & Moradian–Oldak, J. (2010). Perturbed amelogenin secondary structure leads to uncontrolled aggregation in amelogenesis imperfecta mutant proteins. Journal of Biological Chemistry, 285, 40593–40603.

Lee, W. L. (1966). Pigmentation of the marine isopod *Idothea montereyensis*. Comparative Biochemistry and Physiology, 18, 17–36.

Li, R. F., Yu, H. H., Xing, R. G., Liu, S., Qing, Y. K., Li, K. C., Li, B., Meng, X. T., Cui, J. H., & Li, P. C. (2012). Isolation, identification and characterization of a novel antioxidant protein from the nematocyst of the jellyfish *Stomolophus meleagris*. International Journal of Biological Macromolecules, 51, 274–278.

Lieb, B., Altenhein, B., & Markl, J. (2000). The sequence of a gastropod hemocyanin (HtH1 from *Haliotis tuberculata*). Journal of Biological Chemistry, 275, 5675–5681.

Liñán–Cabello, M. A., Paniagua–Michel, J., & Hopkins, P. M. (2002). Bioactive roles of carotenoids and retinoids in crustaceans. Aquaculture Nutrition, 8, 299–309.

Lowry, O. H., Rosebrough, N. J., Farr, A. L., & Randall, R. J. (1951). Protein measurement with the Folin phenol reagent. Journal of Biological Chemistry, 193, 265–275.

Maoka, T. (2011). Carotenoids in marine animals. Marine Drugs, 9, 278–293.

Matsuno, T. (2001). Aquatic animal carotenoids. Fisheries Science, 67, 771–783.

Matsuno, T., & Katsuyama, M. (1982). Metabolism of zeaxanthin to rhodoxanthin in Tilapia *Tilapia nilotica* (In Japanese). Nippon Suisan Gakkaishi, 48, 1491–1493.

Matsuo, E., Sediyama, T., Oliveira, R. D. D., Cruz, C. D., & Oliveria, R. D. T. (2012). Characterization of type and genetic diversity among soybean cyst nematode differentiators. Scientia Agricola, 69, 147–151.

Melville–Smith, R., Cheng, Y. W., & Thomson, A. W. (2003). Factors affecting colour change in 'white' western rock lobsters, *Panulirus cygnus*. Journal of Experimental Marine Biology and Ecology, 291, 111–129.

Michael, F. T., Anita, M., Sara, H., Sutara, S., & Saskia, G. (2009). Morphological colour change in the American lobster (*Homarus americanus*) in response to background colour and UV light. New Zealand Journal of Marine and Freshwater Research, 43, 247–255.

Miller, K. I., Cuff, M. E., Lang, W. F., Varga–Weisz, P., Field, K. G., & van Holde, K. E. (1998). Sequence of the *Octopus dofleini* hemocyanin subunit: structural and evolutionary implications. Journal of Molecular Biology, 278, 827–842.

Newcomer, M. E., Jones, T. A., Aqvist, J., Sundelin, J., Eriksson, U., Rask, L., & Peterson, P. A. (1984). The three–dimensional structure of retinol–binding protein. EMBO Journal, 3, 1451–1454.

Nirmal, N. P., & Benjakul, S. (2009). Melanosis and quality changes of Pacific white shrimp (*Litopenaeus vannamei*) treated with catechin during iced storage. Journal of Agricultural and Food Chemistry, 57, 3578–3586.

Niu, J., Wen, H., Li, C. H., Liu, Y. J., Tian, L. X., Chen, X., Huang, Z., & Lin, H. Z. (2014). Comparison effect of dietary astaxanthin and β–carotene in the presence and absence of cholesterol supplementation on growth performance, antioxidant capacity and gene expression of *Penaeus monodon* under normoxia and hypoxia condition. Aquaculture, 422–423, 8–17.

Nur–E–Borhan, S. A., Okada, S., Watabe, S., & Yamaguchi, K. (1995). Carotenoproteins from the exoskeleton and the muscular epithelium of the black tiger prawn *Penaeus monodon*. Fisheries Science, 61, 337–343.

Palma, A. T., & Steneck, R. S. (2001). Does variable coloration in juvenile marine crabs reduce risk of visual predation? Ecology, 82, 2961–2967.

Papiz, M. Z., Sawyer, L., Eliopoulos, E. E., North, A. C., Findlay, J. B. C., Sivaprasadarao, R., Jones, T. A., Newcomer, M. E., & Kraulis, P. J. (1986). The structure of beta–lactoglobulin and its similarity to plasma retinol–binding protein. Nature, 6095, 383–388.

Parisenti, J., Beirão, L. H., Tramonte, V. L. C. G., Ourique, F., da Silveira, Brito, C. C., & Moreira, C. C. (2011). Preference ranking of colour in raw and cooked shrimps. International Journal of Food Science and Technology, 46, 2558–2561.

Paul, R. J., & Pirow, R. (1997). The physiological significance of respiratory proteins in invertebrates. Zoology, 100, 298–306.

Porter, M. L., Bok, M. J., Robinson, P. R., & Cronin, T. W. (2009). Molecular diversity of visual pigments in Stomatopoda (Crustacea). Visual Neuroscience, 26, 255–265.

Quarmby, B., Norden, D. A., Zagalsky, P. F., Cecaldi, H. J., & Daumas, R. (1977).

Studies on the quaternary structure of the lobster exoskeleton carotenoprotein, crustacyanin. Comparative Biochemistry and Physiology, B–Biochemistry & Molecular Biology, 56, 55–61.

Reszczynskaab, E., Welca, R., Grudzinskia, W., Trebaczb, K., & Gruszeckia, W. I. (2015). Carotenoid binding to proteins, Modeling pigment transport to lipid membranes. Archives of Biochemistry and Biophysics, 584, 125–133.

Ribeiro, E. A., Genofre, G. C., & McNamara, J. C. (2001). Identification and quantification of carotenoid pigments during the embryonic development of the freshwater shrimp *Macrobrachium olfersii* (crustacea, decapoda). Marine and Freshwater Behaviour and Physiology, 34, 105–116.

Sachindra, N. M., Bhaskar, N., & Mahendrakar, N. S. (2005). Carotenoids in different body components of Indian shrimps. Journal of the Science of Food and Agriculture, 85, 167–172.

Saito, A., & Regier, L. W. (1971). Pigmentation of brook trout (*Salvelinus fontinalis*) by feeding dried crustacean waste. Journal of the Fisheries Research Board of Canada, 28, 509–512.

Schidet, K, Leuenberger, F. J., Vecchi, M., & Glinz, E. (1985) Absorption, retention and metabolic transformations of carotenoids in rainbow trout, salmon and chicken. Pure and Applied Chemistry, 57, 685–692.

Schiedt, K., Vecchi, M., & Glinz, E. (1985). Astaxanthin and its metabolites in wild rainbow trout (*Salmogairdneri* R.). Comparative Biochemistry and Physiology Part B: Comparative Biochemistry, 83, 9–12.

Schmittgen, T. D., & Livak, K. J. (2008). Analyzing real–time PCR data by the comparative CT method. Nature Protocols, 3, 1101–1108.

Seidl, M. D., Pirow, R., & Paul, R.J. (2002). Water fleas (*Daphnia magna*) provide a separate ventilatory mechanism for their brood. Zoology, 105, 15–23.

Senphan, T., Benjakul, S., & Kishimura, H. (2014). Characteristics and antioxidative activity of carotenoprotein from shells of pacific white shrimp extracted using hepatopancreas proteases. Food Bioscience, 5, 54–63.

Shahidi, F., Metusalach, & Brown, J. A. (1998). Carotenoid pigments in seafoods and aquaculture. Critical Reviews in Food Science, 38, 1–67.

Sila, A., Nasri, R., Jridi, M., Balti, R., Nasri, M., & Bougatef, A. (2012). Characterisation of trypsin purified from the viscera of Tunisian barbel (*Barbus callensis*) and its application for recovery of carotenoproteins from shrimp wastes. Food Chemistry, 132, 1287–1295.

Silbiger, N., & Munguia, P. (2008). Carapace color change in *Uca pugilator* as a response to temperature. Journal of Experimental Marine Biology and Ecology, 355, 41–46.

Simpson, B. K., Dauphin, L., & Smith, J. P. (1993). Recovery and characteristics of carotenoprotein from lobster (*Homarus americanus*) waste. Journal of Aquatic Food Product Technology, 1, 129–146.

Sreerama, N., & Woody, R. W. (2004). Computation and analysis of protein circular dichroism spectra. Methods in Enzymology, 383, 318–351.

Stevens, M., & Merilaita, S. (2009). Animal camouflage: current issues and new perspectives. Proceedings of the Royal Society B–Biological Sciences, 364, 423–427.

Tabunoki, H., Higurashi, S., Ninagi, O., Fujii, H., Banno, Y., Nozaki, M., Kitajima, M., Miura, N., Atsumi, S., Tsuchida, K., Maekawa, H., & Sato, R. (2004). A carotenoid–binding protein (CBP) plays a crucial role in cocoon pigmentation of silkworm (*Bombyx mori*) larvae. FEBS Letters, 567, 175–178.

Tabunoki, H., Sugiyama, H., Tanaka, Y., Fujii, H., Banno, Y., Jouni, Z. E., Kobayashi, M., Sato, R., Maekawa, H., & Tsuchida, K. (2002). Isolation, characterization, and cDNA sequence of a carotenoid binding protein from the silk gland of *Bombyx mori* Larvae. Journal of Biological Chemistry, 277, 32133–32140.

Thomas, P. D., & Dill, K.A. (1993). Local and nonlocal interactions in proteins and mechanisms of alcohol denaturation. Protein Science, 2, 2050–2065.

Tume, R. K., Sikes, A. L., Tabrett, S., & Smith, D. M. (2009). Effect of background colour on the distribution of astaxanthin in black tiger prawn (*Penaeus monodon*):

Effective method for improvement of cooked colour. Aquaculture, 296, 129–135.

van Holde, K. E., & Miller, K. I. (1995). Hemocyanins. Advances in Protein Chemistry and Structural Biology, 47, 1–81.

van Holde, K. E., Miller, K. I., & Decker, H. (2001). Hemocyanins and invertebrate evolution. Journal of Biological Chemistry, 276, 15563–15566.

Velu, C. S., Czeczuga, B., & Munuswamy, N. (2003). Carotenoprotein complexes in entomostracan crustaceans (*Streptocephalus dichotomus* and *Moina micrura*). Comparative Biochemistry and Physiology. Part B, 135B, 35–42.

Voit, R., Feldmaier–Fuchs, G., Schweikardt, T., Decker, H., & Burmester, T. (2000). Complete sequence of the 24–mer hemocyanin of the Tarantula *Eurypelma californicum*. Journal of Biological Chemistry, 275, 39339–39344.

Wade, N. M., Anderson, M., Sellars, M. J., Tume, R. K., Preston, N. P., & Glencross, B. D. (2012). Mechanisms of colour adaptation in the prawn *Penaeus monodon*. Journal of Experimental Biology, 215, 343–350.

Wade, N. M., Gabaudan, J., & Glencross, B. D. (2017). A review of carotenoid utilization & function in crustacean aquaculture. Aquaculture, 9, 141–156.

Wade, N. M., Melville–Smith, R., Degnan, B. M., & Hall, M. R. (2008). Control of shell colour changes in the lobster, *Panulirus cygnus*. Journal of Experimental Biology, 211, 1512–1519.

Wade, N. M., Tollenaere, A., Hall, M. R., & Degnan, B. M. (2009). Evolution of a novel carotenoid–binding protein responsible for crustacean shell color. Molecular Biology and Evolution, 26, 1851–1864.

Wald, G., & Nathanson, N. (1948). Crustacyanin, the blue carotenoid–protein of the lobster shell. Biology Bulletin, 95, 249.

Wang, J. S. Protein. In: Wang JS, Wang DM, Lv SX (eds). Physicochemical Properties, Vol 6, Chapter 1. Beijing: China Science Publishing & Meida Ltd., 2007; 41–45.

Yanar, Y., Çelik, M., & Yanar, M. (2004). Seasonal changes in total carotenoid contents of wild marine shrimp (*Penaeus semisulcatus* and *Metapenaeus monoceros*) inhabiting the eastern Mediterranean. Food Chemistry, 88, 267–269.

Zadorozhny, P. A., Borisovets, E. E., Yakush, E. V., & Davidyuk, T. S. (2008). Change of carotenoid composition in crabs during embryogenesis. Journal of Evolutionary Biochemistry and Physiology, 44, 450–461.

Zagalsky, P. F. (1985). Invertebrate carotenoproteins. Methods in Enzymology, 111, 216–263.

Zsila, F., Bikádi, Z., & Simonyi, M. (2002). Retinoic acid binding properties of the lipocalin member β–lactoglobulin studied by circular dichroism, electronic absorption spectroscopy and molecular modeling methods. Biochemical Pharmacology, 64, 1651–1660.